

U.S. Department of the Interior
U.S. Geological Survey

Verification of Roughness Coefficients for Selected Natural and Constructed Stream Channels in Arizona

U.S. Geological Survey Professional Paper 1584

Prepared in cooperation with the
Flood Control District of Maricopa County

Property of
Flood Control District of MC Library
Please Return to
2601 W. Durango
Phoenix, AZ 85009



102.909

science for a changing world

Availability of Publications of the U.S. Geological Survey

Order U.S. Geological Survey (USGS) publications from the offices listed below. Detailed ordering instructions, along with prices of the last offerings, are given in the current-year issues of the catalog "New Publications of the U.S. Geological Survey."

Books, Maps, and Other Publications

By Mail

Books, maps, and other publications are available by mail from—

USGS Information Services
Box 25286, Federal Center
Denver, CO 80225

Publications include Professional Papers, Bulletins, Water-Supply Papers, Techniques of Water-Resources Investigations, Circulars, Fact Sheets, publications of general interest, single copies of permanent USGS catalogs, and topographic and thematic maps.

Over the Counter

Books, maps, and other publications of the U.S. Geological Survey are available over the counter at the following USGS Earth Science Information Centers (ESIC's), all of which are authorized agents of the Superintendent of Documents:

- Anchorage, Alaska—Rm. 101, 4230 University Dr.
- Denver, Colorado—Bldg. 810, Federal Center
- Menlo Park, California—Rm. 3128, Bldg. 3, 345 Middlefield Rd.
- Reston, Virginia—Rm. 1C402, USGS National Center, 12201 Sunrise Valley Dr.
- Salt Lake City, Utah—2222 West, 2300 South (books and maps available for inspection only)
- Spokane, Washington—Rm. 135, U.S. Post Office Building, 904 West Riverside Ave.
- Washington, D.C.—Rm. 2650, Main Interior Bldg., 18th and C Sts., NW.

Maps only may be purchased over the counter at the following USGS office:

- Rolla, Missouri—1400 Independence Rd.

Electronically

Some USGS publications, including the catalog "New Publications of the U.S. Geological Survey" are also available electronically on the USGS's World Wide Web home page at <http://www.usgs.gov>

Preliminary Determination of Epicenters

Subscriptions to the periodical "Preliminary Determination of Epicenters" can be obtained only from the Superintendent of

Documents. Check or money order must be payable to the Superintendent of Documents. Order by mail from—

Superintendent of Documents
Government Printing Office
Washington, DC 20402

Information Periodicals

Many Information Periodicals products are available through the systems or formats listed below:

Printed Products

Printed copies of the Minerals Yearbook and the Mineral Commodity Summaries can be ordered from the Superintendent of Documents, Government Printing Office (address above). Printed copies of Metal Industry Indicators and Mineral Industry Surveys can be ordered from the Center for Disease Control and Prevention, National Institute for Occupational Safety and Health, Pittsburgh Research Center, P.O. Box 18070, Pittsburgh, PA 15236-0070.

Mines FaxBack: Return fax service

1. Use the touch-tone handset attached to your fax machine's telephone jack. (ISDN [digital] telephones cannot be used with fax machines.)
2. Dial (703) 648-4999.
3. Listen to the menu options and punch in the number of your selection, using the touch-tone telephone.
4. After completing your selection, press the start button on your fax machine.

CD-ROM

A disc containing chapters of the Minerals Yearbook (1993-95), the Mineral Commodity Summaries (1995-97), a statistical compendium (1970-90), and other publications is updated three times a year and sold by the Superintendent of Documents, Government Printing Office (address above).

World Wide Web

Minerals information is available electronically at <http://minerals.er.usgs.gov/minerals/>

Subscription to the catalog "New Publications of the U.S. Geological Survey"

Those wishing to be placed on a free subscription list for the catalog "New Publications of the U.S. Geological Survey" should write to—

U.S. Geological Survey
903 National Center
Reston, VA 20192

Verification of Roughness Coefficients for Selected Natural and Constructed Stream Channels in Arizona

By JEFF V. PHILLIPS *and* TODD L. INGERSOLL

U.S. GEOLOGICAL SURVEY PROFESSIONAL PAPER 1584

Prepared in cooperation with the

*FLOOD CONTROL DISTRICT OF MARICOPA
COUNTY*



U.S. DEPARTMENT OF THE INTERIOR
BRUCE BABBITT, Secretary

U.S. GEOLOGICAL SURVEY
Thomas J. Casadevall, Acting Director

The use of firm, trade, and brand names in this report is for
identification purposes only and does not constitute
endorsement by the U.S. Government.

Library of Congress Cataloging in Publications Data

Phillips, Jeff V., 1962-

Verification of roughness coefficients for selected natural and
constructed stream channels in Arizona / by Jeff V. Phillips and
Todd L. Ingersoll.

p. cm.-- (U.S. Geological Survey professional paper ; 1584)

"Prepared in cooperation with the Flood Control District of
Maricopa County."

ISBN 0-607-88875-X (alk. paper)

1. Channels (Hydraulic engineering)--Arizona. 2. Frictional
resistance (Hydrodynamics) I. Ingersoll, Todd L., 1970-

II. Flood Control District of Maricopa County. III. Title.

IV. Series.

TC175.P45 1998

627'.23'097921--dc21

97-48313

CIP

For sale by U.S. Geological Survey, Information Services
Box 25286, Federal Center
Denver, CO 80225

CONTENTS

Abstract.....	1
Introduction	1
Purpose and scope	2
Acknowledgments	2
Description of study area.....	2
Field measurements for verified roughness coefficients.....	4
Site selection.....	4
Data collection.....	4
Computation of reach properties and roughness coefficients.....	5
Assumptions and limitations	7
Changing boundary conditions.....	7
Changing vegetation conditions	7
Uncertainties of discharge measurements	8
Flow depth and magnitude	8
Changing bed forms.....	9
Presentation of verified roughness coefficients	10
Hassayampa River near Arlington.....	11
Skunk Creek above Interstate 17.....	16
Agua Fria River below New Waddell Dam.....	23
Cave Creek above Deer Valley Road.....	27
Cave Creek below Cave Buttes Dam	31
Hassayampa River near Morristown	35
Indian Bend Wash above Curry Road.....	40
Salt River above Interstate 10.....	44
Verde River below Beeline Highway	48
West Fork Sycamore Creek near Sunflower.....	52
San Pedro River near Charleston.....	55
Santa Cruz River at Cortaro.....	59
Verde River near Paulden	63
Salt River below Stewart Mountain Dam.....	66
Discussion of significant results	69
Components of Manning's n	69
Base value of Manning's n for gravel-bed streams	69
Influence of vegetation on Manning's n	74
Summary and conclusion.....	74
Selected references	75

FIGURES

1. Map showing study area and n -verification sites in Maricopa, Pima, Cochise, and Yavapai Counties, Arizona.....	3
2. Drawing showing open-channel flow reach in plan and profile views.....	6
3. Graph showing relation of stream power and median grain size to form of bed roughness	9
4A–H. Hassayampa River near Arlington:	
A. Graph showing cross-section 3.....	12
B. Drawing showing plan view	12
C. Graph showing Manning's n and hydraulic radius.....	13
D. Graph showing particle-size distribution for bed material	13

E.	Photograph showing view of typical bed material for low-flow channel	14
F.	Photograph showing view from right bank showing a current-meter measurement made in the low-flow channel	14
G.	Photograph showing view looking upstream from midreach of low-flow channel	15
H.	Photograph showing view from right bank and midreach looking downstream following flow of February 9, 1993	15
5A–K.	Skunk Creek above Interstate 17:	
A.	Graph showing cross-section 2	17
B.	Drawing showing plan view.....	18
C.	Graph showing Manning's n and hydraulic radius.....	18
D.	Graph showing particle-size distribution for bed material.....	19
E.	Photograph showing view of typical bed material in channel reach.....	19
F.	Photograph showing view from left bank and bottom of reach looking upstream during flow of March 1, 1991	20
G.	Photograph showing view from midchannel looking upstream following flow of March 1, 1991	20
H.	Photograph showing view from midchannel and bottom of reach looking upstream following artificial maintenance of the channel vegetation, May 23, 1994.....	21
I.	Photograph showing view from midchannel of reach looking upstream during flow of January 5, 1995	21
J.	Photograph showing view from midchannel looking upstream at regrowth of vegetation	22
K.	Photograph showing view from midchannel looking upstream following flow of August 14, 1996	22
6A–G.	Agua Fria River below New Waddell Dam:	
A.	Graph showing cross-section 2	23
B.	Drawing showing plan view.....	24
C.	Graph showing particle-size distribution for bed material.....	24
D.	Photograph showing view of typical bed material in channel reach.....	25
E.	Photograph showing view from bottom of the reach looking upstream on March 10, 1993	25
F.	Photograph showing view from midchannel looking toward left bank of cross-section 4.....	26
G.	Photograph showing view from midchannel in cross-section 2 of typical vegetation in the reach	26
7A–G.	Cave Creek above Deer Valley Road:	
A.	Graph showing cross-section 2	28
B.	Drawing showing plan view.....	28
C.	Graph showing Manning's n and hydraulic radius.....	28
D.	Graph showing particle-size distribution for bed material.....	29
E.	Photograph showing view of typical bed material in channel reach.....	29
F.	Photograph showing view from bottom of reach looking upstream during flow of January 9, 1995.....	30
G.	Photograph showing view from top of reach looking downstream	30
8A–G.	Cave Creek below Cave Buttes Dam:	
A.	Graph showing cross-section 4	32
B.	Drawing showing plan view.....	32
C.	Graph showing Manning's n and hydraulic radius.....	32
D.	Photograph showing view from cross-section 7 looking upstream toward transition from subcritical to supercritical flow	33
E.	Photograph showing view from cross-section 4 looking upstream toward subcritical flow reach during survey of the water surface, November 2, 1995	33
F.	Photograph showing view from top of reach looking downstream	34
G.	Photograph showing view from midchannel looking downstream.....	34
9A–G.	Hassayampa River near Morristown:	
A.	Plot showing cableway cross section, bed geometry for each current-meter measurement, and water-surface elevations	36
B.	Drawing showing plan view.....	37
C.	Graph showing Manning's n and hydraulic radius.....	37
D.	Graph showing particle-size distribution for bed material.....	38
E.	Photograph showing view upstream from midchannel during no-flow period.....	38

F.	Photograph showing view from cableway looking upstream during flow of February 9, 1993	39
G.	Photograph showing view from cableway looking upstream during flow of February 9, 1993	39
10A–G.	Indian Bend Wash above Curry Road:	
A.	Graph showing cross-section 3	41
B.	Drawing showing plan view.....	41
C.	Graph showing Manning's n and hydraulic radius.....	41
D.	Photograph showing view from midchannel looking downstream at laid-over grass following flow of October 6, 1993	42
E.	Photograph showing view from midreach looking upstream following flow of October 6, 1993.....	42
F.	Photograph showing view from bottom of reach looking upstream during low flow.....	43
G.	Photograph showing view from midchannel looking upstream before flow of December 26, 1994.....	43
11A–G.	Salt River above Interstate 10:	
A.	Graph showing cross-section 1	44
B.	Drawing showing plan view.....	45
C.	Graph showing Manning's n and hydraulic radius.....	45
D.	Graph showing particle-size distribution for bed material.....	46
E.	Photograph showing view of typical bed material in channel reach.....	46
F.	Photograph showing view from top of reach looking downstream during flow of January 15, 1992	47
G.	Photograph showing view from top of reach looking downstream	47
12A–G.	Verde River below Beeline Highway:	
A.	Graph showing cross-section 2	48
B.	Drawing showing plan view for flow of March 28, 1991	49
C.	Graph showing Manning's n and hydraulic radius.....	49
D.	Graph showing particle-size distribution for bed material.....	50
E.	Photograph showing view of typical bed material	50
F.	Photograph showing view from right bank and midreach looking upstream during flow of September 14, 1989.....	51
G.	Photograph showing view from cableway looking downstream during flow of March 28, 1991	51
13A–E.	West Fork Sycamore Creek near Sunflower:	
A.	Graph showing cross-section 2	52
B.	Drawing showing plan view.....	53
C.	Photograph showing view from bottom of reach looking upstream toward cross-section 2, February 25, 1963	53
D.	Photograph showing view from midreach looking upstream toward right bank of cross-section 1, February 25, 1963.....	54
E.	Photograph showing view from bottom of reach looking upstream toward cross-section 3, February 25, 1963	54
14A–E.	San Pedro River near Charleston:	
A.	Graph showing cross-section 2,	56
B.	Drawing showing plan view.....	56
C.	Graph showing particle-size distribution for bed material.....	57
D.	Photograph showing view from left bank looking downstream toward right bank of cross-section 1, October 8, 1964.....	57
E.	Photograph showing view from left bank of cross-section 2 looking downstream, October 8, 1964	58
15A–F.	Santa Cruz River at Cortaro:	
A.	Graph showing cross-section 2	60
B.	Drawing showing plan view.....	60
C.	Graph showing particle-size distribution for bed material.....	61
D.	Photograph showing view from cableway looking downstream, August 5, 1954, at a discharge of 7,000 cubic feet per second.....	61
E.	Photograph showing view from cableway looking downstream, October 2, 1964.....	62

F.	Photograph showing view from midchannel looking upstream toward right bank of cross-section 1 after flow of September 10, 1964.....	62
16A–D.	Verde River near Paulden:	
A.	Graph showing cross-section 2	64
B.	Drawing showing plan view.....	64
C.	Photograph showing view from top of reach looking downstream during low flow.....	65
D.	Photograph showing view from top of reach looking downstream at time of verification measurement, April 16, 1965.....	65
17A–D.	Salt River below Stewart Mountain Dam:	
A.	Graph showing cross-section 2	67
B.	Drawing showing plan view.....	67
C.	Photograph showing view looking upstream along left bank below cross-section 6.....	68
D.	Photograph showing view looking downstream along left bank from cross-section 2.....	68
18.	Graph showing relation of Manning's n and relative roughness for gravel-bed stream channels in Arizona and throughout the world	72
19.	Graph showing relation of vegetation components for vegetated channels studied and the estimated percentage of vegetation that blocks flow	75

TABLES

1.	Flow data and computed roughness coefficients, Hassayampa River near Arlington.....	11
2.	Average-reach properties, Hassayampa River near Arlington.....	11
3.	Flow data and computed roughness coefficients, Skunk Creek above Interstate 17.....	16
4.	Average-reach properties, Skunk Creek above Interstate 17.....	17
5.	Flow data and computed roughness coefficient, Agua Fria River below New Waddell Dam.....	23
6.	Average-reach properties, Agua Fria River below New Waddell Dam.....	23
7.	Flow data and computed roughness coefficients, Cave Creek above Deer Valley Road.....	27
8.	Average-reach properties, Cave Creek above Deer Valley Road	27
9.	Flow data and computed roughness coefficients, Cave Creek below Cave Buttes Dam.....	31
10.	Average-reach properties, Cave Creek below Cave Buttes Dam	31
11.	Flow data and computed roughness coefficients, Hassayampa River near Morristown	35
12.	Data obtained from discharge measurements and field surveys, Hassayampa River near Morristown	36
13.	Flow data and computed roughness coefficient, Indian Bend Wash above Curry Road	40
14.	Average-reach properties, Indian Bend Wash above Curry Road	40
15.	Flow data and computed roughness coefficients, Salt River above Interstate 10.....	44
16.	Average-reach properties, Salt River above Interstate 10.....	44
17.	Flow data and computed roughness coefficients, Verde River below Beeline Highway	48
18.	Average-reach properties, Verde River below Beeline Highway	48
19.	Flow data and computed roughness coefficient, West Fork Sycamore Creek near Sunflower.....	52
20.	Average-reach properties, West Fork Sycamore Creek near Sunflower.....	52
21.	Flow data and computed roughness coefficient, San Pedro River near Charleston	55
22.	Average-reach properties, San Pedro River near Charleston.....	55
23.	Flow data and computed roughness coefficient, Santa Cruz River at Cortaro	59
24.	Average-reach properties, Santa Cruz River at Cortaro	59
25.	Flow data and computed roughness coefficient, Verde River near Paulden.....	63
26.	Average-reach properties, Verde River near Paulden	63
27.	Flow data and computed roughness coefficient, Salt River below Stewart Mountain Dam	66
28.	Average-reach properties, Salt River below Stewart Mountain Dam.....	66
29.	Summary of verification measurements that include magnitude of base n values, factors required to adequately describe flow retardance, channel and hydraulic components, and an estimated percentage of flow that was blocked by vegetation.....	70
30.	Equations for relations among base n values, hydraulic radius, and median diameter of bed material for gravel-bed streams in different parts of the world.....	72

CONVERSION FACTORS

	Multiply	By	To obtain
	inch (in.)	25.4	millimeter
	foot (ft)	0.3048	meter
	cubic foot per second (ft ³ /s)	0.02832	cubic meter per second
	mile (mi)	1.609	kilometer
	square mile (mi ²)	2.590	square kilometer

VERTICAL DATUM

Sea level: In this report, "sea level" refers to the National Geodetic Vertical Datum of 1929 (NGVD of 1929)—a geodetic datum derived from a general adjustment of the first-order level nets of the United States and Canada, formerly called Sea Level Datum of 1929.

GLOSSARY OF TERMS

Antidune: Bed forms of curved symmetrically shaped sand waves that may move upstream, remain stationary, or move downstream. Antidunes occur in trains that are in phase with and strongly interact with gravity water-surface waves. The water-surface waves have larger amplitudes than the coupled sand waves. At large Froude numbers, the waves generally move upstream and grow until they become unstable and break like surf (breaking antidunes). The agitation accompanying the breaking obliterates the antidunes, and the process of antidune initiation and growth is repeated. At smaller Froude numbers, the antidunes generally remain stationary and increase and decrease in amplitude without breaking (standing waves; Simons and Richardson, 1966, p. v).

Backwater: Water backed up or retarded in its course as compared with its normal or natural condition of flow. In stream gaging, a rise in stage produced by a temporary obstruction such as ice or weeds, or by the flooding of the stream below.

Bank, left and right: Reference terms used to specify the banks on the left and right when facing downstream.

Bedform: Alluvial-channel bottom feature whose form depends on bed-material size, flow depth, and flow velocity. Bedforms include ripples, dunes, antidunes, and plane bed.

Conveyance: A measure of the carrying capacity of a channel section and is directly proportional to channel discharge. Conveyance is that part of Manning's equation that excludes the square root of the energy gradient or friction slope.

Crest-stage gage: A device for recording the peak water-surface elevation during a flood by means of a cork line that adheres to a wooden rod placed in a 2-inch-diameter metal pipe that has been secured near the channel margins.

Critical flow: If the flow is critical, the Froude number is equal to unity, and the inertial forces balance the gravitational forces. This balance takes place at the depth at which flow is at its minimum energy.

Dryland: Streams located in regions of semiarid to extremely arid climatic conditions. For the conterminous United States, this would apply to regions that accrue less than 20 in. of precipitation annually.

Ephemeral: A stream or reach of a stream that flows briefly in direct response to precipitation or snowmelt in the immediate vicinity, and whose channel is at all times above the water table.

Flood peak: The largest value of the runoff flow which occurs during a flood, as observed at a particular point in the drainage basin.

- Flood plain:** A flood-prone area, as identified on Federal Emergency Management Agency (FEMA) flood insurance rate maps, generally contains a floodway district and floodway fringe district, or contains areas of land adjoining (or near) the channel of a water course which has been, or may be, covered by floodwaters. A flood plain functions as a temporary channel or reservoir for overbank flows. The lowland that borders a river, usually dry but subject to flooding (Hoyt and Langbein, 1955, p. 12).
- Flow regime:** A range of flows producing similar bed forms, resistance to flow, and mode of sediment transport. The lower flow regime occurs with tranquil flow and produces bed forms of ripples, ripples on dunes, or dunes. The upper flow regime produces bed forms of plane bed with sediment moving, standing waves, or antidunes. Water-surface undulations are generally in phase with bed undulations. Between these two stable regimes is the transition regime, which produces instability in the stage-to-discharge relation and in the typical bed forms.
- Froude number:** A dimensionless number used as an index to characterize the type of flow (subcritical, critical, and supercritical) in an open channel. The Froude number is the ratio of the inertial forces to the gravitational forces, and is computed as the mean flow velocity divided by the square root of the product of the mean depth times the acceleration of gravity.
- Grain size, coarse and fine:** Coarse-grained bed material generally refers to those particles (gravel, cobble, boulder) whose size can be individually measured with a graduated rule or caliper; fine-grained material (sand, silt, clay) is measured by passage through a sieve or by rate of sedimentation. See also particle size.
- High-water marks:** Evidence of the highest stage reached by flow. High-water marks generally consist of debris and scour marks found along the channel boundaries.
- Hydraulic radius:** The ratio of the stream channel's cross-sectional area to its wetted perimeter in a plane normal to the direction of flow.
- Hydrograph:** The functional relation between time and flow discharge, as observed at a particular point within a drainage basin. In the case of a detention and (or) retention facility, an inflow hydrograph depicts the relation of time and runoff inflow to the facility, and an outflow hydrograph is a graph of flow discharge from the facility compared to time.
- Intermittent stream:** A stream that flows only at certain times of the year when it receives water from some surface source (rainfall or snowmelt) or from an intermittent spring and ceases to flow during other periods of the year. The channel is usually above the water table.
- Manning's roughness coefficient (n value):** A measure of the frictional resistance exerted by a channel on the flow. The n value also can reflect other energy losses such as those resulting from unsteady flow, extreme turbulence, and transport of suspended material and debris, that are difficult or impossible to isolate and quantify.
- Particle-size:** The size of material on the bed of a stream, referenced to a specific diameter (either maximum, intermediate, or minimum) of the measured particles.
- Perennial stream:** A stream that discharges continuously all year during dry as well as wet years.
- Relative roughness:** Relative roughness is the ratio of mean depth (usually represented by hydraulic radius, R) to the size of roughness elements (usually represented by the median value of the intermediate diameter of the streambed material, d_{50}).
- Runoff:** The portion of precipitation on land that ultimately reaches streams—especially water from rain or melted snow that flows over the land surface.
- Scour:** Erosion due to flowing water, usually considered as being localized as opposed to general bed degradation.
- Slope, water-surface:** The slope of the water surface, computed as the change in elevation per unit change in the channel's length.

- Slope-area method of discharge measurement:** A computational procedure whereby stream discharge is calculated "on the basis of a uniform-flow equation involving channel characteristics, water-surface profiles, and a roughness coefficient" (Dalrymple and Benson, 1967).
- Stream power:** A measure of energy transfer of the flow. Stream power is computed as $62RSV$, where R , S , and V are the hydraulic radius, in feet; water-surface slope, in feet per foot; and mean velocity, in feet per second, respectively; and 62 is the specific weight of water. Stream power also is defined as the energy dissipated per unit area of streambed per unit time.
- Subcritical flow:** If the flow is subcritical, the Froude number is less than one and the inertial forces are less than the gravitational forces. The flow depth in subcritical flow is greater than the flow depth in critical flow.
- Supercritical flow:** If the flow is supercritical, the Froude number is greater than one and the inertial forces are greater than the gravitational forces. The flow depth in supercritical flow is less than the flow depth in critical flow.
- Uniform flow:** Flow of constant water area, depth, discharge, and average velocity through a reach of a channel.
- Velocity head:** Represents the kinetic energy of the flowing fluid, generally expressed as $V^2/2g$, in feet, but actually is the energy per pound of flowing fluid.
- Velocity-head coefficient:** A factor used to adjust the velocity of the head computed from the mean velocity in a channel section to give the true mean kinetic energy of the flow for nonuniform distribution of velocities.
- Wash load:** The material which is transported by the river but is not found in significant quantities in the bed material.
- Water-surface profile:** A longitudinal plot of the water-surface elevation as a function of the distance downstream through a channel reach.
- Wetted perimeter:** The length of the line of intersection of the channel's wetted surface with a cross-sectional plane normal to the direction of flow.

Verification of Roughness Coefficients for Selected Natural and Constructed Stream Channels in Arizona

By Jeff V. Phillips and Todd L. Ingersoll

ABSTRACT

Physical and hydraulic characteristics are presented for 14 river and canal reaches in Arizona for which 37 roughness coefficients have been determined. The verified roughness coefficients, which ranged from 0.017 to 0.067, were computed from discharges, channel geometry, and water-surface profiles measured at each of the sites. The reaches studied cover a wide range of channel conditions including alluvial channels, boulder channels, constructed channels, and channels containing varying amounts of riparian vegetation. The information given for each stream segment includes bed and bank descriptions, data tables showing channel and hydraulic components, a plan view, a representative cross-section plot, and color photographs that can be used as a comparison standard to aid in determining roughness coefficients for similarly characterized channels.

Relations derived from the data presented relate Manning's roughness coefficient (n) to various hydraulic components. For gravel-bed streams, verified roughness coefficients are related to median grain size of the bed material and hydraulic radius resulting in an equation that can be used to transfer results to similar dryland channels. The equation developed for base values of n for gravel-bed channels in Arizona is significantly different from similarly derived equations for other regions of the United States and the world. Another equation was developed to quantify the magnitude of the vegetation component of

Manning's roughness coefficient for channels in which vegetation is present.

INTRODUCTION

The U.S. Geological Survey, in cooperation with the Flood Control District of Maricopa County, has been studying the hydraulic effects associated with channel-roughness elements in streams in Arizona. Manning's roughness coefficient, n , commonly is used to represent flow resistance for hydraulic computations of flow in open channels. The procedure for selecting n values is subjective and requires judgment and skill that is developed primarily through experience. The expertise necessary for proper selection of roughness coefficients can be obtained, in part, by examining characteristics of channels that have known or verified coefficients. The roughness coefficient can be verified by computations made using data from streamflow measurements and from measurements of the physical features of the channel. Photographs of channel segments where n values have been verified can be used as a comparison standard to aid in assigning n values to similar channels.

Verified values of Manning's n have been presented for streams that represent a wide range of channel conditions in the United States and other countries throughout the world. Past investigations include verified roughness coefficients for 50 selected stream channels in the United States (Barnes, 1967), 21 high-gradient streams in Colorado (Jarrett, 1985), 15 *flood plains* in the southeastern United States (Arcement and Schneider, 1989), 78 rivers and canals in New Zealand (Hicks and Mason, 1991), 11 gravel-bed streams in California (Limerinos, 1970), 67 gravel-

bed streams in Canada (Bray, 1979), and 21 *perennial* channels in New York State (Coon, 1995). However, only a few *n*-verification measurements have been obtained for *dryland* (Graf, 1988) stream channels in arid and semiarid regions of the southwestern United States (Aldridge and Garrett, 1973). Roughness coefficients for a variety of channel conditions are needed to substantiate the validity of guidelines currently used by hydrologists and engineers to assess flow resistance for dryland channels (Aldridge and Garrett, 1973; Thomsen and Hjalmarson, 1991).

Purpose and Scope

The purpose of this report is to present verified Manning's roughness-coefficient values for 37 discharge measurements at 14 selected stream sites in Arizona (fig. 1). The information includes geometry and roughness characteristics of the 14 sites. The selected sites represent a wide range of channel conditions that include unstable alluvial channels, high-gradient boulder-strewn channels, and manmade flood-control channels. Of the sites presented, five were published in previous *n*-value assessment reports and are included herein to increase the range of stream types and transferability of the information (Barnes, 1967; Aldridge and Garrett, 1973).

The verification-measurement data are used to develop empirical relations between channel and hydraulic components and Manning's *n*. The relations presented include an equation for gravel-bed streams that relates Manning's *n* to *relative roughness* and an equation to determine the effect of vegetation on total roughness. These relations can be used to transfer results to similar dryland stream channels in Arizona and the southwestern United States.

This study is the second phase of a two-phase investigation to assess roughness coefficients for stream channels in Arizona. Thomsen and Hjalmarson (1991) concluded the first phase by establishing guidelines for determining roughness coefficients and presented estimated *n* values for 16 stream channels in central Arizona. Some of the 14 verification sites used in this report are on the same streams as those described by Thomsen and Hjalmarson (1991) but at different locations. This report is intended to be used in conjunction with Thomsen and Hjalmarson's report to aid hydrologists and engineers in assessing and estimating *n* values for channels in arid to semiarid environments.

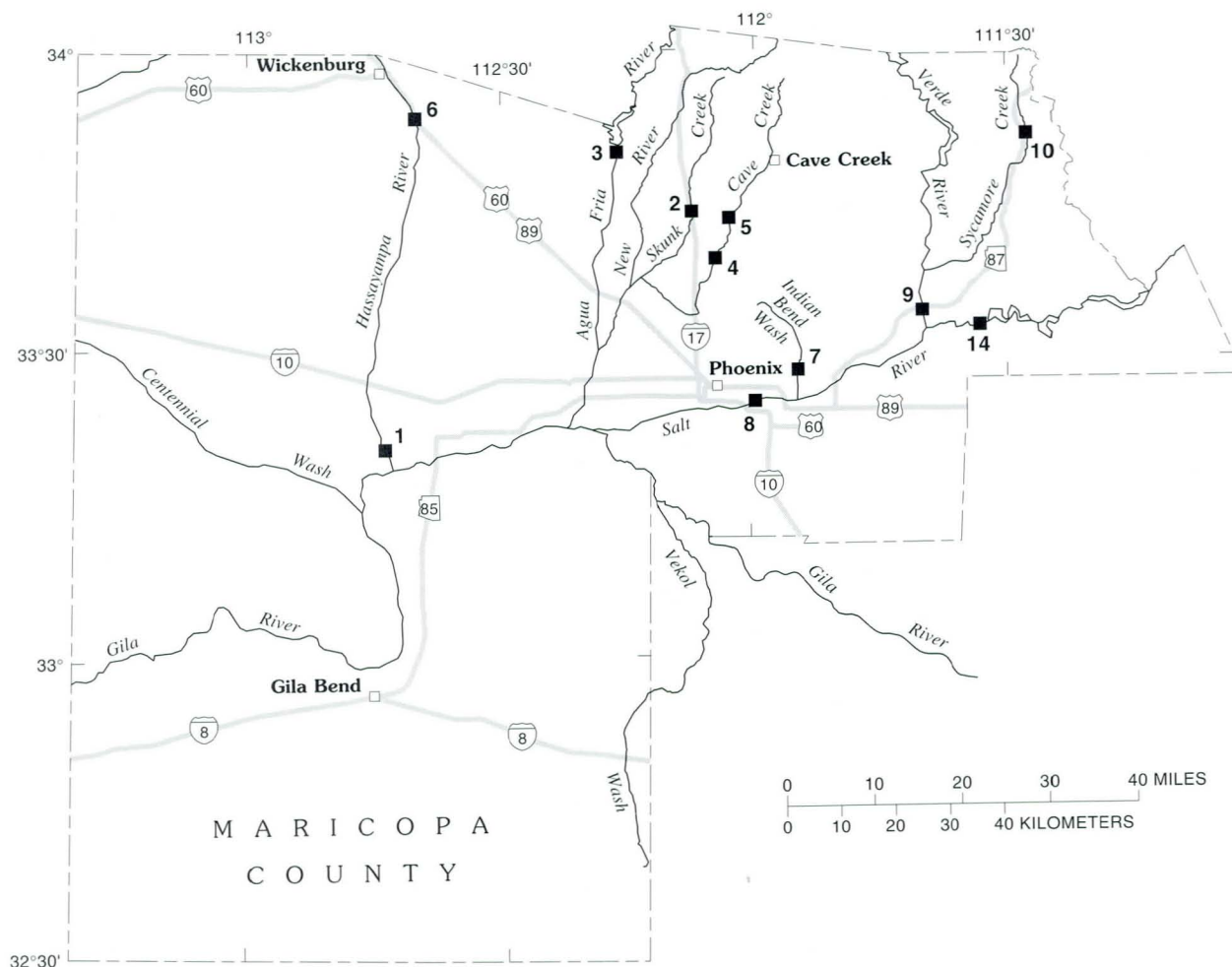
Acknowledgments

B.N. Aldridge, R.D. Jarrett, K.M. Nolan, U.S. Geological Survey; Joseph Tram and Ted Lehman, Flood Control District of Maricopa County; and H.W. Hjalmarson and B.W. Thomsen contributed significantly to the technical substance of this report. Personnel in the USGS, Tempe Office assisted with field and office work during the study.

DESCRIPTION OF STUDY AREA

The basin and range topography typical in most parts of Arizona is characterized by steep block-faulted mountains separated by gently sloping valleys. Dryland streams in the study area cover a wide variety of conditions ranging from unstable alluvial channels, generally stable channels of cobble to boulder-sized bed material, and extremely stable bedrock channels. Sand-dominated streambeds commonly are characterized by unstable boundary conditions, high sediment loads, and long periods of low or no flow punctuated by brief floods that increase discharge several orders of magnitude within minutes (Parker, 1995). Although generally more stable than sand channels, some gravel-dominated channels in Arizona also are *ephemeral* and subject to flooding for brief periods. Flash flooding and the general instability of channel beds of natural channels in Arizona can complicate the task of obtaining accurate flow-rate and channel-geometry measurements that represent conditions during peak discharge. Many stream channels in urban areas are relatively stable, manmade, and composed of either soil cement, concrete, riprap, grouted and wire enclosed rock, grass, or a combination of these materials (NBS Lowry Engineers and Planners and McLaughlin Water Engineers, Ltd., 1992).

The type, distribution, and density of riparian vegetation can vary in the study area. Vegetation types found in and along many streams in central Arizona include saltcedar, willow, cottonwood, mesquite, palo verde, and many brush and grass species. The spatial distribution and density of riparian vegetation mainly depend on water availability, characteristics of flow, and water quality. The few perennial stream channels in the study area have vegetation growing parallel to base-flow channels; whereas vegetation can be found growing randomly throughout the main channel of ephemeral streams. In addition, many effluent-



Base from U.S. Geological Survey digital data, 1:100,000, 1983
 Lambert Conformal Conic projection
 Standard parallels 29°30' and 45°30', central meridian -111°30'

EXPLANATION

- 8 ■ n-VERIFICATION STUDY SITE AND NUMBER
- 1. Hassayampa River near Arlington
- 2. Skunk Creek above Interstate 17
- 3. Agua Fria River below New Waddell Dam
- 4. Cave Creek above Deer Valley Road
- 5. Cave Creek below Cave Buttes Dam
- 6. Hassayampa River near Morristown
- 7. Indian Bend Wash above Curry Road
- 8. Salt River above Interstate 10
- 9. Verde River below Beeline Highway
- 10. West Fork Sycamore Creek near Sunflower
- 11. San Pedro River near Charleston (state map)
- 12. Santa Cruz River near Cortaro (state map)
- 13. Verde River near Paulden (state map)
- 14. Salt River below Stewart Mountain Dam



Figure 1. Study area and *n*-verification sites in Maricopa, Pima, Cochise, and Yavapai Counties, Arizona.

dominated streams in the study area (the lower Hassayampa River, for example) contain elevated nutrient levels resulting in increased vegetation growth. Vegetation conditions in dryland streams in Arizona can be the primary factor in determining total resistance to flow.

Mean annual precipitation in the study area ranges from about 7 in. near Phoenix to more than 30 in. in the adjacent mountain regions. Precipitation in Arizona occurs mainly during two seasons, summer (June through October) and winter (December through March), and rainfall is about equal in each period (Sabol and others, 1990). Summer precipitation normally is produced by convective thunderstorms. These storms are characterized by rainfall of high intensity and short duration, which usually cover small areas and may result in flash floods (Burkham, 1970). Winter precipitation normally is produced by regional frontal systems that are characterized by low-intensity rainfall of long duration that covers a large areal extent. These storms often result in substantial *runoff* volumes and create the potential for major floods. Dissipating tropical cyclones, a third storm type in Arizona, occur primarily in September and October (Hirschboeck, 1985; Webb and Betancourt, 1992). These storms can cause record floods of regional extent (Aldridge and Eychaner, 1984; Roeske and others, 1989). Dissipating tropical cyclones and winter-frontal storms can generate runoff volumes large enough to require discharge from reservoirs in Arizona. Twelve of the 37 verification measurements presented in this report were made during regulated release of waters from upstream reservoirs.

FIELD MEASUREMENTS FOR VERIFIED ROUGHNESS COEFFICIENTS

Site Selection

The verification-site locations were selected to meet, as closely as possible, criteria presented by Dalrymple and Benson (1967) for indirect measurement of discharge by the *slope-area method*, and guidelines presented by Jarrett and Petsch (1985) and Coon (1995) for required hydraulic conditions and reach characteristics for accurate *n*-verification measurements. The site conditions that relate to the specified criteria are summarized as follows.

1. Discharge mainly stayed within the channel banks, and extensive flow in flood plains or overbank areas did not exist. Also, the cross-sectional area of the channels was fully effective and carrying water in accordance with the computed *conveyance*.
2. For verification measurements in which a well-defined stage-discharge rating was used to obtain discharge, good water-surface elevation indicators or *high-water marks* were available to define the *water-surface profile*.
3. Channels generally were straight and uniform for some distance upstream and downstream from the reach. Severe channel bends and channel expansions were avoided.
4. Reaches were long enough to develop adequate fall according to at least one of the following criteria.
 - a. Length of the reach was equal to or greater than 75 times the mean depth.
 - b. Fall in the reach was equal to or greater than the *velocity head*.
 - c. Fall in the reach was equal to or greater than 0.50 ft.

Data Collection

Discharge used for each verification measurement was obtained by the current-meter method or determined from a well-defined stage-discharge relation (Rantz and others, 1982). For verification measurements in which discharge was measured with a current meter, the water surface was marked with flagging at the time the discharge measurement was taken. Adjustments were made to the elevation of the markers if the stage or water surface was rising or falling during the current-meter measurement (Coon, 1995). *Crest-stage gages* were installed at several sites to aid in obtaining accurate peak water-surface elevations at cross sections.

A transit-stadia survey was conducted for each reach either at the time of the current-meter measurement or soon after flow subsided to obtain accurate water-surface elevations and channel-geometry data. Standard surveying techniques were employed throughout the study and are described in detail by Benson and Dalrymple (1967). The information obtained from the surveys was used to plot the channel-geometry data and to determine the required channel-geometry components for computation of Manning's roughness coefficient.

Photographs of the reaches were taken to reflect the major flow-retarding elements in each of the channels. For most n -verification measurements, photographs of the sites were taken during and after the flow.

A *particle-size* distribution of the bed material was measured for most sites because energy losses can be influenced by the size of the bed material (Chow, 1959). For alluvial channels, frequency distributions of bed-material size were determined by sieve analysis. For bed material too large to sieve, such as gravel-bed channels, frequency distributions were obtained by measuring the intermediate axis of particles selected at random from the study reach (Wolman, 1954; Benson and Dalrymple, 1967). These data were used to determine the median grain-size diameter (d_{50}) for most of the study sites.

Suspended-sediment samples also were collected for many flows because large amounts of sediment can become entrained during flooding and may require substantial amounts of energy to transport the material. As indicated by several investigations (Chow, 1959; Costa, 1987; Jarrett, 1987; Glancy and Williams, 1994), suspended sediment can have discernible effects on the fluid characteristics by increasing its density and viscosity, which increase flow resistance and the verified n values. For most of the flows from which verification measurements were made, however, suspended sediment was considered *wash load* and probably had no effect on energy losses.

COMPUTATION OF REACH PROPERTIES AND ROUGHNESS COEFFICIENTS

The fundamental equations on which many open-channel hydraulic computations are based include the Manning's equation, the continuity equation, and the energy equation. The computer program NCALC, developed by Jarrett and Petsch (1985), is based primarily on these equations and was used to compute most of the values of Manning's n in this report. The equations are essentially identical for sites presented in this report for which verified n values were published previously. Manning's equation is defined as:

$$V = \frac{1.486}{n} R^{2/3} S_f^{1/2}, \quad (1)$$

where

- V = mean velocity of flow, in feet per second;
- R = *hydraulic radius*, in feet;
- S_f = energy gradient or friction slope, in feet per foot; and
- n = Manning's roughness coefficient.

The continuity equation is expressed as:

$$Q = AV, \quad (2)$$

where

- Q = discharge, in cubic feet per second;
- A = cross-sectional area of channel, in square feet; and
- V = mean velocity of flow, in feet per second.

Substitution of equation 1 for V in equation 2 yields a variation of Manning's equation often used to compute discharge in open channels:

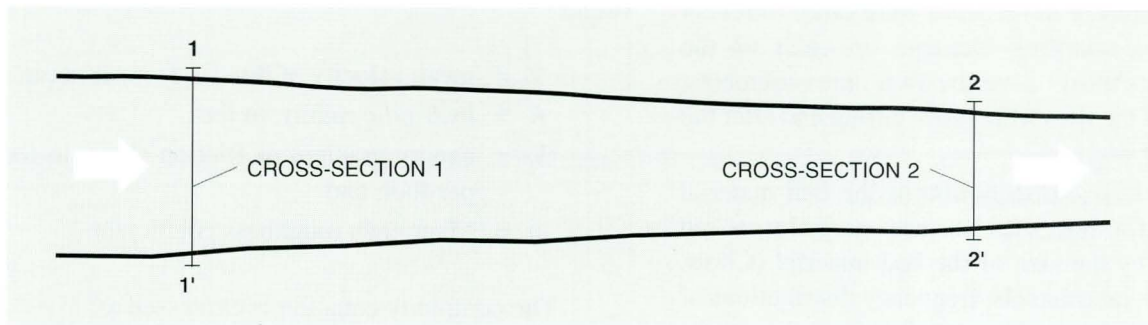
$$Q = \frac{1.486}{n} AR^{2/3} (S_f^{1/2}). \quad (3)$$

The equation was developed for conditions of *uniform flow* in which the water-surface slope and energy gradient are parallel to the streambed, and the area, depth, and velocity are constant throughout the reach. Equation 3 is assumed for nonuniform reaches if the energy gradient is modified to reflect only the losses resulting from boundary friction (Barnes, 1967). The energy equation for a nonuniform stream channel reach between sections 1 and 2 (fig. 2) is:

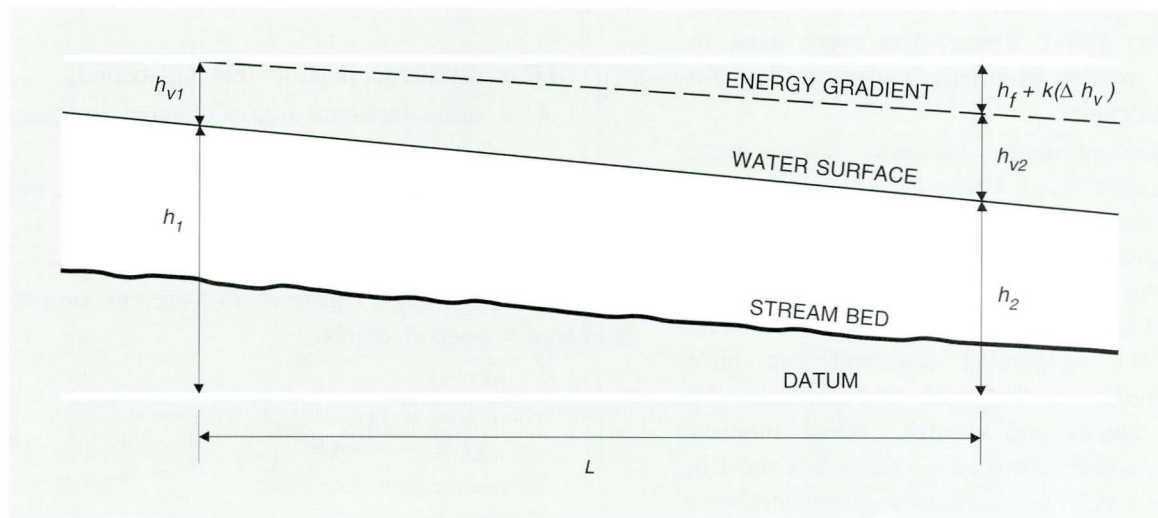
$$(h + h_v)_1 = (h + h_v)_2 + (h_f)_{1-2} + k(\Delta h_v)_{1-2}, \quad (4)$$

where

- h = elevation of the water surface at the respective section above a common datum, in feet;
- h_v = velocity head at the respective section equals $\alpha V^2/2g$, in feet;
- h_f = energy loss due to boundary friction in reach, in feet;



PLAN VIEW



PROFILE VIEW

Figure 2. Open-channel flow reach in plan and profile views (modified from Dalrymple and Benson, 1967, fig. 1).

Δh_v = upstream velocity head minus the downstream velocity head, in feet;

$k(\Delta h_v)$ = energy loss due to acceleration of velocity in a contracting reach, or deceleration of velocity in an expanding reach, in feet; and

k = coefficient assumed to be equal to 0 for contracting reaches, and 0.5 for expanding reaches (Barnes, 1967).

where

α = velocity-head coefficient; and

g = acceleration due to gravity, in feet per second per second.

In computing the values of n using this method, the value of α is always considered to be 1.00. This

requirement limits verification computations to unit channels that do not require segmenting or subdividing (Jarrett and Petsch, 1985). Although α can be much larger than 1.00 in natural channels (Jarrett, 1985), any resulting error in the computation of n is assumed to be minimal because the effect of α actually depends on the relative difference between the velocity-head coefficients from upstream and downstream cross sections rather than their actual magnitudes (Coon, 1995).

The friction slope, S_f , to be used in Manning's equation is defined as:

$$S_f = \frac{h_f}{L} = \frac{\Delta h + \Delta h_v - k(\Delta h_v)}{L}, \quad (5)$$

where

Δh = difference in water-surface elevation at the two sections, in feet; and

L = length of the reach (Dalrymple and Benson, 1967), in feet.

In Manning's equation, the quantity $(1.486/n)AR^{2/3}$ is called conveyance, K , and is computed for each cross section. The mean conveyance in the reach between any two sections is computed as the geometric mean of the conveyance of the two sections. The discharge equation in terms of conveyance is expressed as:

$$Q = (K_1 K_2 S_f)^{1/2}. \quad (6)$$

In this investigation, n is computed for each reach of known discharge, the water-surface profile, and the hydraulic properties of the reach as defined by the cross sections. The following equation was primarily used to compute n for this study and is applicable to a multisection reach of M cross sections, designated 1, 2, 3, ... $M - 1$, M :

$$n = \frac{1.486}{Q} \sqrt{\frac{\beta - [(k\Delta h_v)_{1-2} + (k\Delta h_v)_{2-3} + \dots + (k\Delta h_v)_{(M-1)-M}]}{\frac{L_{1-2}}{Z_1 Z_2} + \frac{L_{2-3}}{Z_2 Z_3} + \dots + \frac{L_{(M-1)-M}}{Z_{(M-1)} Z_M}}}, \quad (7)$$

where

$$\beta = (h + h_v)_1 - (h + h_v)_2$$

$$Z = AR^{2/3} \text{ (Barnes, 1967).}$$

ASSUMPTIONS AND LIMITATIONS

Although efforts were made to strictly follow the site-selection and data-collection criteria, assumptions were required for some of the verification measurements as channel and hydraulic conditions were not always ideal. The main sources of potential errors in calculations of roughness coefficients for dryland channels include changing boundary and vegetation conditions, discharge measurement uncertainties, and changing *bedforms*. The verification measurements presented in this report are qualified or rated on the basis of these four factors. Additionally,

transfer of results presented in this report to similar sites may be limited because of uncertainties associated with extrapolating n values obtained for relatively low flows to flows of greater magnitudes.

The accuracy of verification measurements presented in this report is rated as either good, fair, or estimated. These categories correspond to potential percent errors of less than 10, 15, or 20 percent, respectively. Verification measurements with an error of greater than 20 percent were not considered for publication in this report.

Changing Boundary Conditions

In the performance of hydraulic computations of flow in streams that are dominated by sand-sized material, constant-bed geometry often is assumed to persist throughout flow events. Several investigators indicate sand-dominated streams do not *scour* appreciably in a uniform segment of river channel (Culbertson and Dawdy, 1964; Benson and Dalrymple, 1967). Although most of the channel segments studied for this report are uniform, scour of substrate material during the rise and peak of the flow and subsequent backfill during the flow recession requires consideration. Accuracy ratings for the n -verification measurements made in sand-dominated streams where changing boundary conditions are possible, thus, were downgraded according to the potential amount of scour and fill.

Although the channel-geometry changes may not be as significant as with sand-dominated streams, flood-stage flows in gravel-bed streams also may mobilize and transport bed material. Hydraulic components measured for the verification measurements made in gravel-bed streams, however, probably were not large enough to cause a considerable change in boundary conditions resulting from substantial movement of the bed material.

Changing Vegetation Conditions

In arid and semiarid environments, vegetation commonly grows throughout the main channel of dryland streams. The vegetation can significantly impede flow and result in large increases in roughness coefficients, as suggested by several past studies (Aldridge and Garrett, 1973; Thomsen and Hjalmarsen, 1991). The force and power of flows,

however, can lay over and even remove vegetation, thereby decreasing channel roughness and increasing channel conveyance (Burkham, 1976; Phillips and Hjalmarson, 1994).

The flow-induced changes in vegetation conditions are commonly assumed to occur before peak flow, and postflow vegetation conditions are assumed to reflect the roughness conditions when the high-water marks were formed. However, for certain conditions, this may be an erroneous assumption. Water-level indicators in vegetated channels surveyed following flows may not actually represent the water-surface during the time of peak discharge. The force and power of flow may be large enough to substantially affect (lay over or remove) vegetation just before peak flow and thus cause the water surface to drop dramatically because of the decrease in flow resistance. This phenomenon may result in a lower water-surface elevation during peak discharge than that suggested by the high-water indicators. This phenomenon may have occurred for the flow of February 9, 1993, at Hassayampa River near Arlington. The high-water indicators may actually have been deposited before and not during peak discharge. This verification measurement, therefore, was rated as estimated. Vegetation documented during and shortly after flow at the other study sites appeared to have little or no change compared to preflow conditions.

Uncertainties of Discharge Measurements

The accuracy of the verified n values directly depends on the precision of the measured discharge. As mentioned previously, discharge was determined either by a current-meter measurement or from a well-defined stage-discharge relation. Current-meter measurements made by the USGS are rated as excellent, good, fair, or poor depending on factors that include the number of subsections in the measurement, stability of the channel, and accuracy of the equipment (Rantz and others, 1982). These ratings correspond to possible errors of less than 2, 5, 8, or greater than 8 percent of the actual discharge, respectively. Errors for discharges determined from a well-defined and stable stage-discharge relation are assumed to be less than 10 percent. Discharge accuracy is considered when determining the overall accuracy rating for each of the n -verification measurements.

Flow Depth and Magnitude

In the absence of bank vegetation and other obstructions, the roughness for low flows in a uniform gravel-bed stream generally decreases with increasing depth of flow. As flow approaches bank-full stage, however, roughness may asymptotically approach a constant value, as shown by several previous investigations (Limerinos, 1970; Bray, 1979; Sargent, 1979; Griffiths, 1981; Jarrett, 1985; Blodgett, 1986; Hicks and Mason, 1991; Coon, 1995).

The basic roughness coefficient for these streams should not vary greatly with depth of flow if the relative roughness is greater than about 5 (Benson and Dalrymple, 1967). Many of the verification measurements presented in this report, however, have values of relative roughness that are less than or close to 5, and the variation in Manning's roughness coefficient with depth is apparent.

For many previously published n -verification manuals and for this report, verified n values are obtained from flow discharge data that may not result in a reliable value for studies requiring estimates of roughness coefficients for design purposes. Design discharge typically is determined on the basis of the estimated flood having a particular recurrence interval (100-year flood, for example). Roughness-coefficient verification studies, however, generally are limited to flows that may not exceed even the 5-year flood (Wahl, 1994). This limitation is caused by the relatively short duration of n -value studies and the difficult logistics involved in making n -verification measurements during floodflows. Roughness coefficients can be extrapolated to the design discharges using relations between hydraulic components, such as R and n ; however, large uncertainties may be associated with these extrapolations (Wahl, 1994). Water-resource managers and engineers need to be aware of these limitations when using this and other n -verification manuals.

For sand-dominated streams, the amount of variance in Manning's n with depth is much more difficult to describe and quantify compared to gravel-bed streams. Roughness in sand-dominated streams depends not only on grain size but also on flow regime and type of bedform manifested. As indicated by the verification measurements made at the Hassayampa River near Morristown, the relation of Manning's n to flow depth (hydraulic radius) can actually be the inverse of the relation for gravel-bed streams (fig. 9C, see p. 37).

Changing Bed Forms

Resistance to flow can vary greatly in sand channels because the bed material is unstable and may take on different configurations or bedforms throughout a single period of flow. The type of bedform is a function of many components that include flow velocity, grain size, shear stress, temperature, and other variables (Aldridge and Garrett, 1973). The magnitude of Manning's roughness coefficient may relate directly to the type of bed form that is manifested, which makes accurate assessment of n values in sand channels a difficult and complex procedure.

On the basis of data obtained with the aid of laboratory flumes, Simons and Richardson (1966) proposed that median grain size and *stream power* can be used to determine the *flow regime* and the type of bed form that will develop in sand channels. Stream power is determined from the equation:

$$SP = 62RSV, \quad (8)$$

where

- SP = stream power, in foot-pounds per second per square foot;
- 62 = specific weight of water, in pounds per cubic foot;

R = hydraulic radius, in feet;

S = water-surface slope, in feet per foot; and

V = mean velocity, in feet per second.

Other investigators have modified results presented by Simons and Richardson (1966, p. J24, fig. 28) in order to develop practical criteria for determining Manning's roughness coefficient in sand-dominated streams (Benson and Dalrymple, 1967). As shown in figure 3, flow in sand channels can be classified as either lower-regime or upper-regime flow separated by a transition zone.

In lower-regime flow (fig. 3), the bed may have a plane surface with little or no movement of sand or small uniform waves (ripples), or large irregular waves (dunes) that are formed by sediment moving downstream. Water-surface undulations manifested in lower-regime flow generally are out of phase with the bed surface. The fact that the water surface is out of phase with the bed surface is a positive indication that the flow is tranquil or *subcritical* (*Froude number* < 1 ; Simons and Richardson, 1966, p. J9).

The bed configuration in the transition zone can be erratic and may range from that typical of the lower-flow regime to that typical of the upper-flow regime depending mainly on antecedent conditions (Simons and Richardson, 1966, p. J11). Resistance to flow and sediment transport also have the same variability as the

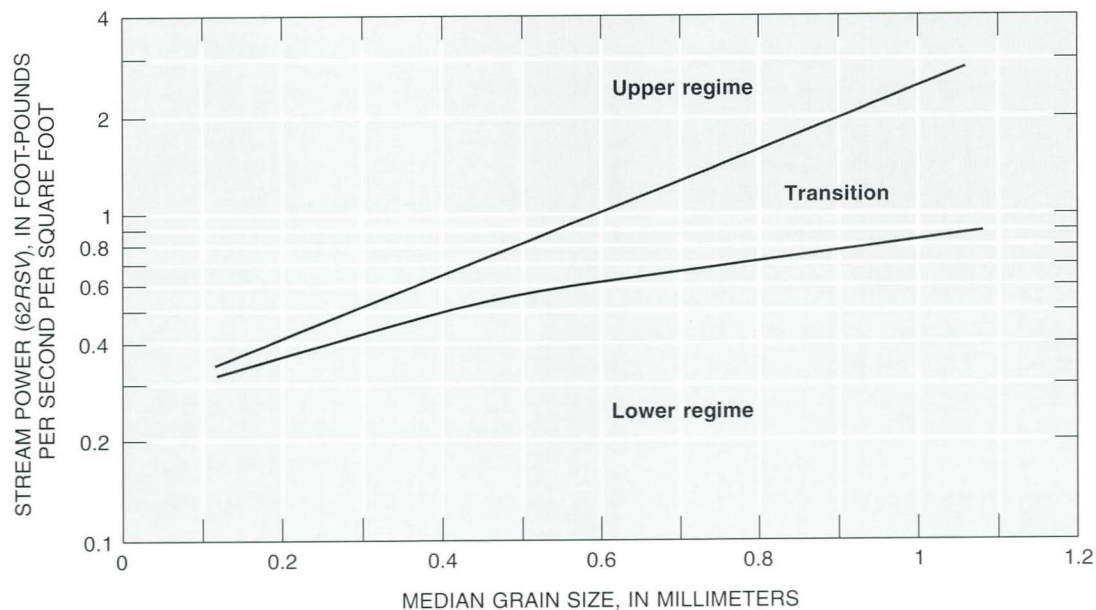


Figure 3. Relation of stream power and median grain size to form of bed roughness. (Modified from Benson and Dalrymple, 1967.)

bed configuration in the transition zone. A discontinuity in stage-discharge relations may occur at the transition between lower-regime and upper-regime flow (Culbertson and Dawdy, 1964).

In upper-regime flow, the bed may have a plane surface or it may have long smooth sand formations in phase with the surface waves (Leopold and others, 1964, and Karim, 1995). These waves are known as standing waves or antidunes where, during upper-regime flow conditions, roughness can be much larger than for plane-bed conditions (Simons and Richardson, 1966). As the size of the antidunes grow, the water-surface slope on the upstream side of the waves becomes steeper, and the antidune may eventually collapse. Following collapse of antidunes, the flow generally will shift back to plane-bed conditions. If the antidunes do not collapse, however, resistance to flow can be about the same as for plane-bed conditions. When antidune formation occurs in upper-regime flow and the water and bed surfaces are in phase, the flow is rapid or *supercritical* (Froude number > 1 ; Simons and Richardson, 1966, p. J9).

On the basis of criteria presented by Simons and Richardson (1966) and Benson and Dalrymple (1967), upper-regime flow conditions were exhibited for all verification measurements that were made in sand-dominated streams (sites 6 and 12, fig. 1). In addition to the uncertainties associated with changing boundary conditions for sand channels, the possibility of intermittent antidune formation and subsequent collapse of the antidunes could result in intermittent surging of the water surface along the banks of the channel. The surges may result in super elevation of high-water marks that normally are surveyed when the flow subsides. This phenomenon occurred on March 6, 1995, about 1,000 ft upstream from the USGS streamflow-gaging station at Hassayampa River near Morristown. Discharge was about 9,000 ft³/s, and the authors witnessed trains of large antidunes (about 6 ft from trough to crest) that were forming and collapsing at regular intervals. The collapse resulted in a surge of the water surface along the channel banks of more than 1 ft in elevation. Following collapse of the antidunes, the flow would return to plane-bed conditions until another train of antidunes formed.

Intermittent surging of the water surface causing super elevation of the high-water marks along the channel banks complicates the task of obtaining accurate and representative water-surface elevations for *n*-verification measurements made in sand

channels, and may introduce errors into the hydraulic computations. The accuracy of the verification measurements that were made in sand channels, therefore, was qualified according to the potential amount of error resulting from difficulties in obtaining accurate water-surface elevations and channel-boundary configuration.

PRESENTATION OF VERIFIED ROUGHNESS COEFFICIENTS

A total of 37 verified *n* values are presented for discharge measurements at 14 separate stream locations in Arizona. Data for 4 of the 14 sites are from Aldridge and Garrett (1973), and data for Salt River below Stewart Mountain Dam is from Barnes (1967). General information is presented on the location of the site, drainage area of the stream, date and discharge of each measurement, computed roughness coefficients for the reach, median size of bed material (if available), concentration of suspended sediment (if available), and a general description of the channel. Tabulated data presented are from field surveys and hydraulic computations. These data include average values for area, top width, hydraulic radius, mean velocity, and Froude numbers. The total reach length and fall in water surface also are included. Plan-view sketches are presented to show the location of the cross sections and general shape of the channel. A representative cross section is illustrated with water-surface elevations shown for each flow. Information for two or more discharges is available for most sites to show changes in roughness with depth. The changes are demonstrated by plots of Manning's *n* and hydraulic radius. The assumption is made that hydraulic radius closely approximates mean flow depth for each of the sites. Color photographs are presented for each study reach to be used as a comparison standard to aid transfer of results to sites with similar channel and hydraulic characteristics. Selected photographs also show flow conditions at the time of the measurement. The average water level corresponding to the measured flow is indicated in certain photographs by a horizontal rod. The frame of the square grid (painted orange) in several photographs has an outside dimension of 1.5 ft and an internal grid spacing of 1 in.

Hassayampa River near Arlington

Reach location: Latitude 33°20'50", longitude 112°20'30". Reach begins about 1,000 ft downstream from streamflow-gaging station 09517000, Hassayampa River near Arlington.

Drainage area: 1,471 mi².

Bed-material size: Low-flow channel = 87 mm (0.28 ft); Overbank area = 0.53 mm (0.0017 ft).

Channel description: The channel is straight and uniform throughout the study reach, and cross sections are trapezoidal in shape. The low-flow channel is approximately 25 ft wide, and the bed consists primarily of cobble-sized material. Overbanks are mainly composed of coarse sand and small gravel-sized material. Grass and small brush grow on the overbanks and appear to have kept the overbank-bed material fairly stable during the flow of February 9, 1993. The site is in a section of the river that is considered *intermittent*. The nearly constant low flows are dominated by irrigation return flow.

Remarks: Following the flow of February 9, 1993, the grass was in a prone position and the brush was bent in the direction of flow. The timing of the vegetation changes is not known. A thin layer of fine sand appears on the overbanks that probably was deposited following the peak. No significant amount of scour or fill was apparent in the reach during any of the flows recorded. For the three low-flow verifications, water mainly consisted of irrigation return flow and appeared to be clear [suspended sediment was 172.8 mg/L for a sample taken during a low-flow period (June 20, 1995) and was considered as wash load]. Suspended-sediment concentrations can exceed 35,000 mg/L for flows that result from runoff in upstream basins.

Table 1. Flow data and computed roughness coefficients, Hassayampa River near Arlington

Date of flow	Discharge, in cubic feet per second	Roughness coefficient	Rating
02-09-93	5,580	0.027	Estimate
07-06-94	80.5	.034	Good
06-16-94	45.5	.036	Good
06-15-94	17.0	.036	Good

Table 2. Average-reach properties, Hassayampa River near Arlington

Date	Area, in square feet	Top width, in feet	Hydraulic radius, in feet	Mean velocity, in feet per second	Froude number	Total length, in feet	Total fall, in feet	Water-surface slope
02-09-93	725	174	4.12	7.75	0.67	715	2.44	0.0034
07-06-94	24.8	18.2	1.29	3.26	.49	571	2.22	.0039
06-16-94	17.5	17.3	.97	2.61	.46	571	2.22	.0039
06-15-94	9.29	15.7	.58	1.86	.43	571	2.25	.0039

Hassayampa River near Arlington—Continued

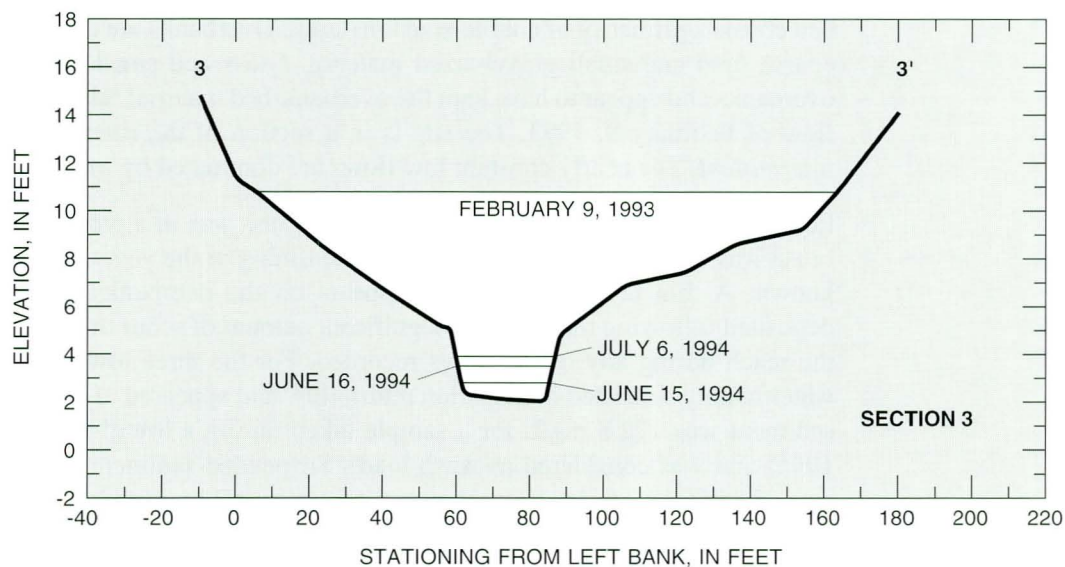


Figure 4A. Cross-section 3, Hassayampa River near Arlington.

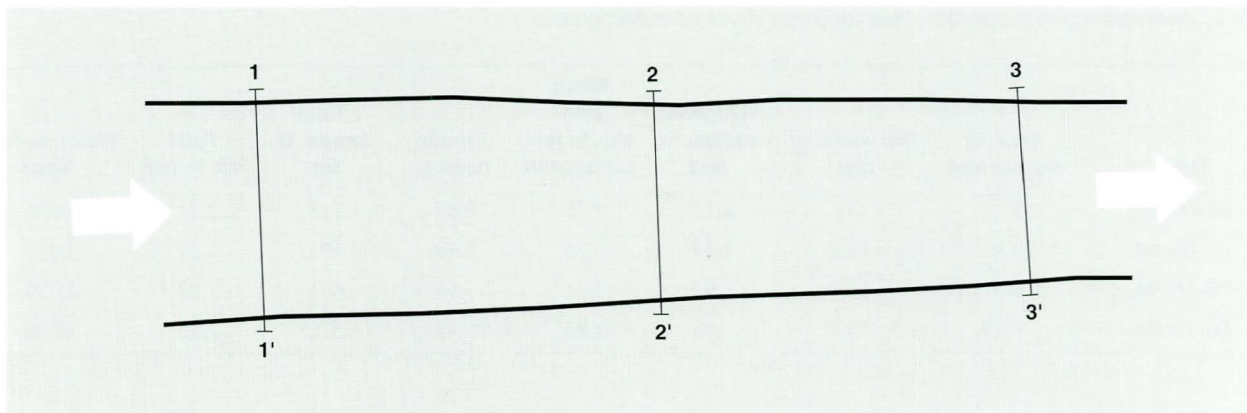


Figure 4B. Plan view, Hassayampa River near Arlington.

Hassayampa River near Arlington—Continued

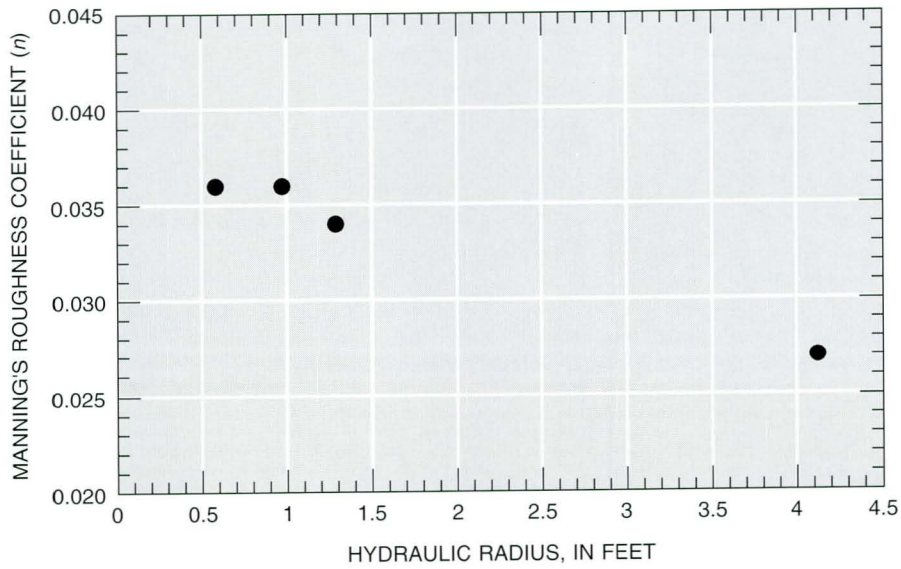


Figure 4C. Manning's n and hydraulic radius, Hassayampa River near Arlington.

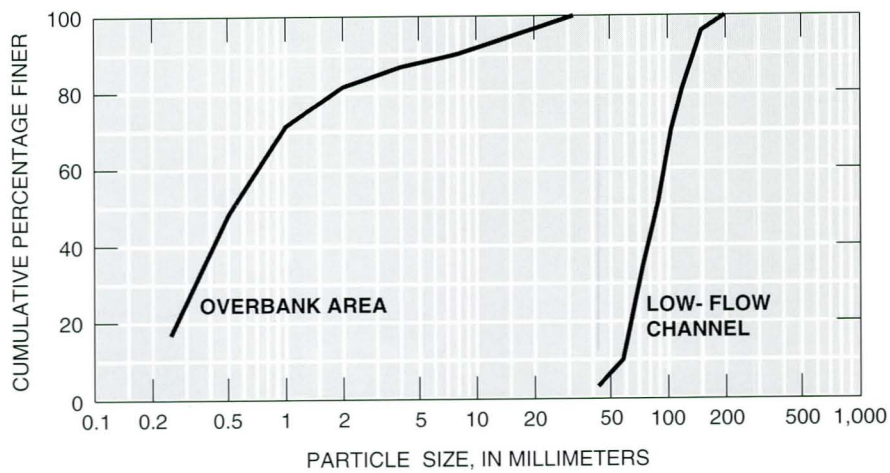


Figure 4D. Particle-size distribution for bed material, Hassayampa River near Arlington.

Hassayampa River near Arlington—Continued



Figure 4E. View of typical bed material for low-flow channel, Hassayampa River near Arlington. The square grid (painted orange) has an outside dimension of 1.5 feet and an internal grid spacing of 1 inch.



Figure 4F. View from right bank showing a current-meter measurement made in the low-flow channel, Hassayampa River near Arlington.

Hassayampa River near Arlington—Continued



Figure 4G. View looking upstream from midreach of low-flow channel, Hassayampa River near Arlington.



Figure 4H. View from right bank and midreach looking downstream following flow of February 9, 1993, Hassayampa River near Arlington.

Skunk Creek above Interstate 17

<u>Reach location:</u>	Latitude 33°43'56", longitude 112°06'57". Reach begins about 1,000 ft upstream from streamflow-gaging station 09513860, Skunk Creek near Phoenix.
<u>Drainage area:</u>	64.9 mi ² .
<u>Bed-material size:</u>	$d_{50} = 88$ mm (0.29 ft).
<u>Channel description:</u>	The constructed channel is fairly uniform, and bed material is mainly cobble-sized clasts partially surrounded by finer silt- and sand-sized material. Vegetation consists of brush of moderate spatial density and grows randomly throughout the channel. The stream is ephemeral and flow is unregulated.
<u>Remarks:</u>	Nine verification measurements were made for several stages of vegetation growth within the study reach. The first measurement on March 1, 1991, was made when the vegetation was fully grown (average height, about 5 ft). Verifications 2–5 were made after the reach had been artificially maintained and cleared of all the vegetation. Verifications 6 and 7 were made during a period of regrowth (average height was about 2 ft). Verifications 8 and 9 were made after the vegetation was again fully grown (average height, about 5 ft). Although flow magnitude was greater for the postmaintenance measurement of January 26, 1995, compared to the premaintenance measurement of March 1, 1991, the water-surface elevations were lower (fig. 5A). The vegetation was little affected by flow for all measurements. According to survey data, channel geometry and bed conditions did not appear to change significantly after clearing of the vegetation. For the flow of September 28, 1995, the suspended-sediment concentration was 198.8 mg/L and was considered wash load. Suspended-sediment concentrations probably did not exceed wash-load conditions for any of the verification measurements.

Table 3. Flow data and computed roughness coefficients, Skunk Creek above Interstate 17

Condition of reach	Date of flow	Discharge, in cubic feet per second	Roughness coefficient	Rating
Premaintenance of vegetation	03-01-91	618	0.048	Good
Postmaintenance of vegetation	01-26-95	723	.031	Fair
Do.	01-05-95	393	.034	Fair
Do.	01-26-95	180	.035	Good
Do.	01-05-95	168	.037	Good
Partial regrowth of vegetation	09-28-95	822	.035	Fair
Do.	11-01-95	500	.039	Fair
Regrowth of vegetation	08-14-96	403	.048	Fair
Do.	09-02-96	215	.052	Fair

Skunk Creek above Interstate 17—Continued

Table 4. Average-reach properties, Skunk Creek above Interstate 17

Date	Area, in square feet	Top width, in feet	Hydraulic radius, in feet	Mean velocity, in feet per second	Froude number	Total length, in feet	Total fall, in feet	Water-surface slope
03-01-91	176	88.3	1.97	3.52	0.44	658	3.61	0.0055
01-26-95	140	81.8	1.71	5.18	.70	677	3.93	.0058
01-05-95	97.5	76.1	1.28	4.06	.63	677	4.19	.0062
01-26-95	63.2	70.8	.90	2.91	.55	677	3.92	.0058
01-05-95	57.6	69.6	.83	3.07	.61	677	4.55	.0067
09-28-95	162	84.2	1.91	5.09	.64	677	4.18	.0062
11-01-95	130	80.7	1.60	3.16	.54	677	3.71	.0055
08-14-96	126	78.6	1.60	3.24	.45	677	3.54	.0052
09-02-96	88.1	73.5	1.20	2.48	.40	677	3.67	.0054

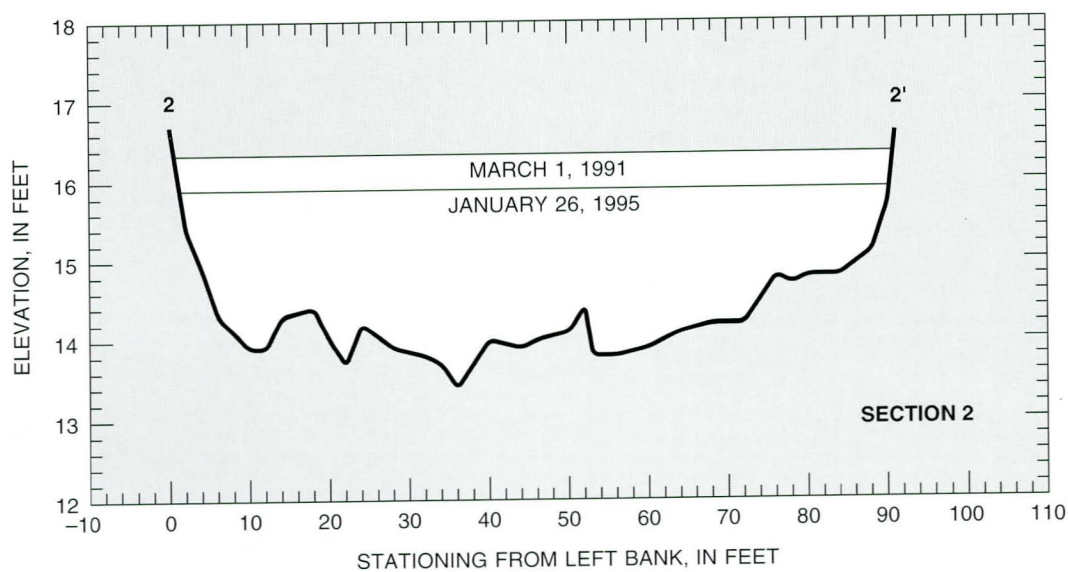


Figure 5A. Cross-section 2, Skunk Creek above Interstate 17.

Skunk Creek above Interstate 17—Continued

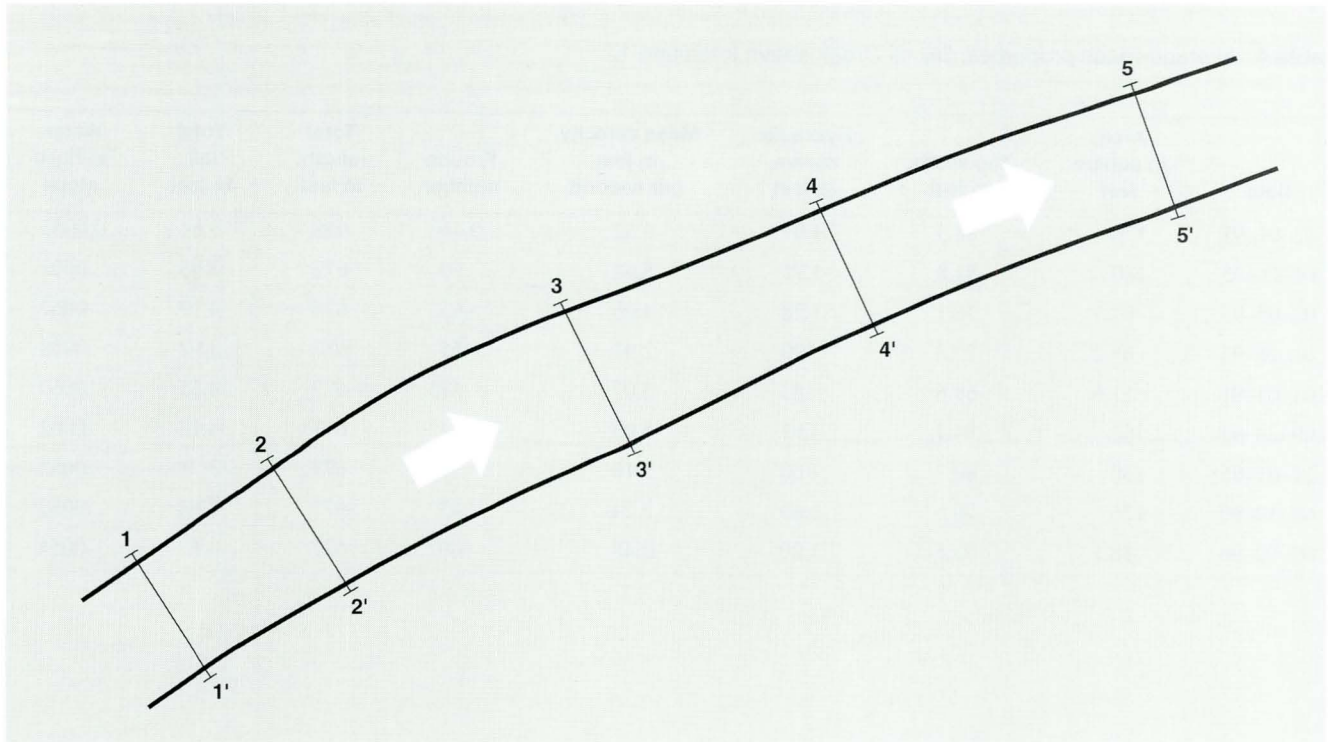


Figure 5B. Plan view, Skunk Creek above Interstate 17.

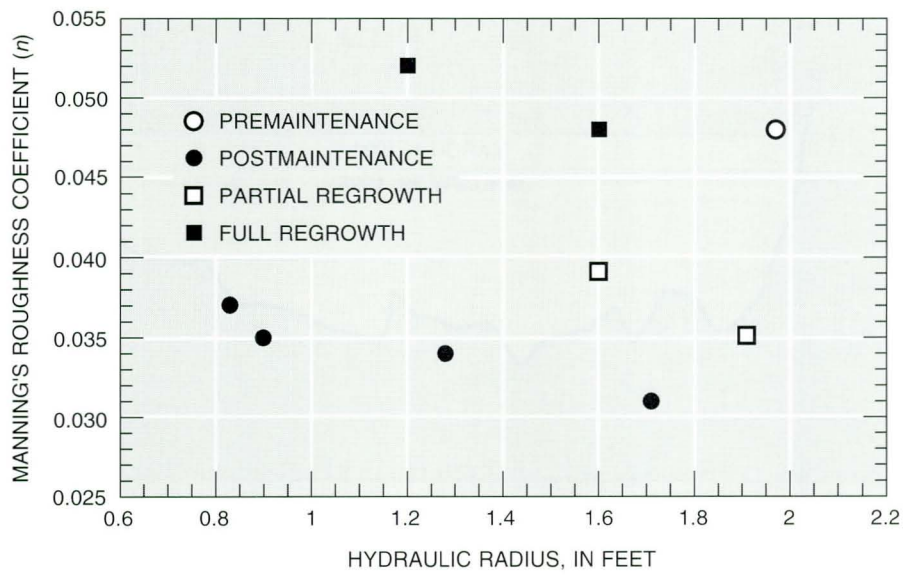


Figure 5C. Manning's n and hydraulic radius, Skunk Creek above Interstate 17.

Skunk Creek above Interstate 17—Continued

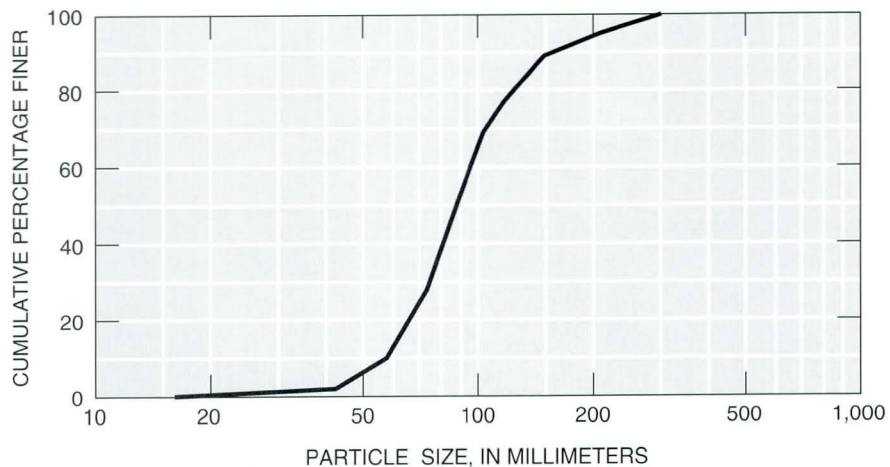


Figure 5D. Particle-size distribution for bed material, Skunk Creek above Interstate 17.



Figure 5E. View of typical bed material in channel reach, Skunk Creek above Interstate 17. The square grid (painted orange) has an outside dimension of 1.5 feet and an internal grid spacing of 1 inch (painted green).

Skunk Creek above Interstate 17—Continued



Figure 5F. View from left bank and bottom of reach looking upstream during flow of March 1, 1991, Skunk Creek above Interstate 17.



Figure 5G. View from midchannel looking upstream following flow of March 1, 1991, Skunk Creek above Interstate 17. Vegetation was little affected by flow.

Skunk Creek above Interstate 17—Continued



Figure 5H. View from midchannel and bottom of reach looking upstream following artificial maintenance of the channel vegetation, May 23, 1994, Skunk Creek above Interstate 17. The crest-stage gages were installed in surveyed cross sections to aid in obtaining accurate water-surface elevations and profiles.



Figure 5I. View from midchannel looking upstream during flow of January 5, 1995, Skunk Creek above Interstate 17.

Skunk Creek above Interstate 17—Continued



Figure 5J. View from midchannel looking upstream at regrowth of vegetation, Skunk Creek above Interstate 17. The brush is about 2 feet in height and was little affected by flow.

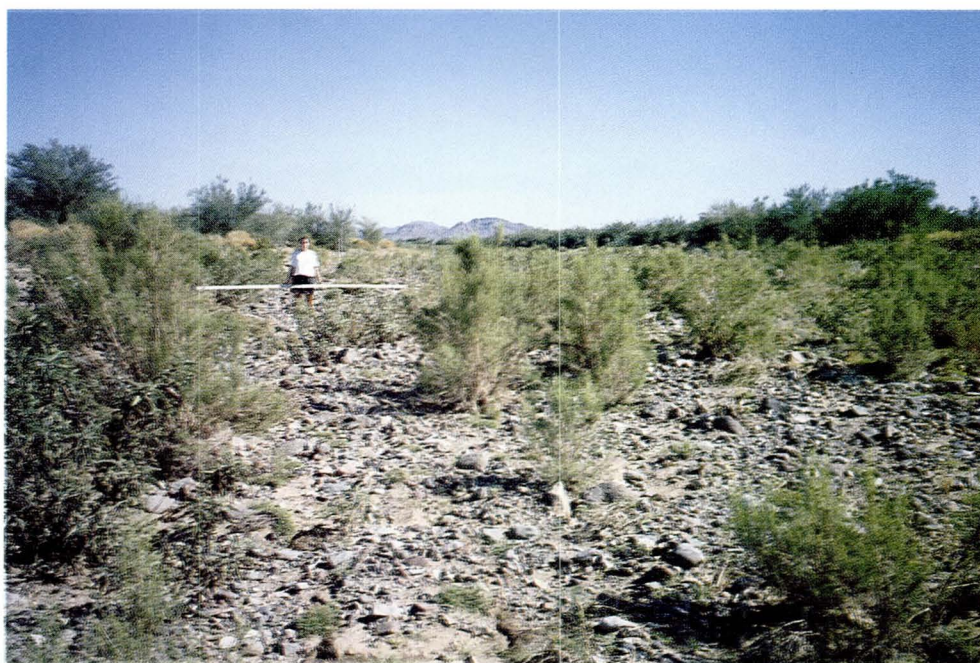


Figure 5K. View from midchannel looking upstream following flow of August 14, 1996, Skunk Creek above interstate 17.

Agua Fria River below New Waddell Dam

Reach location: Latitude 33°50'03", longitude 112°16'33". The reach begins about 3,000 ft below New Waddell Dam.

Drainage area: 1,459 mi².

Bed-material size: $d_{50} = 82$ mm (0.27 ft).

Channel description: The channel generally is straight throughout the reach. The reach narrows considerably from cross-sections 1 to 4. A small ridge is along the middle of the reach with poorly defined low-flow channels on either side. Outcroppings of bedrock are near the *left bank* of cross-sections 3 and 4. Saltcedar ranges in height from about 5–10 ft in the reach and grows mostly along the middle ridge. The channel bed consists mainly of small- to medium-sized cobbles. The stream was perennial before construction of Waddell Dam.

Remarks: Following the recorded flow, the saltcedar appeared to be little affected by the flow. A small nonconveying area is at the right bank of cross-section 4 (investigation of the debris deposited by the flow indicated a zone of separation and a *backwater* area) that was not included in the verification computations.

Table 5. Flow data and computed roughness coefficient, Agua Fria River below New Waddell Dam

Date of flow	Discharge, in cubic feet per second	Roughness coefficient	Rated
02-09-93	9,000	0.042	Fair

Table 6. Average-reach properties, Agua Fria River below New Waddell Dam

Date	Area, in square feet	Top width, in feet	Hydraulic radius, in feet	Mean velocity, in feet per second	Froude number	Total length, in feet	Total fall, in feet	Water-surface slope
02-09-93	1,978	418	4.78	4.6	0.37	447	1.11	0.0025

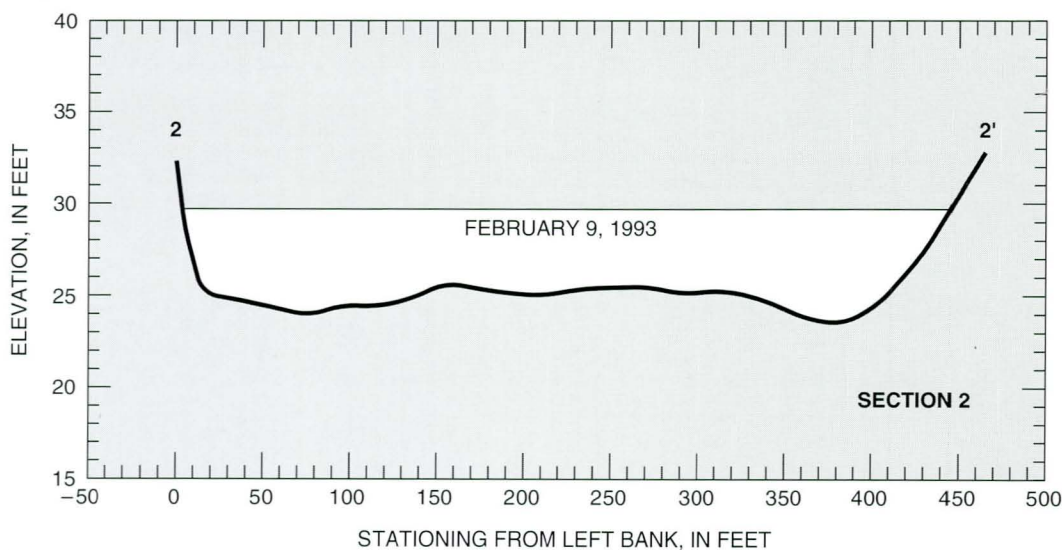


Figure 6A. Cross-section 2, Agua Fria River below New Waddell Dam.

Agua Fria River below New Waddell Dam—Continued

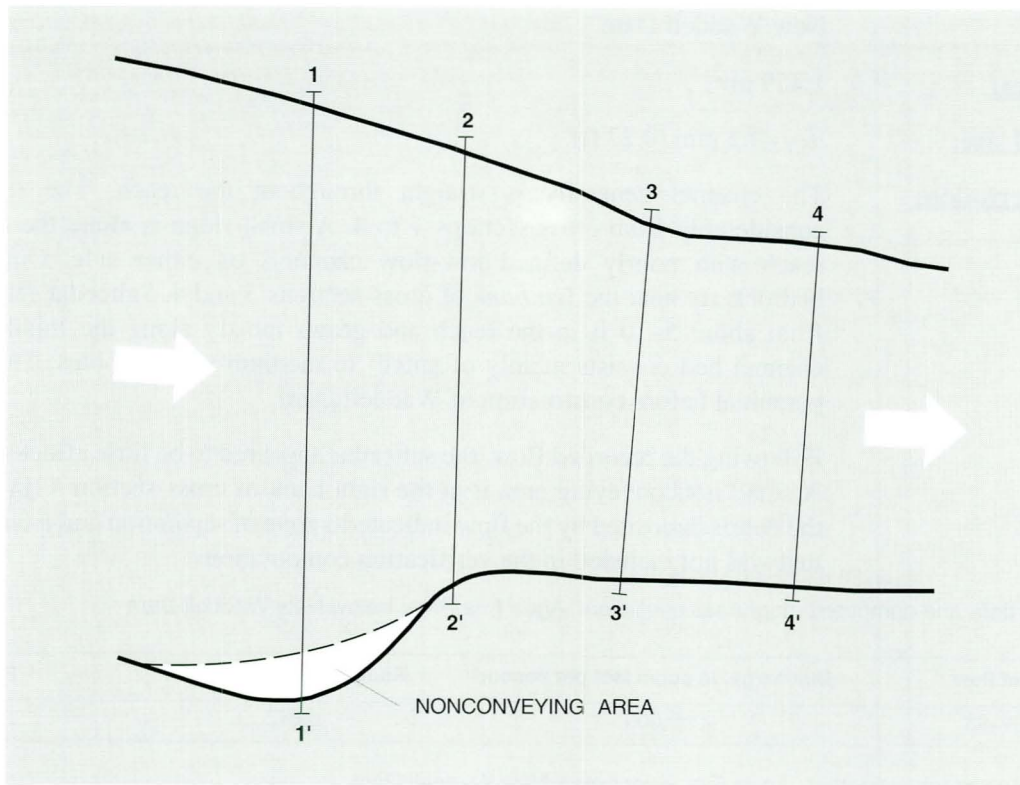


Figure 6B. Plan view, Agua Fria River below New Waddell Dam.

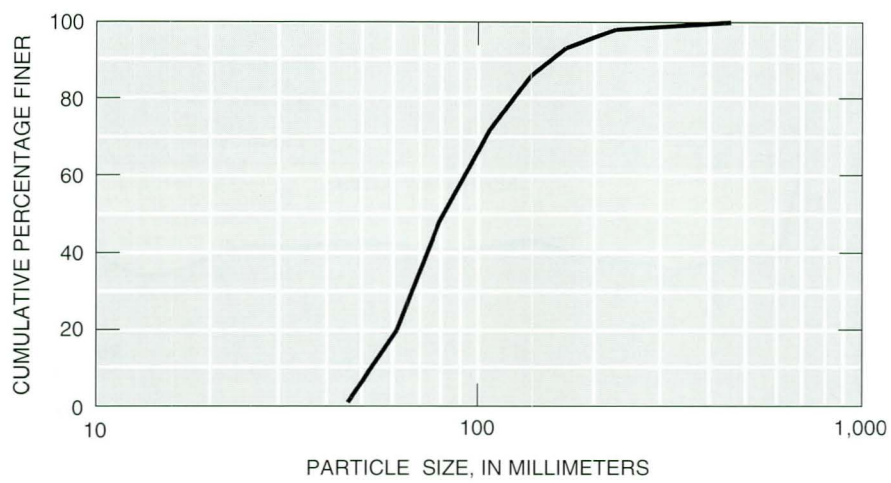


Figure 6C. Particle-size distribution for bed material, Agua Fria River below New Waddell Dam.

Agua Fria River below New Waddell Dam—Continued



Figure 6D. View of typical bed material in channel reach, Agua Fria River below New Waddell Dam. The square grid (painted orange) has an outside dimension of 1.5 feet and an internal grid spacing of 1 inch.

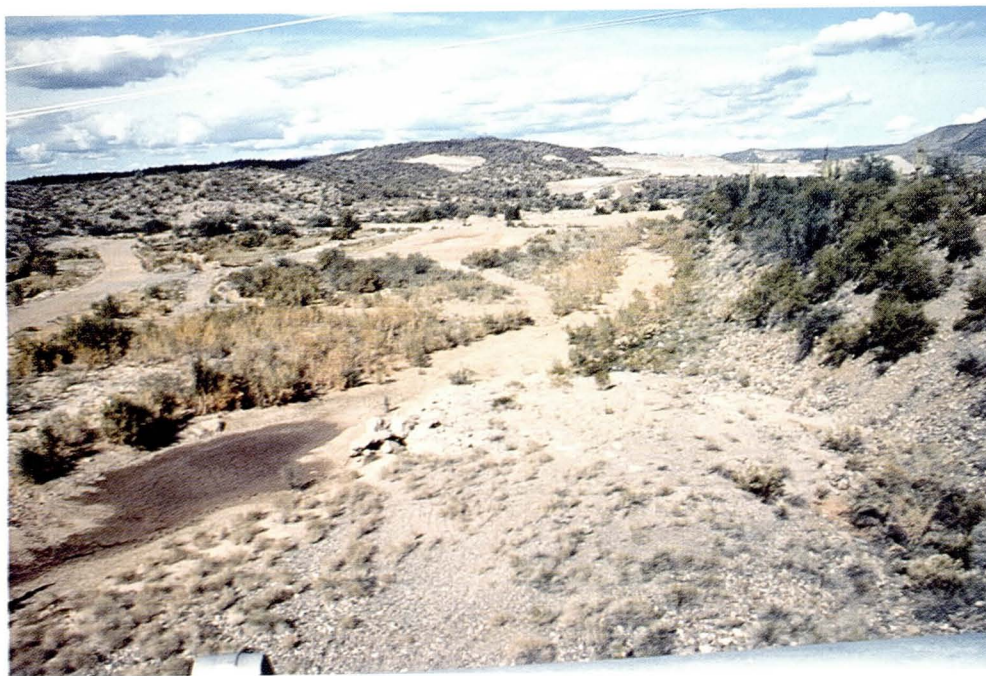


Figure 6E. View from bottom of reach looking upstream on March 10, 1993, Agua Fria River below New Waddell Dam.

Agua Fria River below New Waddell Dam—Continued



Figure 6F. View from midchannel looking toward left bank of cross-section 4, Agua Fria River below New Waddell Dam.



Figure 6G. View from midchannel in cross-section 2 of typical vegetation in the reach, Agua Fria River below New Waddell Dam. Length of measuring rod, 6 feet. Photograph taken at time of survey on May 19, 1993.

Cave Creek above Deer Valley Road

Reach location: Latitude 33°41'13", longitude 112°03'32". Reach ends about 1,000 ft above Deer Valley Road.

Bed-material size: $d_{50} = 91$ mm (0.30 ft).

Channel description: The channel is straight and uniform throughout the reach. The cross sections are trapezoidal in shape, and vegetation of moderate spatial density is along the banks. Bed material found in the reach is mostly small- to medium-sized cobbles. The stream is ephemeral, and flow is regulated by Cave Buttes Dam.

Remarks: The bank vegetation probably had a discernible effect on total flow retardance for the two larger flows. This bank vegetation was little affected by flows. The suspended-sediment concentration was 228 mg/L for the flow on January 9, 1995, and is assumed to be indicative of suspended-sediment concentrations for all three flows. The suspended sediment was regarded as wash load and was considered to have negligible effects on n values.

Table 7. Flow data and computed roughness coefficients, Cave Creek above Deer Valley Road

Date of flow	Discharge, in cubic feet per second	Roughness coefficient	Rating
01-06-95	297	0.033	Estimate
01-09-95	193	.033	Good
01-10-95	39	.034	Good

Table 8. Average-reach properties, Cave Creek above Deer Valley Road

Date	Area, in square feet	Top width, in feet	Hydraulic radius, in feet	Mean velocity, in feet per second	Froude number	Total length, in feet	Total fall, in feet	Water-surface slope
01-06-95	58.2	22.8	2.33	5.13	0.57	225	1.03	0.0046
01-09-95	48.9	21.8	2.07	3.96	.49	225	.65	.0029
01-10-95	17.5	17.4	.98	2.32	.42	225	.55	.0024

Cave Creek above Deer Valley Road—Continued

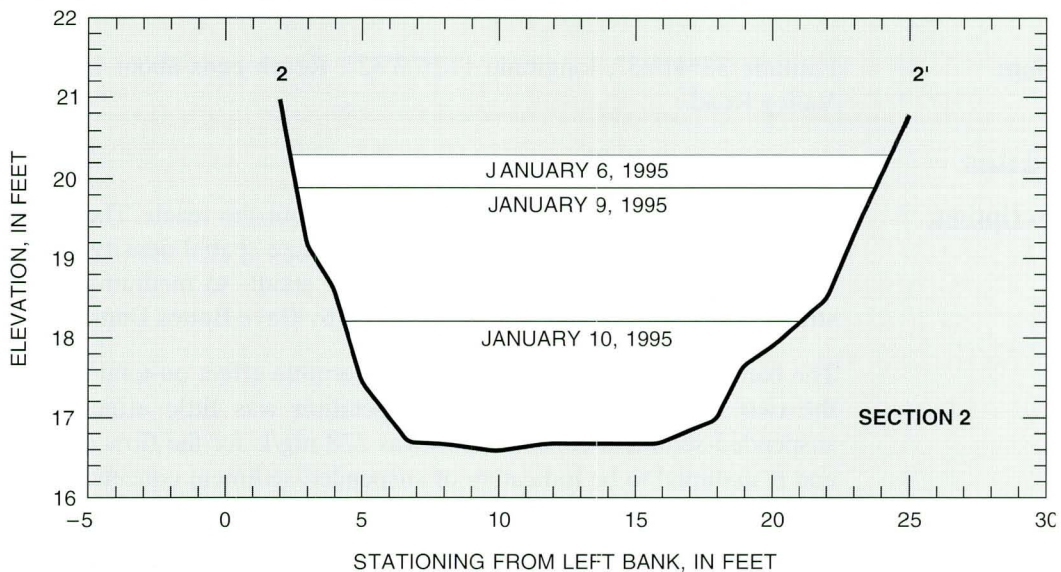


Figure 7A. Cross-section 2, Cave Creek above Deer Valley Road.

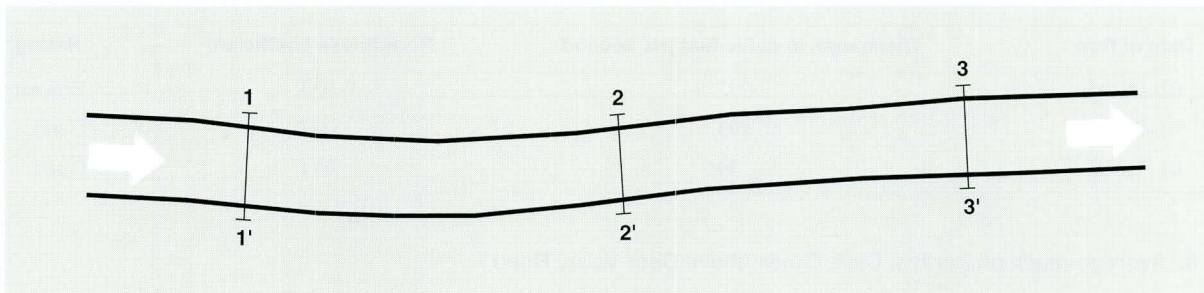


Figure 7B. Plan view, Cave Creek above Deer Valley Road.

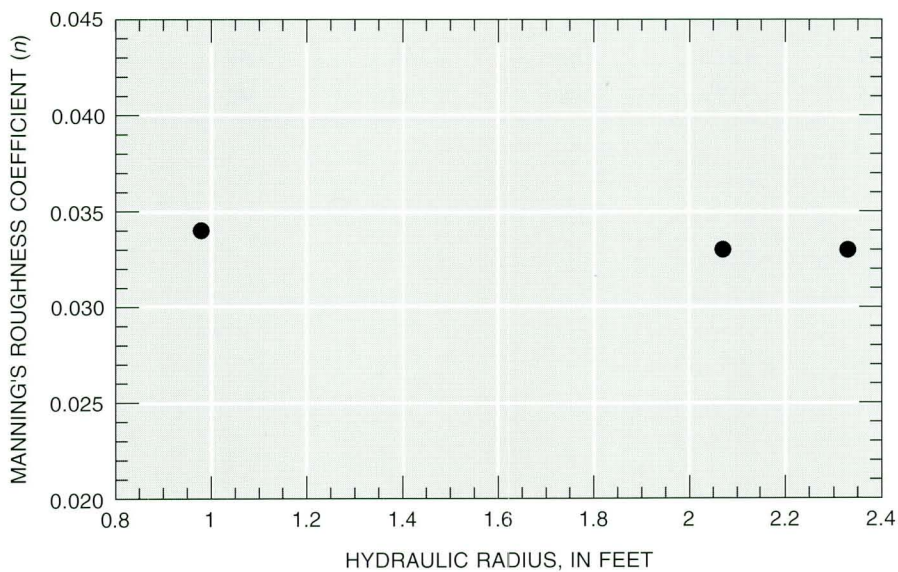


Figure 7C. Manning's n and hydraulic radius, Cave Creek above Deer Valley Road.

Cave Creek above Deer Valley Road—Continued

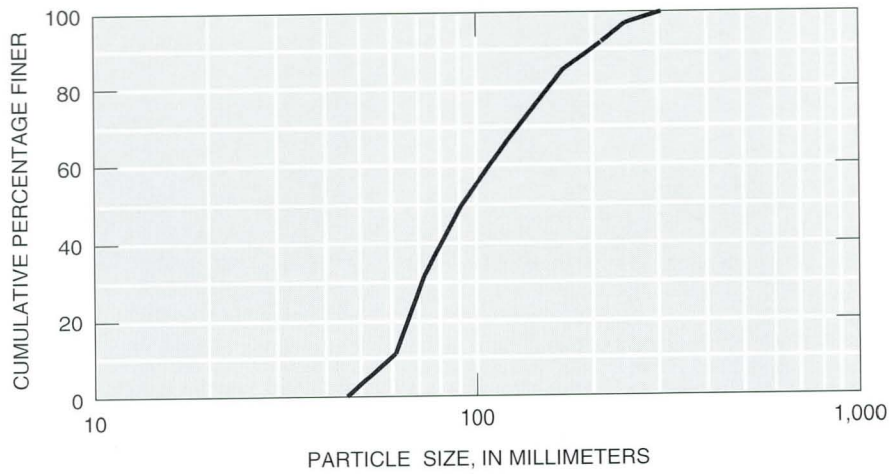


Figure 7D. Particle-size distribution for bed material, Cave Creek above Deer Valley Road.

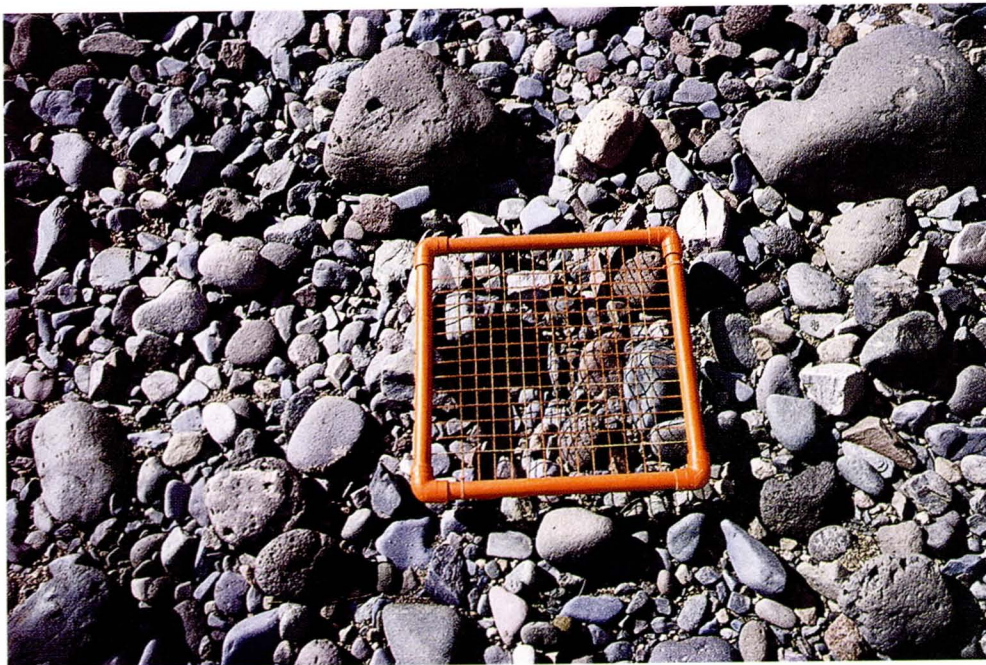


Figure 7E. View of typical bed material in channel reach, Cave Creek above Deer Valley Road. The square grid (painted orange) has an outside dimension of 1.5 feet and an internal grid spacing of 1 inch.

Cave Creek above Deer Valley Road—Continued



Figure 7F. View from bottom of reach looking upstream during flow of January 9, 1995, Cave Creek above Deer Valley Road.



Figure 7G. View from top of reach looking downstream, Cave Creek above Deer Valley Road. Rod indicates water-surface elevation for the peak flow of January 6, 1995.

Cave Creek below Cave Buttes Dam

Reach location: Latitude 33°42'55", longitude 112° 02'44". Reach begins about 500 ft below Cave Buttes Dam.

Bed-material size: See *channel description*.

Channel description: The constructed reach is straight, and cross sections are trapezoidal in shape. The bottom and sides of the channel are composed of rounded cobbles imbedded in a matrix of cement (approximate mean diameter of the rock projections was 80 mm, about half of which seemed to be exposed to flow). Roughness elements are constant throughout the reach. The channel gradient increases from about 0.002 ft/ft at cross-section 1 to about 0.010 ft/ft at cross-section 8. The stream is ephemeral, and flow is regulated by Cave Buttes Dam.

Remarks: Roughness coefficients were determined for both subcritical (Froude number < 1.0) and supercritical (Froude number > 1.0) flow regimes. The Froude number at cross-section 5 approximated 1.0 (*critical flow*) for both flows and was not incorporated in the analyses. A decrease in Manning's *n* occurred when flow transitioned from subcritical flow to supercritical flow. This change could be the result of unstable flow conditions as investigated by Koloseus and Davidian (1966). According to their results, roughness depends on the Froude number when unstable flow conditions occur (generally flow is considered unstable if Froude numbers are larger than about 1.6). Although Froude numbers in the supercritical reach averaged about 1.6 or less, the Froude number increased to over 1.8 in cross-section 8. The suspended-sediment concentration was 224 mg/L for the flow of January 9, 1995, and may be indicative of suspended-sediment concentration for the flow on November 2, 1995. This amount of suspended sediment is considered as wash load and to have negligible effects on *n* values.

Table 9. Flow data and computed roughness coefficients, Cave Creek below Cave Buttes Dam

Date of flow	Discharge, in cubic feet per second	Roughness coefficient		Rating
		Subcritical	Supercritical	
01-09-95	197	0.025	0.017	Good
11-02-95	165	.025	.017	Good

Table 10. Average-reach properties, Cave Creek below Cave Buttes Dam

Date	Area, in square feet	Top width, in feet	Hydraulic radius, in feet	Mean velocity, in feet per second	Froude number	Total length, in feet	Total fall, in feet	Water-surface slope
Subcritical flow regime (cross-sections 1-4)								
01-09-95	46.6	21.4	2.03	4.36	0.53	311	0.94	0.0030
Supercritical flow regime (cross-sections 6-8)								
01-09-95	21.9	19.1	1.12	9.21	1.54	148	2.19	.0148
Subcritical flow regime (cross-sections 1-4)								
11-02-95	42.0	20.4	1.91	4.06	.51	311	.95	.0031
Supercritical flow regime (cross-sections 6-8)								
11-02-95	18.1	17.9	.99	9.16	1.61	148	1.92	.0130

Cave Creek below Cave Buttes Dam—Continued

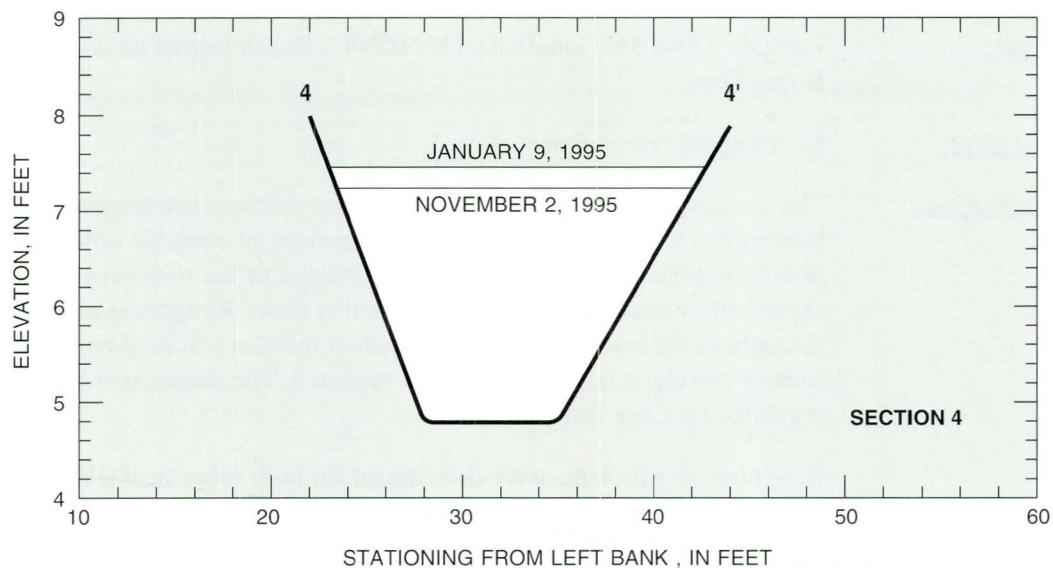


Figure 8A. Cross-section 4, Cave Creek below Cave Buttes Dam.

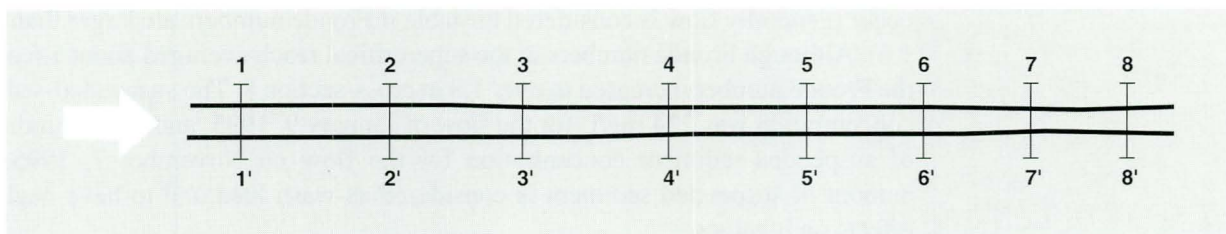


Figure 8B. Plan view, Cave Creek below Cave Buttes Dam.

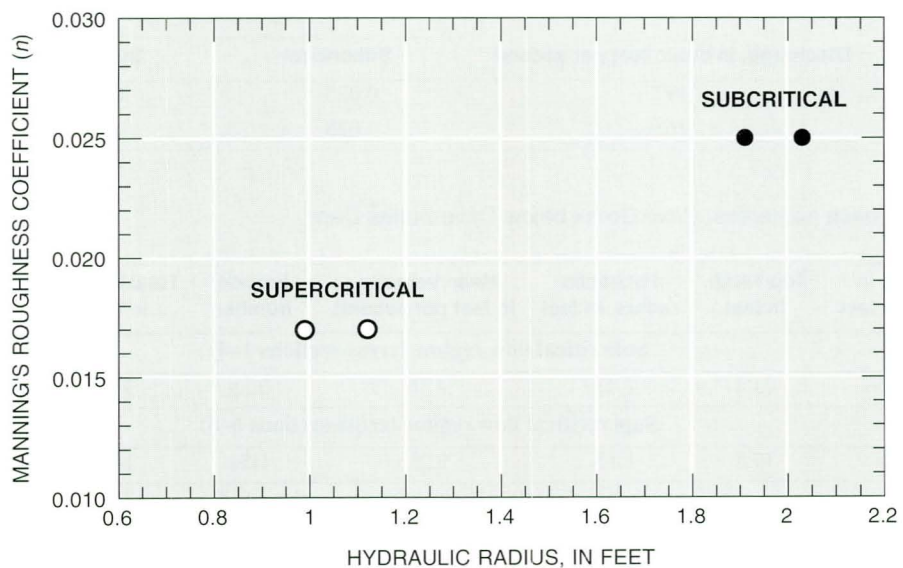


Figure 8C. Manning's n and hydraulic radius, Cave Creek below Cave Buttes Dam.

Cave Creek below Cave Buttes Dam—Continued



Figure 8D. View from cross-section 7 looking upstream toward transition from subcritical to supercritical flow, Cave Creek below Cave Buttes Dam.



Figure 8E. View from cross-section 4 looking upstream toward subcritical flow reach during survey of the water surface, November 2, 1995, Cave Creek below Cave Buttes Dam.

Cave Creek below Cave Buttes Dam—Continued



Figure 8F. View from top of reach looking downstream, Cave Creek below Cave Buttes Dam.



Figure 8G. View from midchannel looking downstream, Cave Creek below Cave Buttes Dam.

Hassayampa River near Morrystown

Reach location: Latitude 33°53'06", longitude 112°39'41". Reach is at streamflow-gaging station 09516500, Hassayampa River near Morrystown.

Drainage area: 796 mi².

Bed-material size: $d_{50} = 0.42$ mm (0.0014 ft).

Channel description: The channel bed in the reach consists of sand-sized material, and the channel is straight and uniform. The right bank is a straight vertical railway embankment, and the left bank is a vertical bedrock cliff. The sparse vegetation is mainly mesquite along the right bank. The stream is intermittent, and flow is unregulated.

Remarks: Data from current-meter measurements were used to obtain an accurate representation of the bed configuration. This technique was required because the bed is highly unstable and may take on different configurations during moderate to high flows (fig. 9A). Only channel-geometry measurements obtained during flow from this one section, therefore, were used for the n -verification computations. The measured water-surface slope is assumed to approximate the slope of the energy-gradient line. Uniformity of the reach probably prevents significant energy losses due to expansion and contraction. Potential errors incurred by the required assumptions probably are offset by the accurate measurements of the channel configuration during flows on this highly unstable bed. Upper-regime flow conditions were encountered during all of the verification measurements (fig. 3). Plane-bed or nearly plane-bed conditions were reported for the two lower flow measurements, and waves that slowly propagated downstream, nearly extended bank to bank, and periodically collapsed were observed during the two high-flow measurements. Increased suspended-sediment concentrations and turbulence generated by the waves probably resulted in the larger verified n values. The suspended-sediment concentration was 18,916 mg/L at a flow rate of about 9,000 ft³/s on March 6, 1995.

Table 11. Flow data and computed roughness coefficients, Hassayampa River near Morrystown

Date of flow	Discharge, in cubic feet per second	Roughness coefficient	Rating
02-20-93	7,330	0.025	Estimate
02-09-93	6,180	.026	Estimate
01-19-93	2,470	.019	Estimate
01-21-93	787	.018	Estimate

Hassayampa River near Morristown—Continued

Table 12. Data obtained from discharge measurements and field surveys, Hassayampa River near Morristown
[N/A, not applicable]

Date	Area, in square feet ¹	Top width, in feet ¹	Hydraulic radius, in feet ¹	Mean velocity, in feet per second ¹	Froude number ¹	Total length, in feet	Total fall, in feet	Water-surface slope
02-20-93	652	173	3.8	11.20	1.01	N/A	N/A	0.0062
02-09-93	518	172	3.4	11.93	1.13	N/A	N/A	.0062
01-19-93	300	165	1.8	8.23	1.09	N/A	N/A	.0050
01-21-93	155	170	.9	5.08	.94	N/A	N/A	.0043

¹Obtained from current-meter measurements.

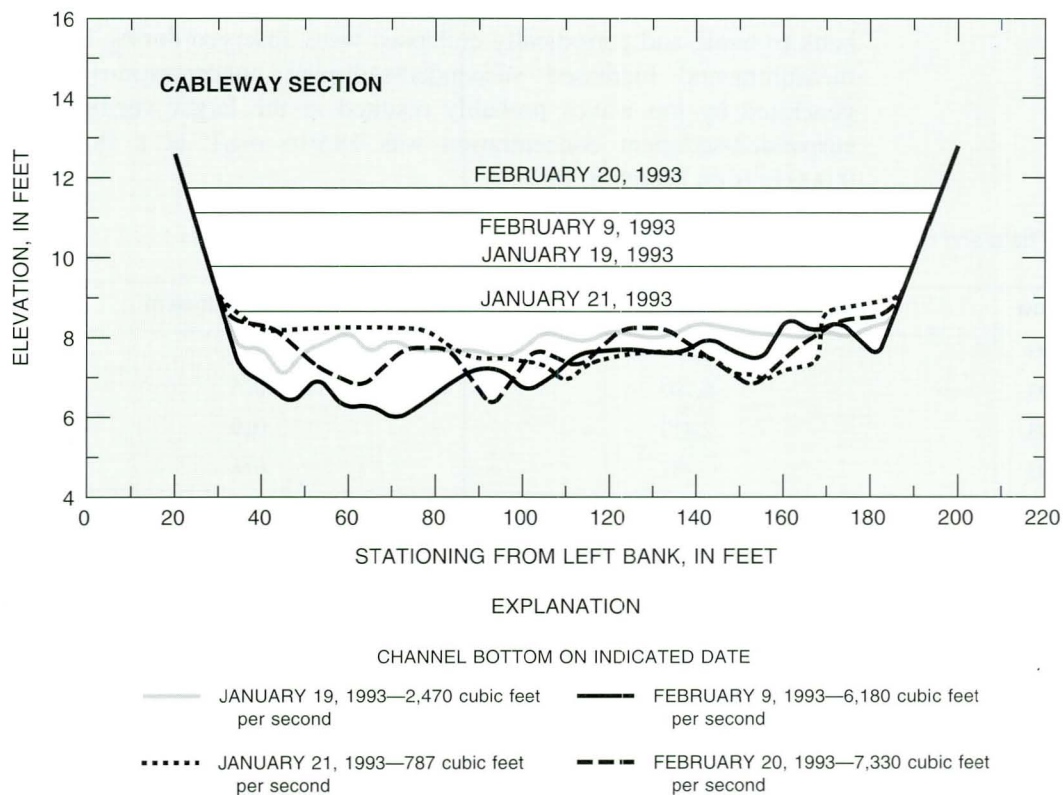


Figure 9A. Cableway cross section, bed geometry for each current-meter measurement, and water-surface elevations, Hassayampa River near Morristown.

Hassayampa River near Morrystown—Continued

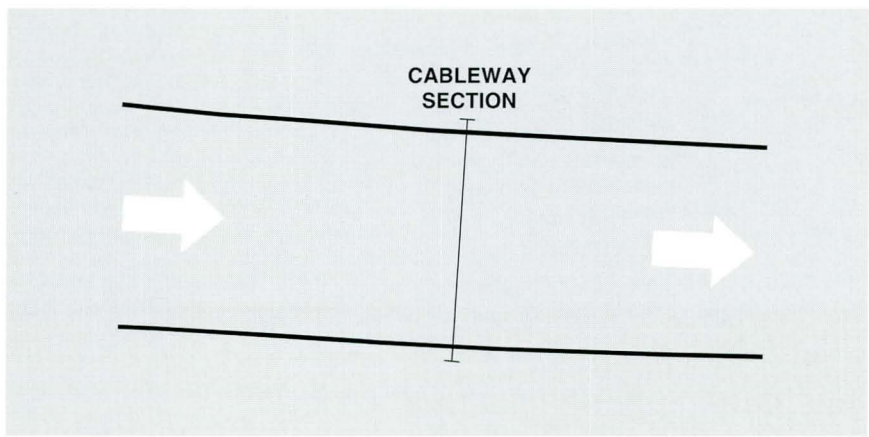


Figure 9B. Plan view, Hassayampa River near Morrystown.

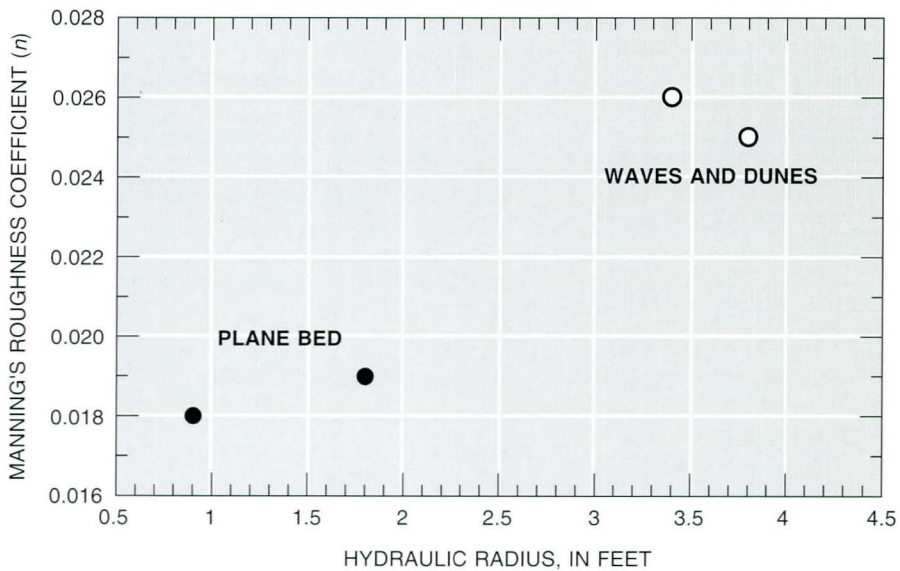


Figure 9C. Manning's n and hydraulic radius, Hassayampa River near Morrystown.

Hassayampa River near Morrystown—Continued

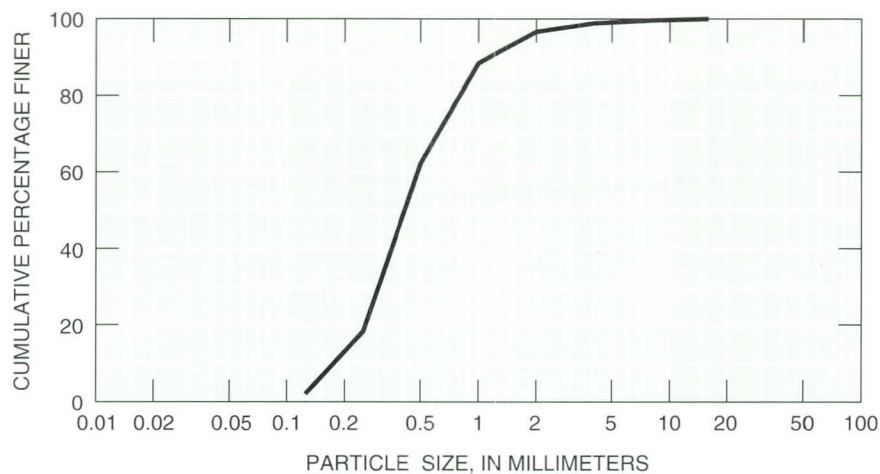


Figure 9D. Particle-size distribution for bed material, Hassayampa River near Morrystown.



Figure 9E. View upstream from midchannel during no-flow period, Hassayampa River near Morrystown. Rod indicates water-surface elevation for the peak flow of January 8, 1993.

Hassayampa River near Morristown—Continued



Figure 9F. View from cableway looking upstream during flow of February 9, 1993, Hassayampa River near Morristown. Disturbance is a wave propagating slowly downstream and is indicative of hydraulic characteristics in alluvial channels during upper-regime flow conditions.



Figure 9G. View from cableway looking upstream during flow of February 9, 1993, Hassayampa River near Morristown. Disturbance is a wave propagating slowly downstream and is indicative of hydraulic characteristics in alluvial channels during upper-regime flow conditions. Photograph taken soon after photograph shown in figure 9F.

Indian Bend Wash above Curry Road

Reach location: Latitude 33°26'50", longitude 111°54'55". Reach begins about 1,500 ft upstream from streamflow-gaging station 09512162, Indian Bend Wash at Curry Road.

Drainage area: 82.0 mi².

Bed-material size: See *channel description*.

Channel description: The constructed channel is uniform and cross sections are trapezoidal in shape. The channel bottom is firm earth with seasonal growth of grasses and small brush. The stream is ephemeral.

Remarks: The grass generally was laid over following the flow on October 6, 1993, and in a direction parallel to flow, whereas the sparse brush appeared to be little affected by the flow. Postflow conditions indicate that the flow of December 26, 1994, did not significantly affect either the brush or the grass. Suspended-sediment concentration was 365.4 mg/L at a discharge of about 500 ft³/s on September 28, 1995, and was considered wash load. As the drainage area is mainly urbanized, this wash-load condition probably is indicative of suspended-sediment concentrations for most flows at this site (Fossum and Davis, 1996).

Table 13. Flow data and computed roughness coefficient, Indian Bend Wash above Curry Road

Date of flow	Discharge, in cubic feet per second	Roughness coefficient	Rating
10-06-93	6,480	0.024	Fair
12-26-94	449	.036	Good

Table 14. Average-reach properties, Indian Bend Wash above Curry Road

Date	Area, in square feet	Top width, in feet	Hydraulic radius, in feet	Mean velocity, in feet per second	Froude number	Total length, in feet	Total fall, in feet	Water-surface slope
10-06-93	905	167	5.36	7.16	0.54	878	1.27	0.0014
12-26-94	200	132	1.52	2.25	.32	851	1.36	.0016

Indian Bend Wash above Curry Road—Continued

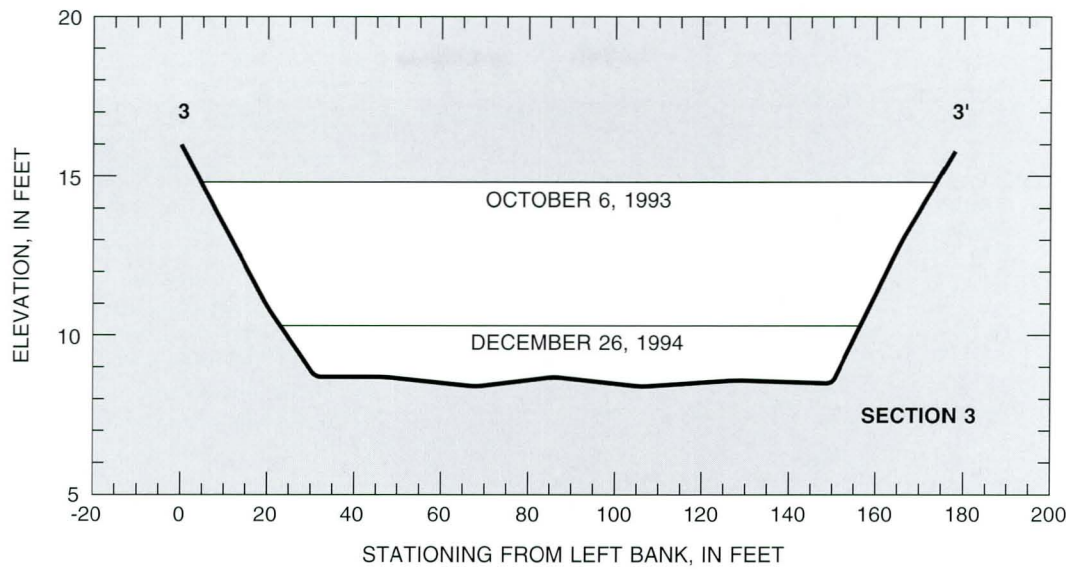


Figure 10A. Cross-section 3, Indian Bend Wash above Curry Road.

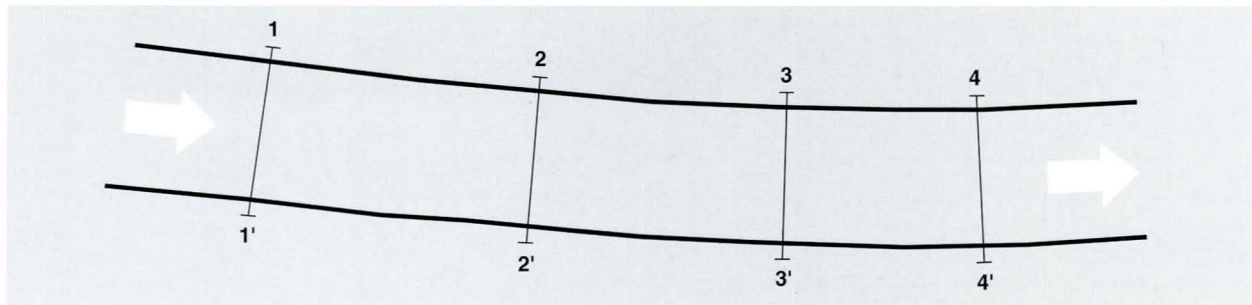


Figure 10B. Plan view, Indian Bend Wash above Curry Road.

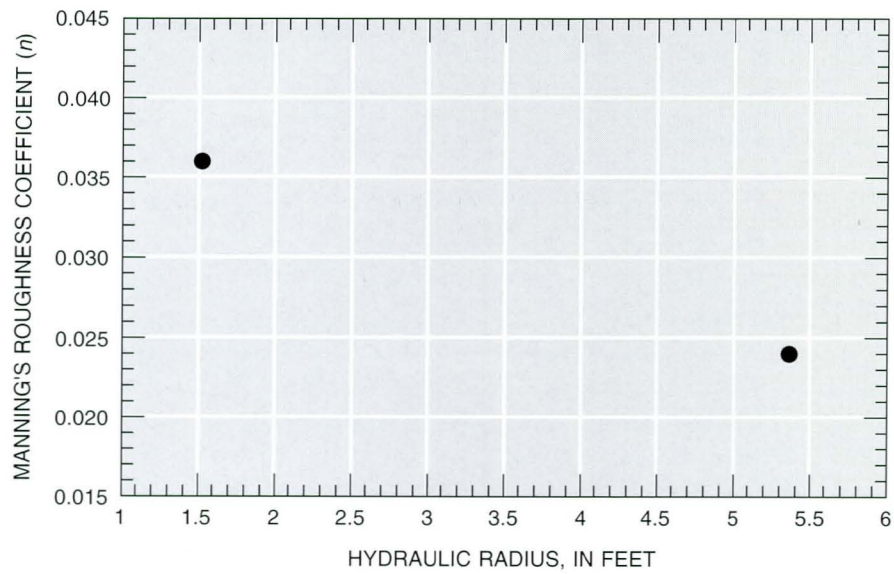


Figure 10C. Manning's *n* and hydraulic radius, Indian Bend Wash above Curry Road.

Indian Bend Wash above Curry Road—Continued



Figure 10D. View from midchannel looking downstream at laid-over grass following flow of October 6, 1993, Indian Bend Wash above Curry Road. The square grid (painted orange) has an outside dimension of 1.5 feet and an internal grid spacing of 1 inch.



Figure 10E. View from midreach looking upstream following flow of October 6, 1993, Indian Bend Wash above Curry Road.

Indian Bend Wash above Curry Road—Continued

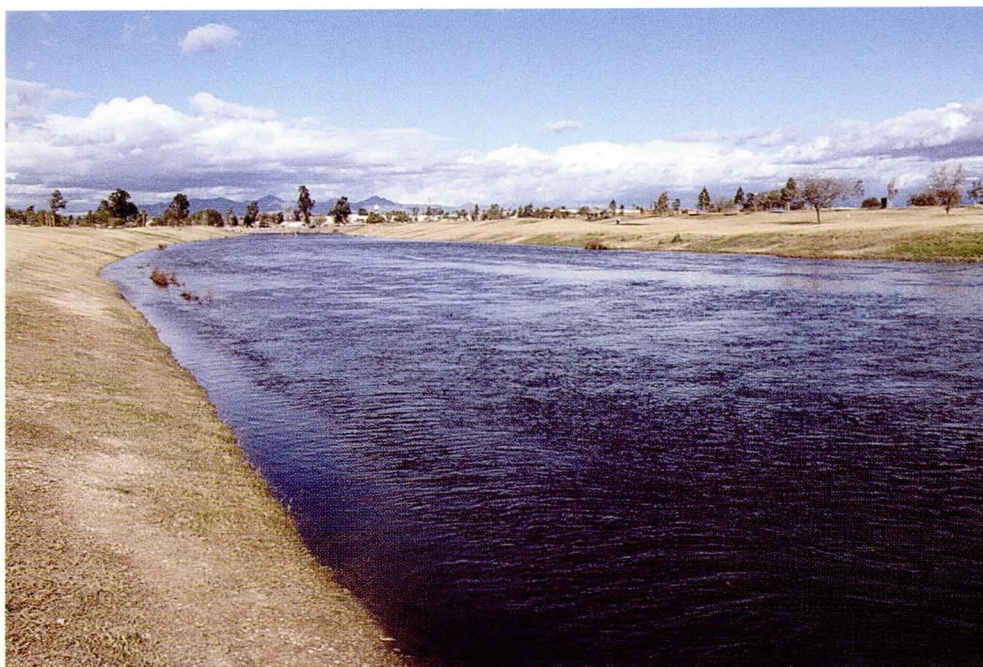


Figure 10F. View from bottom of reach looking upstream during low flow, Indian Bend Wash above Curry Road.



Figure 10G. View from midchannel looking upstream before flow of December 26, 1994, Indian Bend Wash above Curry Road.

Salt River above Interstate 10

Reach location: Latitude 33°25'53", longitude 111°59'16". Reach begins about 3,000 ft above Interstate 10.

Drainage area: 13,300 mi².

Bed-material size: $d_{50} = 94$ mm (0.31 ft).

Channel description: The constructed channel has a uniform geometry and cross sections generally are rectangular in shape. Bed material is dominated by medium-sized rounded cobbles. The river was perennial before construction of upstream reservoirs.

Remarks: Sparse growth of algae sometimes is observed growing on the cobbles following prolonged releases from the upstream reservoirs. Flow appeared to be clear during the three discharge measurements. Suspended-sediment data are not available.

Table 15. Flow data and computed roughness coefficients, Salt River above Interstate 10

Date of flow	Discharge, in cubic feet per second	Roughness coefficient	Rating
02-18-92	4,900	0.030	Good
01-15-92	2,070	.034	Good
01-09-92	1,000	.038	Good

Table 16. Average-reach properties, Salt River above Interstate 10

Date	Area, in square feet	Top width, in feet	Hydraulic radius, in feet	Mean velocity, in feet per second	Froude number	Total length, in feet	Total fall, in feet	Water-surface slope
02-18-92	1,090	416	2.61	4.50	0.49	1,497	3.71	0.0025
01-15-92	665	405	1.64	3.13	.43	1,497	3.99	.0027
01-09-92	462	399	1.16	2.18	.36	1,497	3.91	.0026

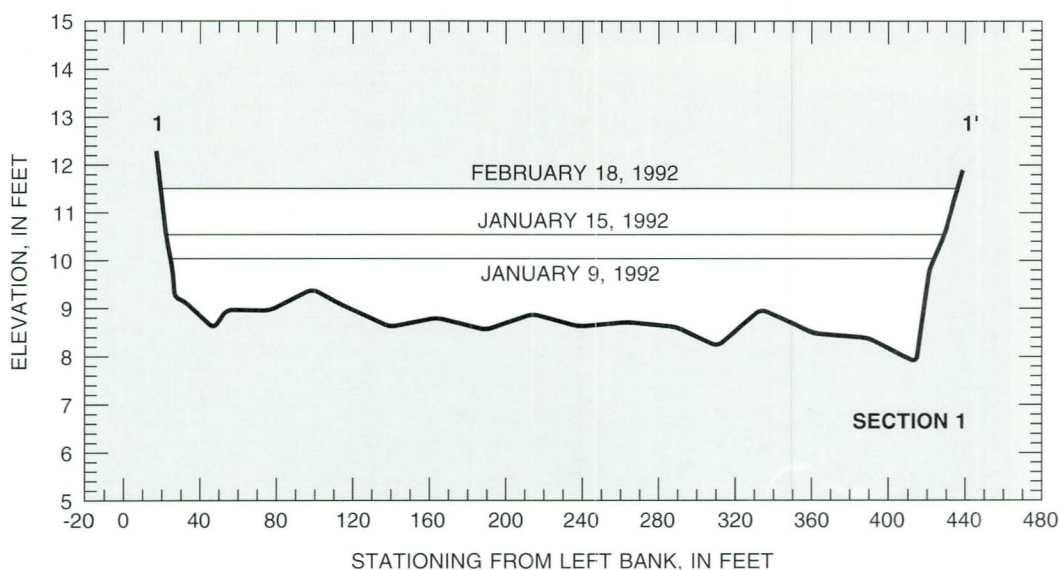


Figure 11A. Cross-section 1, Salt River above Interstate 10.

Salt River above Interstate 10—Continued

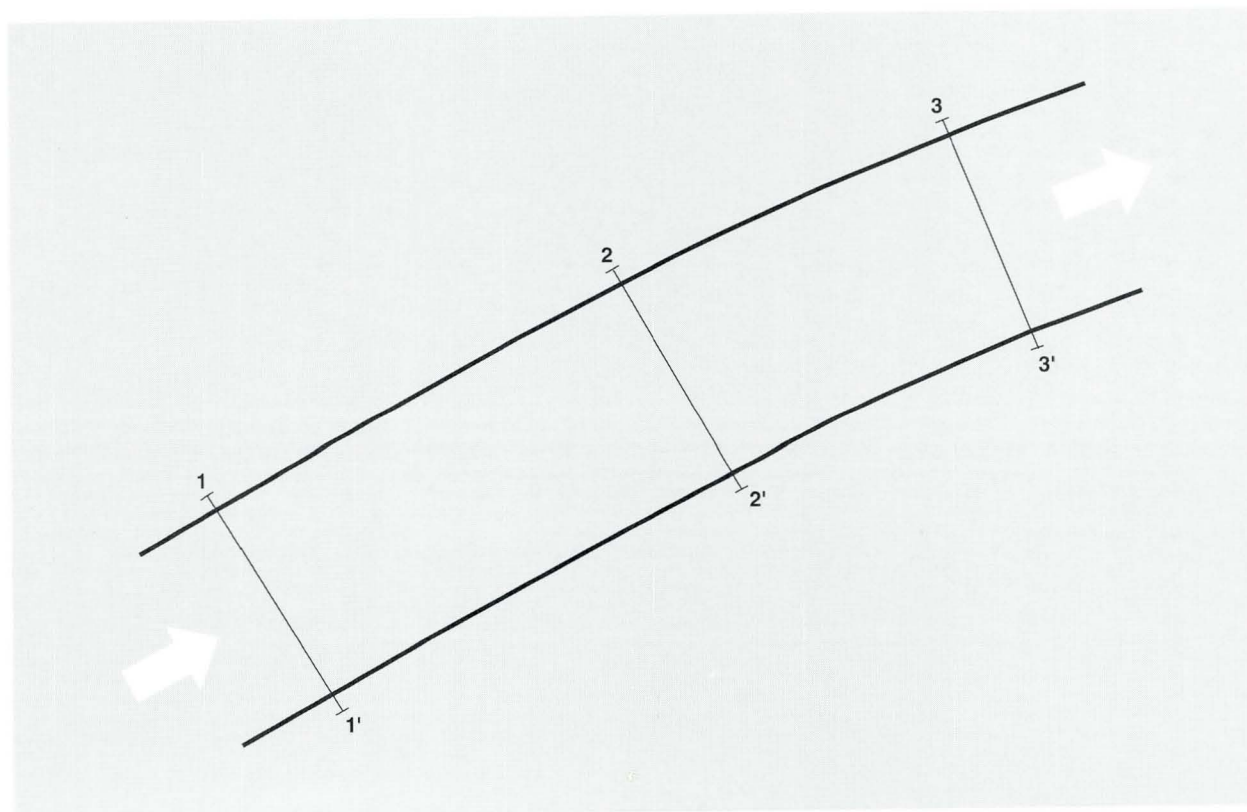


Figure 11B. Plan view, Salt River above Interstate 10.

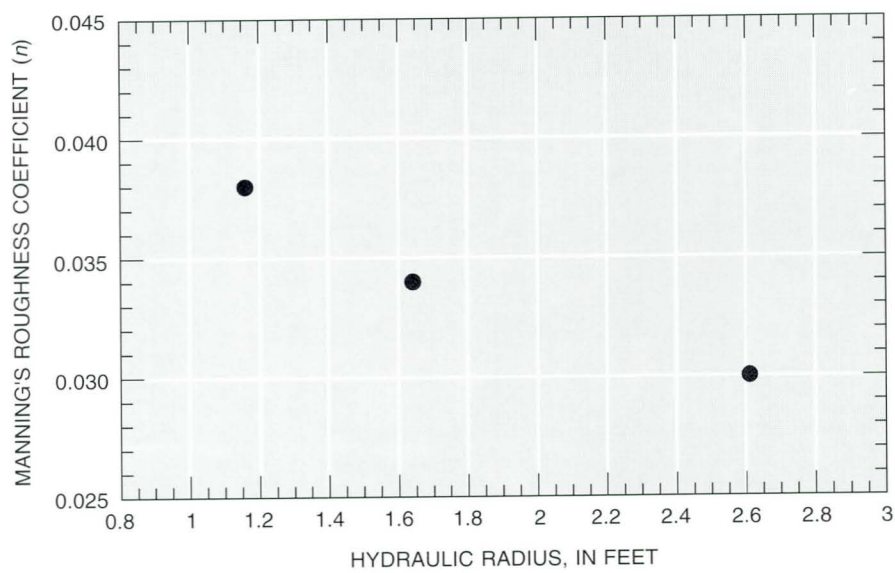


Figure 11C. Manning's n and hydraulic radius, Salt River above Interstate 10.

Salt River above Interstate 10—Continued

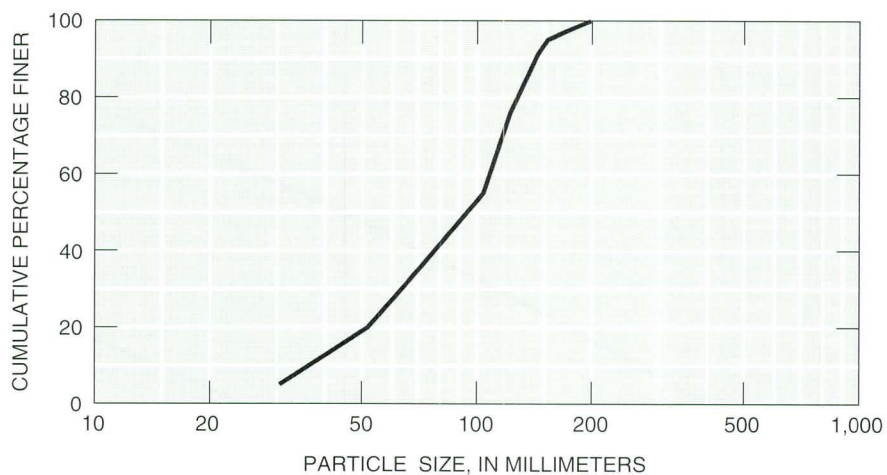


Figure 11D. Particle-size distribution for bed material, Salt River above Interstate 10.



Figure 11E. View of typical bed material in channel reach, Salt River above Interstate 10. The square grid (painted orange) has an outside dimension of 1.5 feet and an internal grid spacing of 1 inch.

Salt River above Interstate 10—Continued



Figure 11F. View from top of reach looking downstream during flow of January 15, 1992, Salt River above Interstate 10.



Figure 11G. View from top of reach looking downstream, Salt River above Interstate 10.

Verde River below Beeline Highway

Reach location: Latitude 33°33'31", longitude 111°40'07". Reach begins about 200 ft downstream from streamflow-gaging station 09511300, Verde River near Scottsdale.

Drainage area: 6,615 mi².

Bed-material size: $d_{50} = 110$ mm (0.36 ft).

Channel description: Although there is a slight curvature of the reach as indicated in the plan view (fig. 12B), the channel is fairly uniform and consists mainly of cobble-sized material. The left bank is steep and is primarily bare soil. Root systems of the vegetation at higher elevations seem to keep the bank material fairly stable. Sparse vegetation (brush) is in the channel. The river is perennial and flow is regulated by upstream reservoirs.

Remarks: The effect of the sparse brush in the main channel on flow resistance was considered negligible. Additionally, the bank vegetation evident in figure 12G was above the high-water line and did not affect flow. The low-flow verification measurement was made in a short section of the channel reach (not shown in figures).

Table 17. Flow data and computed roughness coefficients, Verde River below Beeline Highway

Date of flow	Discharge, in cubic feet per second	Roughness coefficient	Rating
03-28-91	2,860	0.030	Good
09-14-89	225	.036	Good

Table 18. Average-reach properties, Verde River below Beeline Highway

Date	Area, in square feet	Top width, in feet	Hydraulic radius, in feet	Mean velocity, in feet per second	Froude number	Total length, in feet	Total fall, in feet	Water-surface slope
03-28-91	610	157	3.94	4.69	0.42	1,045	1.38	0.0013
09-14-89	87.9	87.4	1.00	2.57	.45	243	.92	.0038

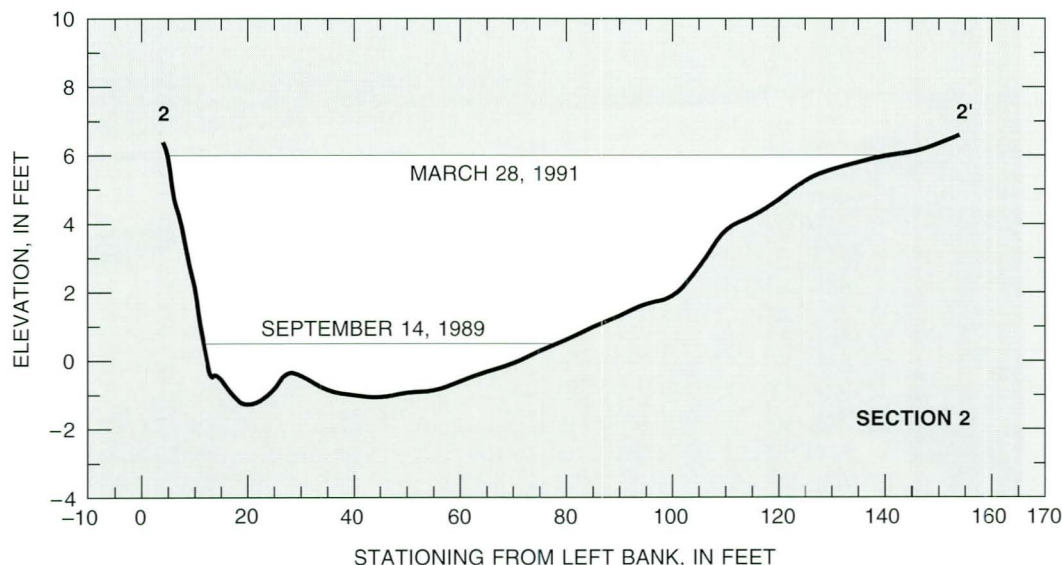


Figure 12A. Cross-section 2, Verde River below Beeline Highway.

Verde River below Beeline Highway—Continued

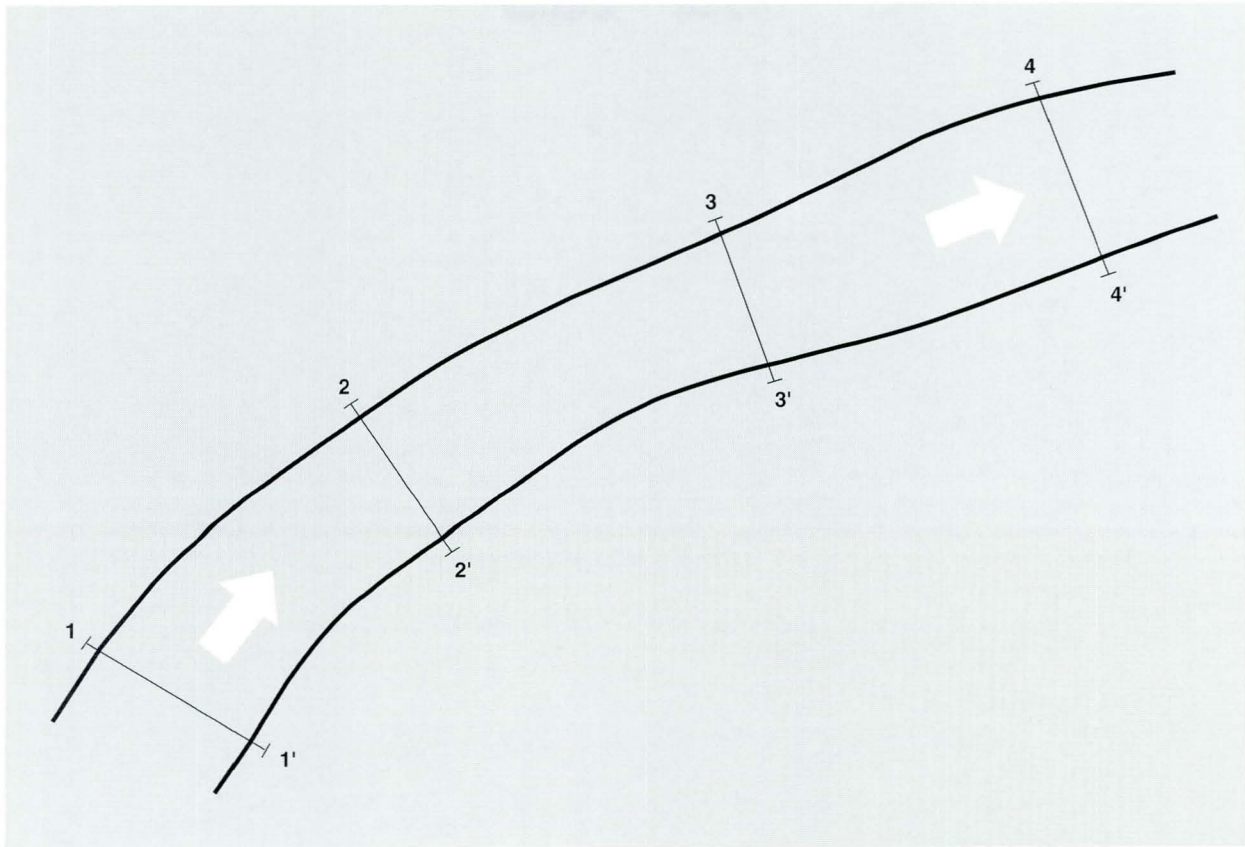


Figure 12B. Plan view for flow of March 28, 1991, Verde River below Beeline Highway. The reach in which the low-flow verification measurement was made is between cross-sections 1 and 2.

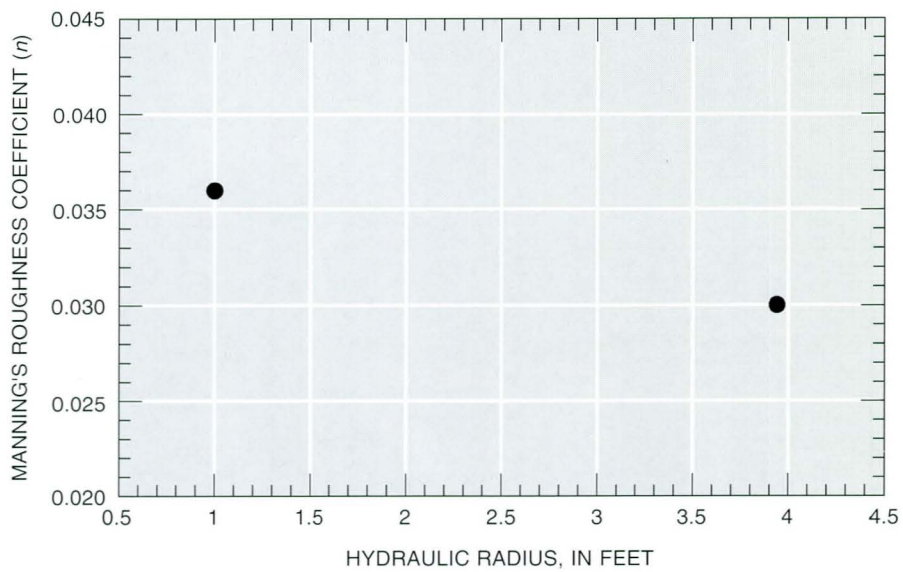


Figure 12C. Manning's n and hydraulic radius, Verde River below Beeline Highway.

Verde River below Beeline Highway—Continued

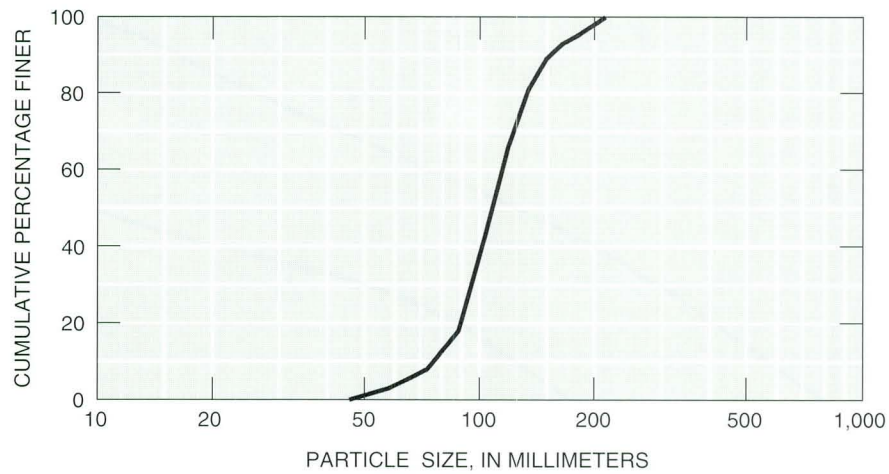


Figure 12D. Particle-size distribution for bed material, Verde River below Beeline Highway



Figure 12E. View of typical bed material, Verde River below Beeline Highway. The square grid (painted orange) has an outside dimension of 1.5 feet and an internal grid spacing of 1 inch.

Verde River below Beeline Highway—Continued

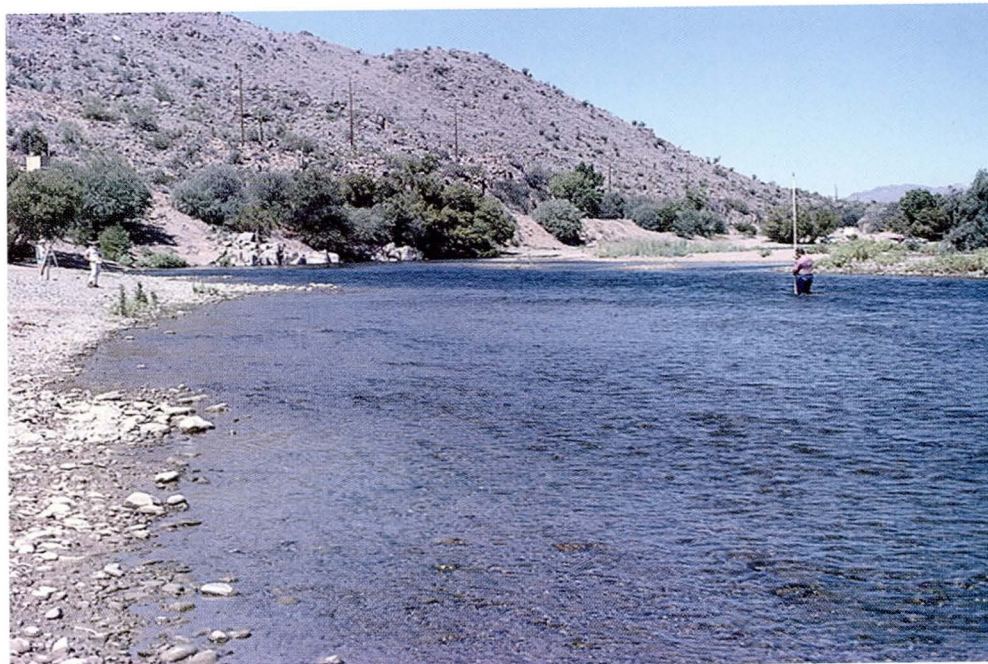


Figure 12F. View from right bank and midreach looking upstream during flow of September 14, 1989, Verde River below Beeline Highway.



Figure 12G. View from cableway looking downstream during flow of March 28, 1991, Verde River below Beeline Highway.

West Fork Sycamore Creek near Sunflower

Reach location: Latitude 33°57'20", longitude 111°29'25". Reach begins about 350 ft downstream from streamflow-gaging station 09510120, West Fork Sycamore Creek near Sunflower (Aldridge and Garrett, 1973).

Drainage area: 8.6 mi².

Bed-material size: See *channel description*.

Channel description: The channel is fairly uniform throughout the study reach. The channel bottom consists mostly of pebble to boulder-size clasts. No grain-size analysis is available. A few trees are near the channel margins (figs. 13C–E). The stream is intermittent, and flow is unregulated.

Remarks: The trees probably had a slight effect on total flow resistance. Discharge was obtained from a well-defined stage-discharge relation. High-water indicators were plentiful and were rated good to excellent (E.E. Denis, hydrologist, U.S. Geological Survey, written commun., 1963).

Table 19. Flow data and computed roughness coefficient, West Fork Sycamore Creek near Sunflower

Date of flow	Discharge, in cubic feet per second	Roughness coefficient	Rating
02-11-63	117	0.067	Good

Table 20. Average-reach properties, West Fork Sycamore Creek near Sunflower

Date	Area, in square feet	Top width, in feet	Hydraulic radius, in feet	Mean velocity, in feet per second	Froude number	Total length, in feet	Total fall, in feet	Water-surface slope
02-11-63	36.2	29.4	1.21	3.29	0.53	108	1.96	0.0181

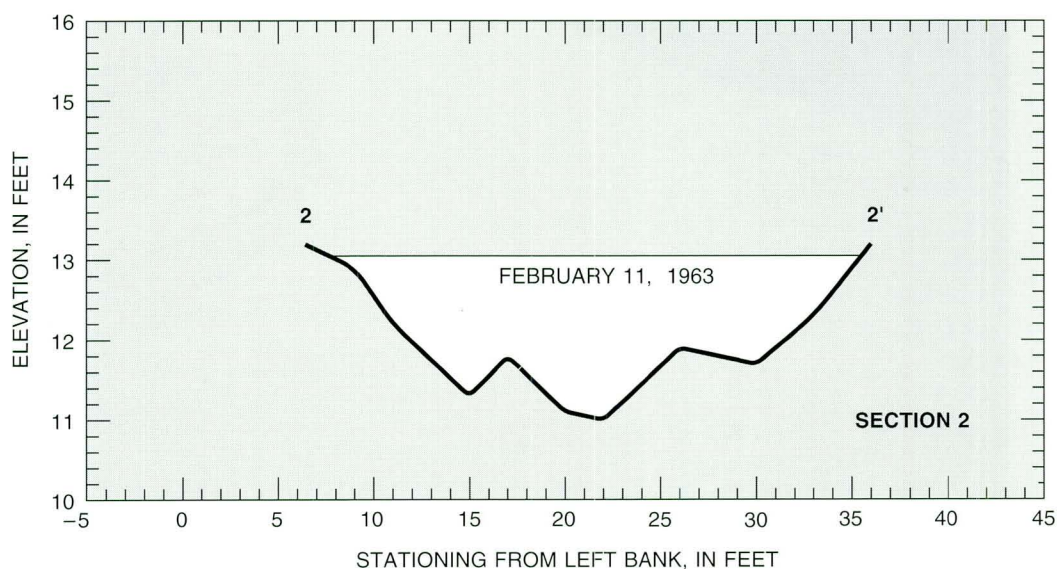


Figure 13A. Cross-section 2, West Fork Sycamore Creek near Sunflower.

West Fork Sycamore Creek near Sunflower—Continued

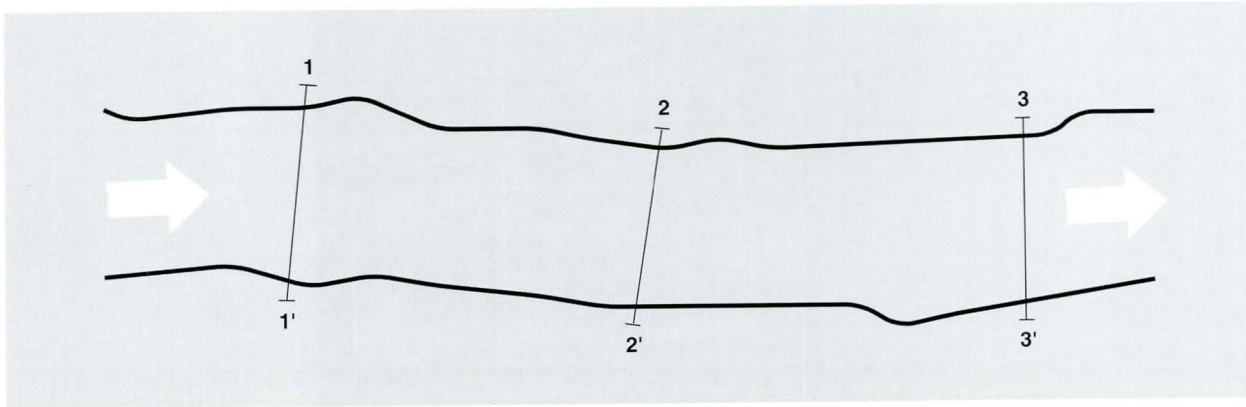


Figure 13B. Plan view, West Fork Sycamore Creek near Sunflower.

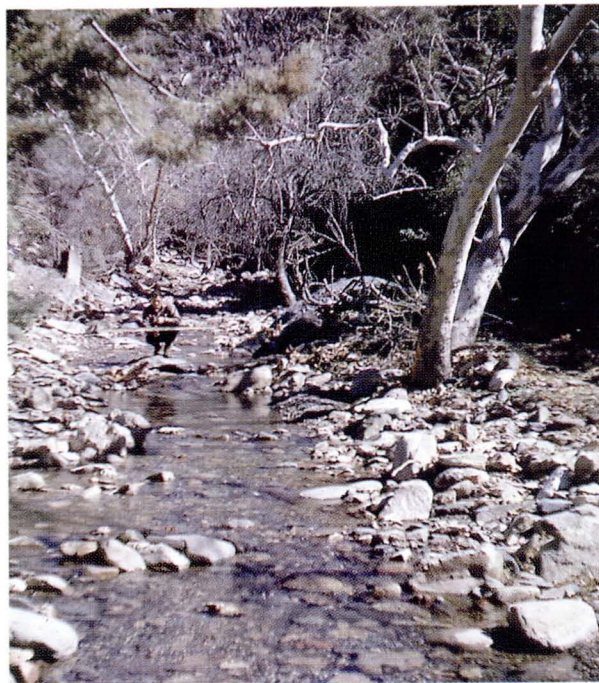


Figure 13C. View from bottom of reach looking upstream toward cross-section 2, February 25, 1963, West Fork Sycamore Creek near Sunflower.

West Fork Sycamore Creek near Sunflower—Continued

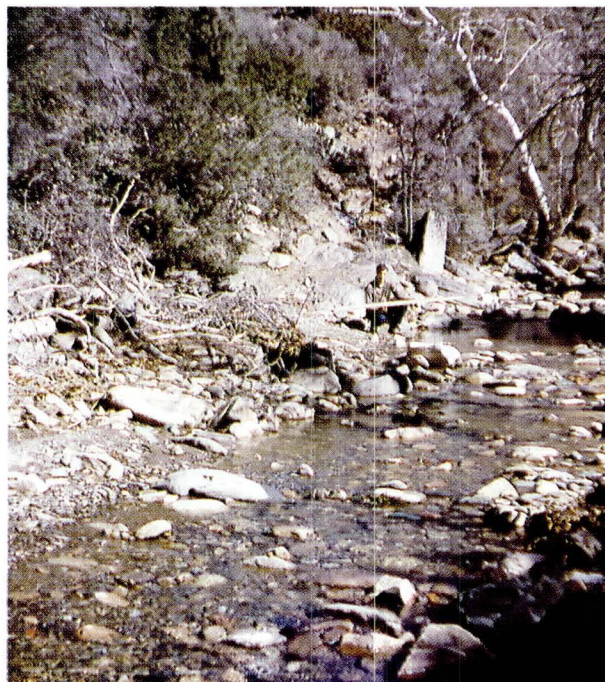


Figure 13D View from midreach looking upstream toward right bank of cross-section 1, February 25, 1963, West Fork Sycamore Creek near Sunflower.

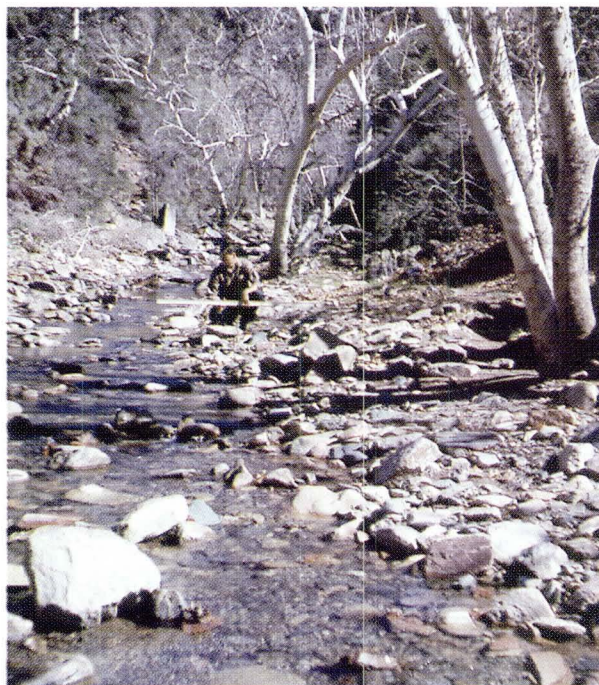


Figure 13E. View from bottom of reach looking upstream toward cross-section 3, February 25, 1963, West Fork Sycamore Creek near Sunflower.

San Pedro River near Charleston

Reach location: Latitude 31°37'33", longitude 110°10'26". Reach is just downstream from streamflow-gaging station 09471000, San Pedro River near Charleston (Aldridge and Garrett, 1973).

Drainage area: 1,234 mi².

Bed-material size: See *channel description*.

Channel description: The bed material is mainly hard conglomerate overlain by deposits that range from sand to angular and rounded boulders 2 to 3 ft (610 to 920 mm) in diameter. The material surrounding the boulders has a median grain size of 1.2 mm (fig. 14C). At the upper end of the reach, conglomerate projections are exposed across the entire channel. The projections are several feet across, and many stand 2 to 3 ft (610 to 920 mm) above the average bed level. Grass and small brush grow along bars at the channel sides. The stream is perennial, and flow is unregulated.

Remarks: Two other channel reaches also were used to verify roughness coefficients for this same discharge measurement. These reaches were in sections of the stream where the bed was primarily composed of sand-sized material and was considered highly unstable. Owing to the uncertainty of channel geometry during peak flow (D.E. Click, hydrologist, U.S. Geological Survey, written commun., 1964), these reaches were not included in this report.

Table 21. Flow data and computed roughness coefficient, San Pedro River near Charleston

Date of flow	Discharge, in cubic feet per second	Roughness coefficient	Rating
08-14-64	7,550	0.048	Fair

Table 22. Average-reach properties, San Pedro River near Charleston

Date	Area, in square feet	Top width, in feet	Hydraulic radius, in feet	Mean velocity, in feet per second	Froude number	Total length, in feet	Total fall, in feet	Water-surface slope
08-14-64	1,268	276	4.62	5.9	0.44	293	1.42	0.0048

San Pedro River near Charleston—Continued

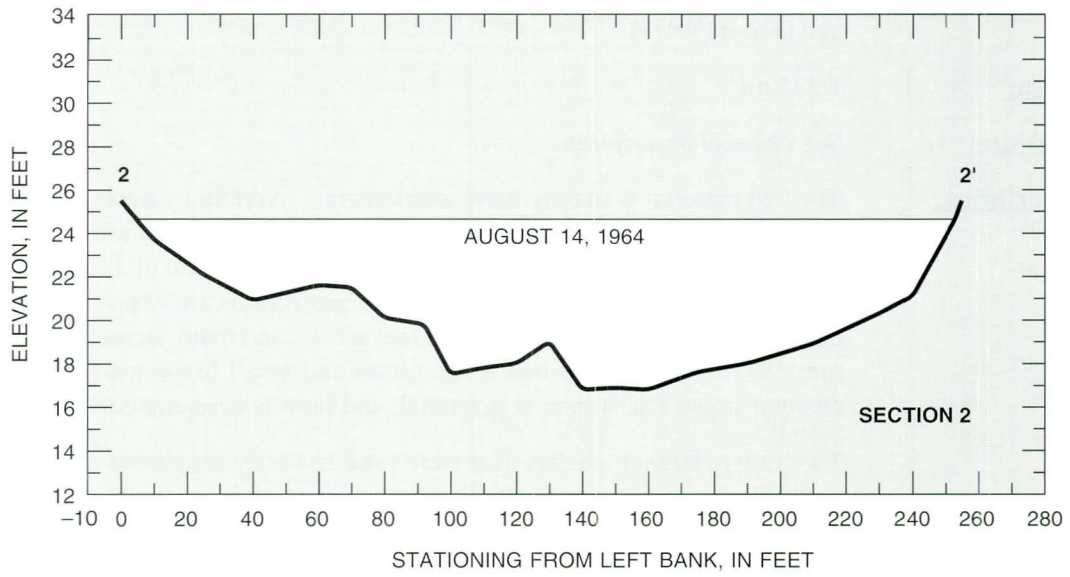


Figure 14A. Cross-section 2, San Pedro River near Charleston.

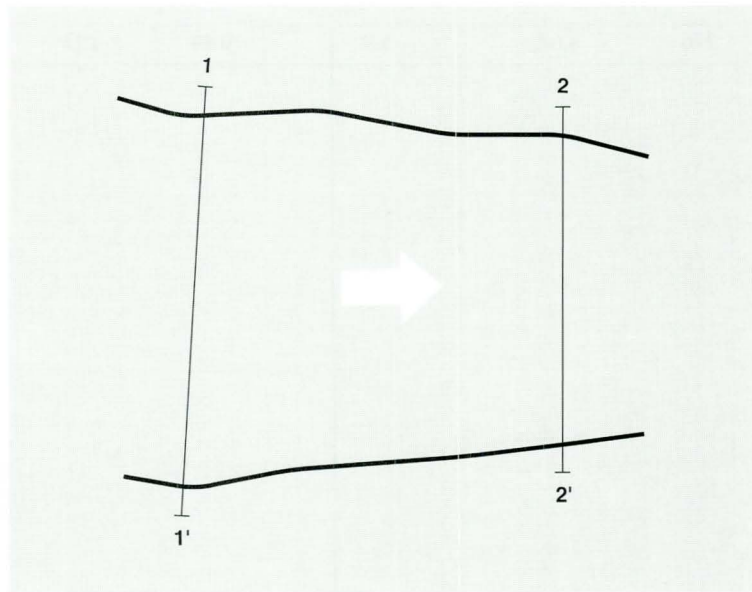


Figure 14B. Plan view, San Pedro River near Charleston.

San Pedro River near Charleston—Continued

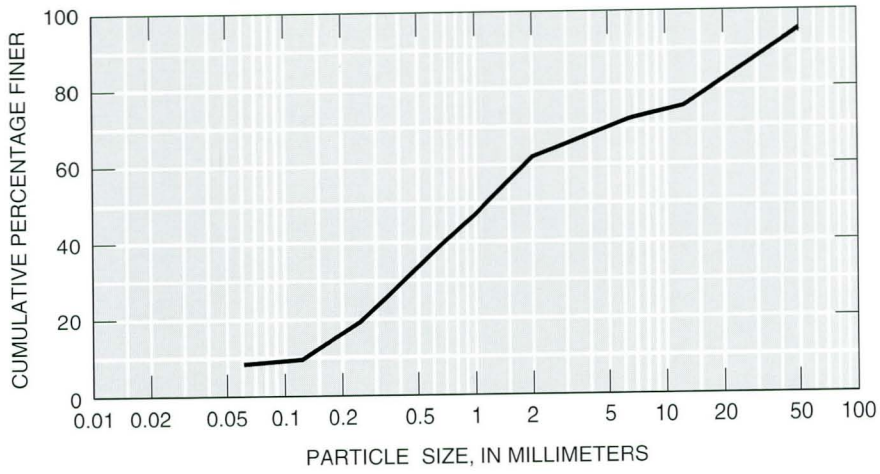


Figure 14C. Particle-size distribution for bed material, San Pedro River near Charleston.



Figure 14D. View from left bank looking downstream toward right bank of cross-section 1, October 8, 1964, San Pedro River near Charleston.

San Pedro River near Charleston—Continued



Figure 14E. View from left bank of cross-section 2 looking downstream, October 8, 1964, San Pedro River near Charleston.

Santa Cruz River at Cortaro

Reach location: Latitude 32°21'04", longitude 111°05'38". Reach begins about 1,200 ft downstream from streamflow-gaging station 09486500, Santa Cruz River at Cortaro (Aldridge and Garrett, 1973, p. 48).

Drainage area: 3,503 mi².

Bed-material size: $d_{50} = 1.2$ mm (0.0039 ft).

Channel description: The channel is fairly straight and uniform and has steeply sloping dirt banks. Heavy brush covers the banks. The cross sections are trapezoidal in shape. The bed is composed mainly of sand-sized material. The river is ephemeral, and flow is unregulated.

Remarks: A current-meter measurement was made at the time of peak discharge. Upper-flow regime conditions persisted during the discharge measurement (fig. 3). High-water marks surveyed after flow were rated good to excellent. J.J. Ligner (hydrologist, U.S. Geological Survey, written commun., 1964) made the following observations during flow on September 10, 1964.

"The river carried a great deal of drift of all sizes, ranging from seeds and twigs to large desert-type trees. As we watched, we were able to see the material that forms the normal high water mark as it advanced up the river bank. It was interesting to note that the grass and small shrubs acted as a fine sieve, and that there was clear water usually from 3 to 6 in. (laterally) ahead of the drift line. It appeared to us that the very top of the drift pile was a close approximation of the ultimate elevation of the water surface. During most of the time we observed the flow, there were chains of standing waves building and breaking into antidunes. There were a number of times that I observed rather long waves that were formed parallel to the flow of the river and that would break (almost like an antidune) towards the right bank."

Table 23. Flow data and computed roughness coefficient, Santa Cruz River at Cortaro

Date of flow	Discharge, in cubic feet per second	Roughness coefficient	Rating
09-10-64	14,200	0.020	Fair

Table 24. Average-reach properties, Santa Cruz River at Cortaro

Date	Area, in square feet	Top width, in feet	Hydraulic radius, in feet	Mean velocity, in feet per second	Froude number	Total length, in feet	Total fall, in feet	Water-surface slope
09-10-64	1,137	175	6.36	12.5	0.87	860	3.16	0.0037

Santa Cruz River at Cortaro—Continued

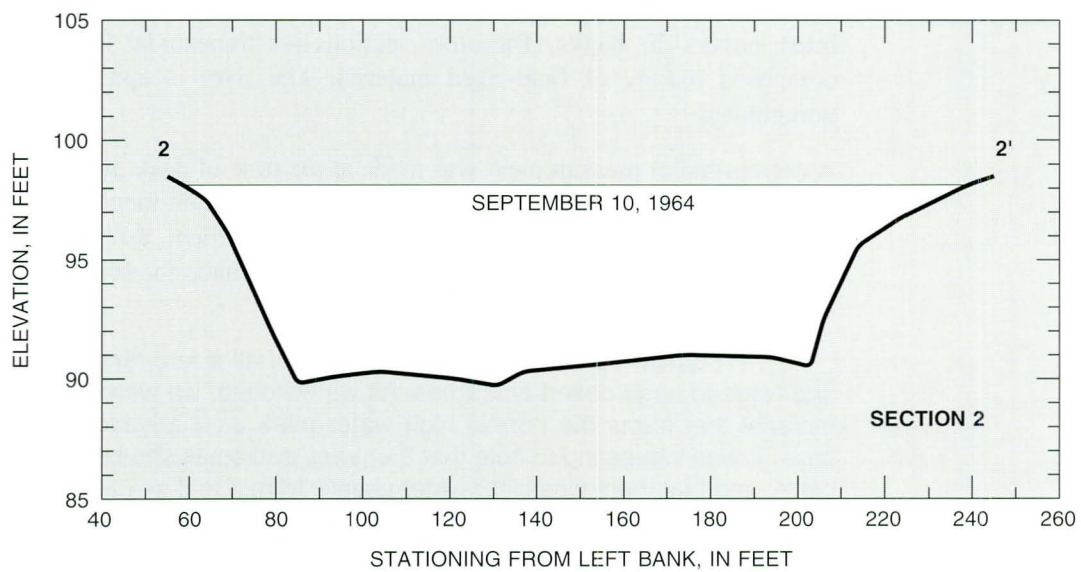


Figure 15A. Cross-section 2, Santa Cruz River at Cortaro.

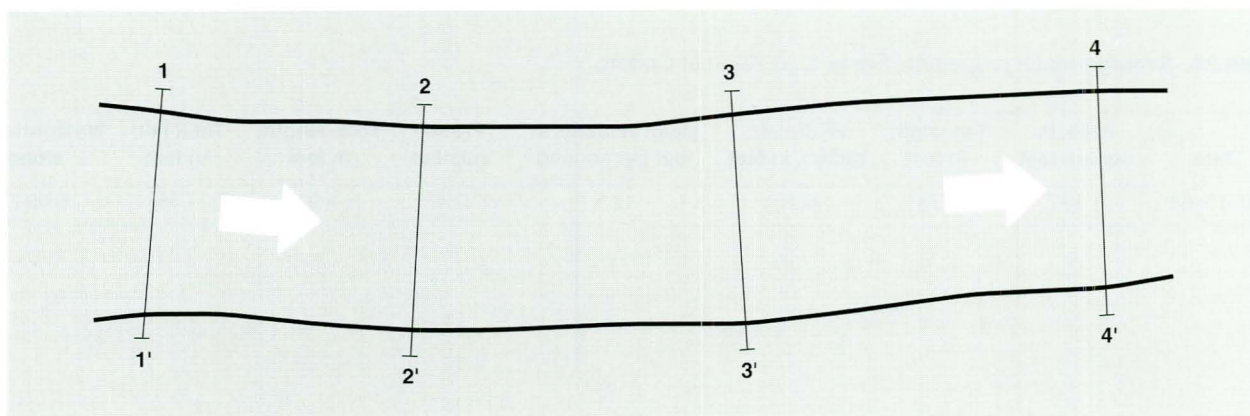


Figure 15B. Plan view, Santa Cruz River at Cortaro.

Santa Cruz River at Cortaro—Continued

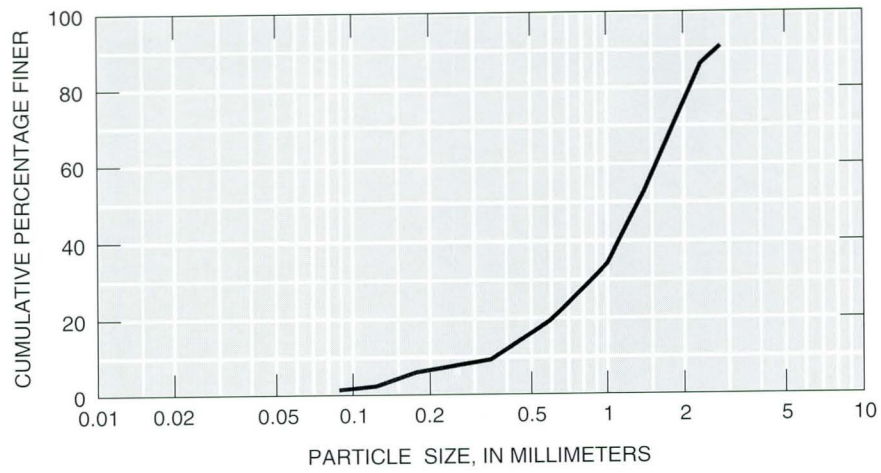


Figure 15C. Particle-size distribution for bed material, Santa Cruz River at Cortaro.



Figure 15D. View from cableway looking downstream, August 5, 1954, at a discharge of 7,000 cubic feet per second, Santa Cruz River at Cortaro.

Santa Cruz River at Cortaro—Continued



Figure 15E. View from cableway looking downstream, October 2, 1964, Santa Cruz River at Cortaro.



Figure 15F. View from midchannel looking upstream toward right bank of cross-section 1 after flow of September 10, 1964, Santa Cruz River at Cortaro.

Verde River near Paulden

Reach location: Latitude 34°53'40", longitude 112°20'32". Reach begins about 80 ft below streamflow-gaging station 09503700, Verde River near Paulden (Aldridge and Garrett, 1973).

Drainage area: 2,530 mi².

Bed-material size: See *channel description*.

Channel description: The low-flow channel is 40 to 50 ft wide and has irregular, vertical banks about 2 ft high. The bed of the low-flow channel is composed of compacted sand, cobbles, and scattered boulders as much as 2 ft (610 mm) in diameter. Above this channel are grass-covered benches. The right bench is narrow and bare except for a growth of very short grass; the bank slopes steeply above the bench. The slope of the left bank is gentle. The reach expands slightly throughout its length. The river is perennial, and flow is unregulated.

Remarks: H.W. Hjalmanson (hydrologist, U.S. Geological Survey, written commun., 1965) stated:

"The computed n value seems lower than would be indicated by the size of the bed material, but most of the rocks were immersed in a smooth flow of water and caused very little turbulence. The top of the surge was marked throughout the reach before and after the current-meter measurement."

Table 25. Flow data and computed roughness coefficient, Verde River near Paulden

Date of flow	Discharge, in cubic feet per second	Roughness coefficient	Rating
04-16-65	313	0.029	Fair

Table 26. Average-reach properties, Verde River near Paulden

Date	Area, in square feet	Top width, in feet	Hydraulic radius, in feet	Mean velocity, in feet per second	Froude number	Total length, in feet	Total fall, in feet	Water-surface slope
04-16-65	139	68.3	2.19	2.19	0.27	333	0.26	0.0008

Verde Valley near Paulden—Continued

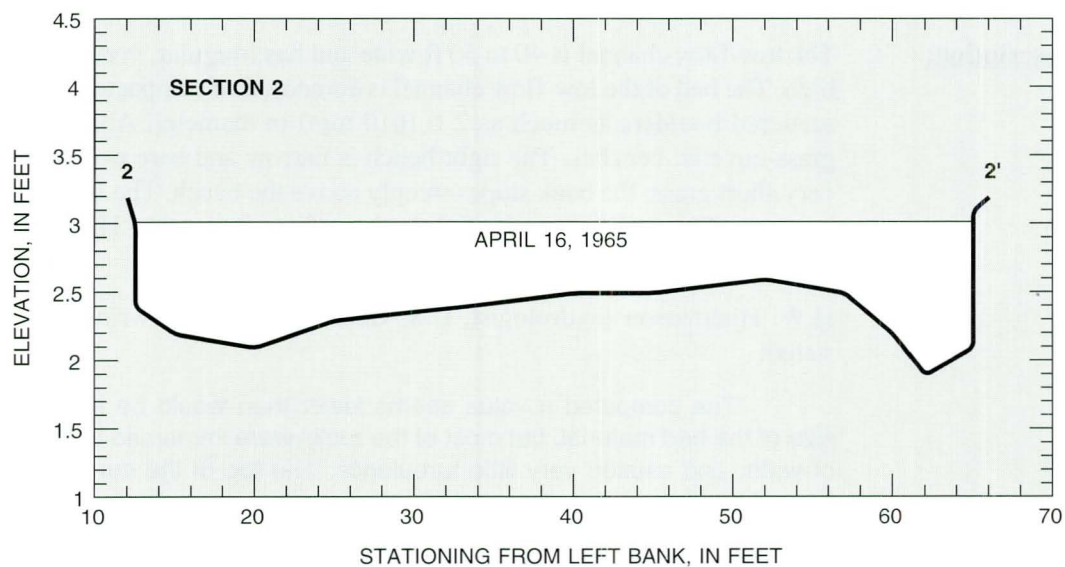


Figure 16A. Cross-section 2, Verde River near Paulden.

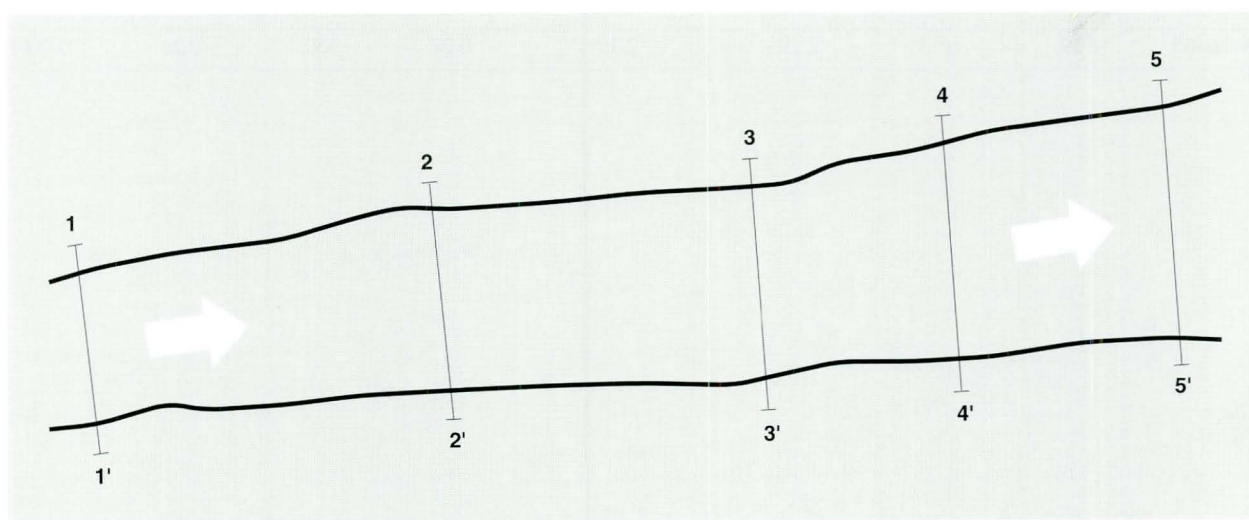


Figure 16B. Plan view, Verde River near Paulden.

Verde River near Paulden—Continued



Figure 16C. View from top of reach looking downstream during low flow, Verde River near Paulden.



Figure 16D. View from top of reach looking downstream at time of verification measurement, April 16, 1965, Verde River near Paulden.

Salt River below Stewart Mountain Dam

Reach location: Latitude 33°33'00", longitude 111°34'31". The reach begins about 2.25 mi downstream from streamflow-gaging station 09502000, Salt River below Stewart Mountain Dam (Barnes, 1967).

Drainage area: 6,230 mi².

Bed-material size: See *channel description*.

Channel description: The reach is fairly uniform and slightly contracting in a downstream direction. Bed and bank material consist of smooth cobbles that range from 4 to 10 in. (100 to 250 mm) in diameter. As indicated in the photographs, a sand-and-pebble matrix is between the cobbles. A grain-size analysis was not available. The river is perennial, and flow is regulated by upstream reservoirs.

Table 27. Flow data and computed roughness coefficient, Salt River below Stewart Mountain Dam

Date of flow	Discharge, in cubic feet per second	Roughness coefficient	Rating
03-24-50	1,280	0.032	Good

Table 28. Average-reach properties, Salt River below Stewart Mountain Dam

Date	Area, in square feet	Top width, in feet	Hydraulic radius, in feet	Mean velocity, in feet per second	Froude number	Total length, in feet	Total fall, in feet	Water-surface slope
03-24-50	405	190	2.14	3.22	0.39	1,886	3.59	0.0019

Salt River below Stewart Mountain Dam—Continued

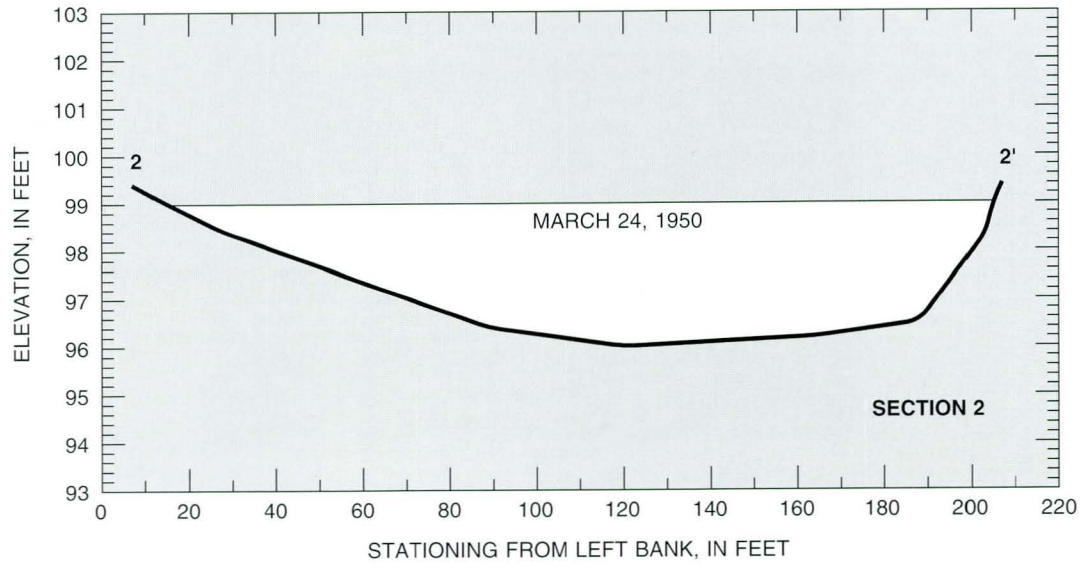


Figure 17A. Cross-section 2, Salt River below Stewart Mountain Dam.

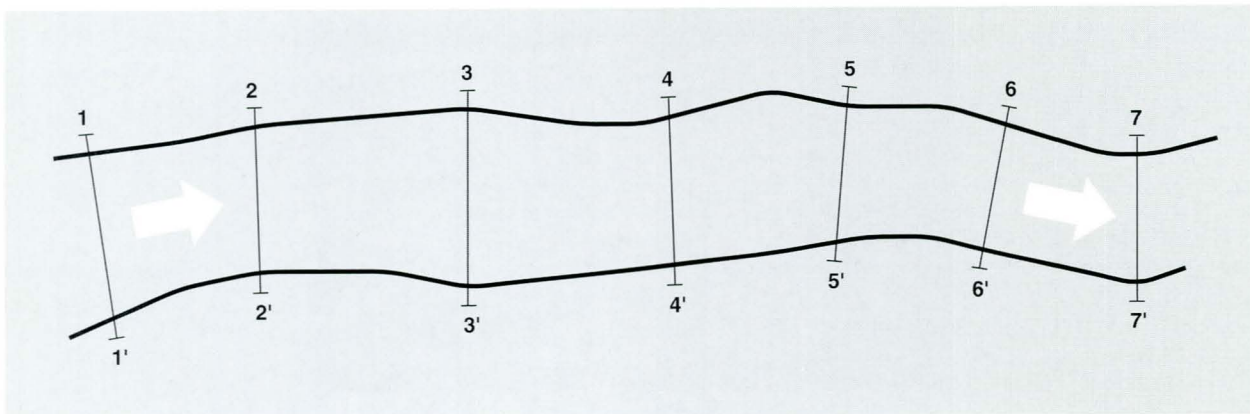


Figure 17B. Plan view, Salt River below Stewart Mountain Dam.

Salt River below Stewart Mountain Dam—Continued

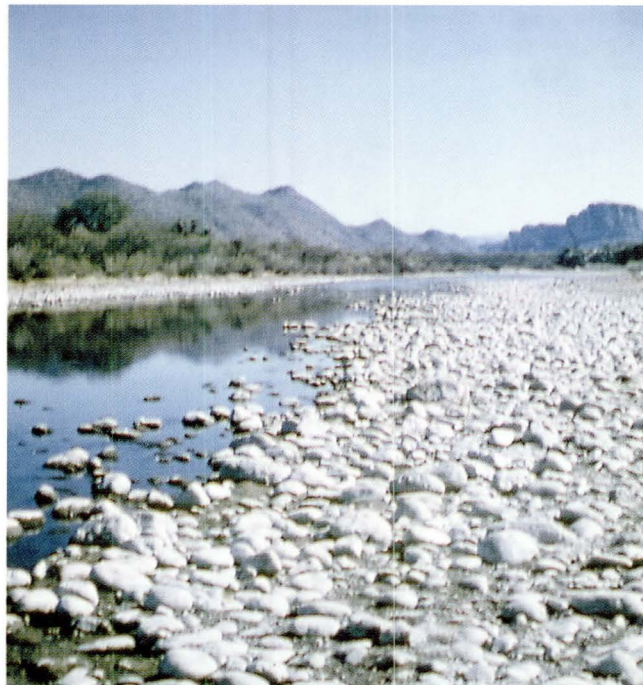


Figure 17C. View looking upstream along left bank below cross-section 6, Salt River below Stewart Mountain Dam.

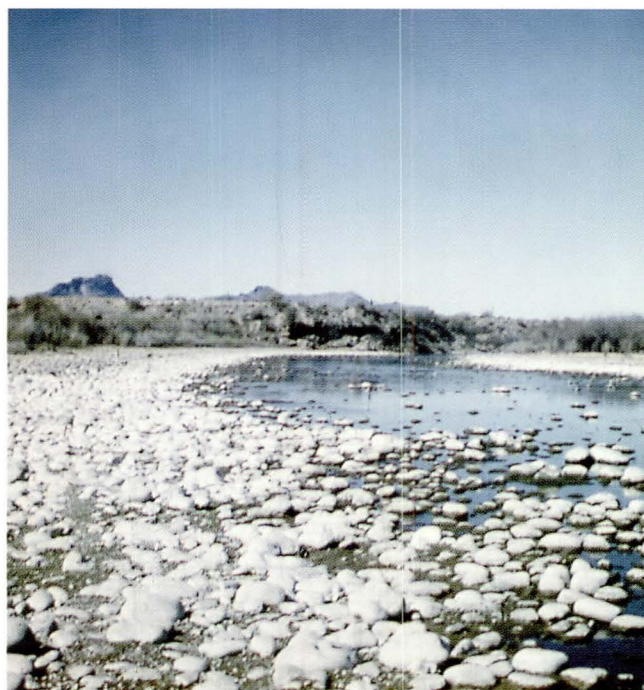


Figure 17D. View looking downstream along left bank from cross-section 2, Salt River below Stewart Mountain Dam.

DISCUSSION OF SIGNIFICANT RESULTS

Components of Manning's n

Attempts were made, using various techniques, to quantify the separate components or adjustment factors of Manning's n for each of the verification measurements presented in this report (table 29). The purpose of presenting this information is to supply additional aid to designers and engineers who need to assess roughness characteristics of stream channels for hydraulic studies in arid to semiarid environments. According to current guidelines (Thomsen and Hjalmarson, 1991), the general approach for estimating resistance to flow in stream channels is to first select a base value of Manning's n for the bed material. The base value of Manning's n is represented by the size and shape of the grains of the material that form the *wetted perimeter* and that produce a retarding effect on flow (Chow, 1959). Cross-section irregularities, channel alignment, vegetation, obstructions, and other factors that increase roughness then are added to the base value of n . The following equation, first introduced by Cowan (1956), is used to compute the equivalent total Manning's n for a channel using this approach:

$$n = (n_b + n_1 + n_2 + n_3 + n_4) m \quad (9)$$

where

- n_b = base value of n for a straight uniform channel,
- n_1 = surface irregularities,
- n_2 = variations in shape and size of the channel,
- n_3 = obstructions,
- n_4 = vegetation, and
- m = correction factor for meandering or sinuosity of the channel.

Detailed explanations for each adjustment factor can be found in Cowan (1956), Chow (1959), Aldridge and Garrett (1973), and Thomsen and Hjalmarson (1991).

Base Value of Manning's n for Gravel-Bed Streams

A variety of techniques and methods have been presented in literature that aid in estimating the base value of Manning's n for hydraulic computations in gravel-bed streams. Referencing tables and photographs of verified roughness coefficients is one method; another is the use of equations that relate Manning's n to easily measured hydraulic and channel parameters.

Previous investigators have presented data that indicate trends exist among hydraulic radius, median grain-size diameter, and verified base values of n for gravel-bed streams in specific regions of the world. For example, Limerinos (1970) examined verified values of n for 11 gravel-bed streams in California. Other researchers, such as Bray (1979) and Griffiths (1981), presented similar information for gravel-bed streams in Canada and New Zealand, respectively (table 30). These three investigators developed equations that relate Manning's n to hydraulic radius and median-grain size of the bed material (table 30). A similar equation was developed for gravel-bed streams in Arizona in which the base n value was the only factor that contributed to total roughness (table 30; Phillips and Ingersoll, 1997).

The four equations are plotted to show the relation between Manning's n and relative roughness (R/d_{50}) for gravel-bed streams in different parts of the world (fig. 18). In order to perform this simple comparison of equations, a constant d_{50} value of 0.30 ft was used, and hydraulic-radius values ranged from 0.6 to 7.5 ft (fig. 18).

The plots in figure 18 have a similar trend that is fairly steep for relative roughness values less than about 5. Although the general trend among the different relations is similar and, for relative roughness values larger than about 5, all the trend lines asymptotically approach constant values, a significant shift is apparent in the relation for verified n values presented in this report (fig. 18). As indicated by the three equations developed for areas outside Arizona, the asymptotic n values range between approximately 0.036 and 0.041. According to the data presented for dryland gravel-bed streams in Arizona, however, the data trend asymptotically approaches a base n value of about 0.028. If the equations presented are to be properly used as aids in determining base values of Manning's n , adequate descriptions of channel characteristics from which the data were obtained must be presented.

Table 29. Summary of verification measurements that include magnitude of base n values, factors required to adequately describe flow retardance, channel and hydraulic components, and an estimated percentage of flow that was blocked by vegetation

[n , Manning's roughness coefficient; n_b , base value of n for a straight uniform channel; n_1 , surface irregularities; n_2 , variations in shape and size of the channel; n_3 , obstructions; n_4 , vegetation; m , correction factor for meandering or sinuosity of the channel; R , hydraulic radius, in feet; S_{ws} , water-surface slope (no dimensions); d_{50} , median diameter of bed material, in feet; R/d_{50} , relative roughness (no dimensions); B , estimated percentage of flow blocked by vegetation. Dashes indicate no data or component not applicable for measurement.]

Date	Discharge, in cubic feet per second	n	n_b	n_1	n_2	n_3	n_4	m	R	S_{ws}	d_{50}	R/d_{50}	B
Hassayampa River near Arlington													
02-09-93	5,580	0.027	0.024	---	---	---	¹ 0.003	1.0	4.12	0.0034	---	---	5
07-06-94	80.5	.034	.034	---	---	---	---	1.0	1.29	.0039	.28	4.61	---
06-16-94	45.5	.036	.036	---	---	---	---	1.0	.97	.0039	.28	3.46	---
06-15-94	17.0	.036	.036	---	---	---	---	1.0	.58	.0039	.28	2.07	---
Skunk Creek above Interstate 17													
03-01-91	618	.048	² .031	---	---	---	.017	1.0	1.97	.0055	.29	6.79	20
01-05-95	393	.034	.034	---	---	---	---	1.0	1.28	.0062	.29	4.41	---
01-05-95	168	.037	.037	---	---	---	---	1.0	.83	.0067	.29	2.86	---
01-26-95	723	.031	.031	---	---	---	---	1.0	1.71	.0058	.29	5.90	---
01-26-95	180	.035	.035	---	---	---	---	1.0	.90	.0058	.29	3.10	---
09-28-95	822	.035	² .031	---	---	---	.004	1.0	1.91	.0062	.29	6.59	5
11-01-95	500	.039	² .032	---	---	---	.007	1.0	1.60	.0055	.29	5.52	10
08-14-96	403	.048	² .032	---	---	---	.016	1.0	1.60	.0052	.29	5.52	20
09-02-96	215	.052	² .034	---	---	---	.018	1.0	1.20	.0054	.29	4.14	25
Agua Fria River below New Waddell Dam													
02-09-93	9,000	.042	² .028	---	0.007	---	¹ .007	1.0	4.78	.0025	.27	17.7	10
Cave Creek above Deer Valley Road													
01-06-95	297	0.033	² .031	---	---	---	.002	1.0	2.33	.0046	.30	7.77	5
01-09-95	193	.033	² .031	---	---	---	.002	1.0	2.07	.0029	.30	6.90	3
01-10-95	39	.034	.034	---	---	---	---	1.0	.98	.0024	.30	3.27	---
Cave Creek below Cave Buttes Dam													
11-02-95	165	.025	.025	---	---	---	---	1.0	1.91	.0031	---	---	---
11-02-95	165	.017	.017	---	---	---	---	1.0	.99	.0130	---	---	---
01-09-95	197	.025	.025	---	---	---	---	1.0	2.03	.0030	---	---	---
01-09-95	197	.017	.017	---	---	---	---	1.0	1.12	.0148	---	---	---
Hassayampa River near Morrystown													
02-20-93	7,330	.025	.022	---	---	---	¹ .003	1.0	3.8	.0062	.0014	---	5

Table 29. Summary of verification measurements that include magnitude of base n values, factors required to adequately describe flow retardance, channel and hydraulic components, and an estimated percentage of flow that was blocked by vegetation—Continued

Date	Discharge, in cubic feet per second	n	n_b	n_1	n_2	n_3	n_4	m	R	S_{ws}	d_{50}	R/d_{50}	B
Hassayampa River near Morristown													
02-09-93	6,180	0.026	0.023	---	---	---	¹ 0.003	1.0	3.4	0.0062	0.0014	---	5
01-19-93	2,470	.019	.016	---	---	---	¹ .003	1.0	1.8	.0050	.0014	---	5
01-21-93	787	.018	.015	---	---	---	¹ .003	1.0	.9	.0043	.0014	---	5
Indian Bend Wash above Curry Road													
10-06-93	6,480	.024	.021	---	---	---	¹ .003	1.0	5.36	.0014	---	---	5
12-26-94	449	.036	.025	---	---	---	¹ .011	1.0	1.52	.0016	---	---	15
Salt River above Interstate 10													
02-18-92	4,900	.030	.030	---	---	---	---	1.0	2.61	.0025	.31	8.42	---
01-15-92	2,070	.034	.034	---	---	---	---	1.0	1.64	.0027	.31	5.29	---
01-09-92	1,000	.038	.038	---	---	---	---	1.0	1.16	.0026	.31	3.74	---
Verde River below Beeline Highway													
03-28-91	2,860	.030	.030	---	---	---	---	1.0	3.94	.0013	.36	10.9	---
09-14-89	225	.036	.036	---	---	---	---	1.0	1.00	.0038	.36	2.78	---
West Fork Sycamore Creek near Sunflower													
02-11-63	117	.067	.064	---	---	---	¹ .003	1.0	1.21	.0181	---	---	5
San Pedro River near Charleston													
08-14-64	7,550	.048	.039	---	0.006	---	¹ .003	1.0	4.62	.0048	---	---	5
Santa Cruz River at Cortaro													
09-10-64	14,200	.020	.017	---	---	---	¹ .003	1.0	6.36	.0037	.0039	---	5
Verde River near Paulden													
04-16-65	313	.029	.025	---	.001	---	¹ .003	1.0	2.19	.0008	---	---	5
Salt River below Stewart Mountain Dam													
03-24-50	1,280	.032	.032	---	---	---	---	1.0	2.14	.0019	---	---	---

¹Obtained from equation 14.

²Obtained from equation 13.

Table 30. Equations for relations among base n values, hydraulic radius, and median diameter of bed material for gravel-bed streams in different parts of the world

[Equations 10–12 are from Coon (1995)]

Source	Equation	Range in d_{50} (ft)	Location
	(10)		
Limerinos (1970)	$n = \frac{0.0926 R^{1/6}}{0.35 + 2.0 \log (R/d_{50})}$	0.02 to 0.83	California, U.S.A.
	(11)		
Griffiths (1981)	$n = \frac{0.0927 R^{1/6}}{0.760 + 1.98 \log (R/d_{50})}$	0.04 to 0.99	New Zealand
	(12)		
Bray (1979)	$n = \frac{0.0927 R^{1/6}}{0.248 + 2.36 \log (R/d_{50})}$	0.06 to 0.48	Alberta, Canada
	(13)		
n verification ¹	$n = \frac{0.0926 R^{1/6}}{1.46 + 2.23 \log (R/d_{50})}$	0.28 to 0.36	Arizona, U.S.A.

¹Phillips and Ingersoll (1997).

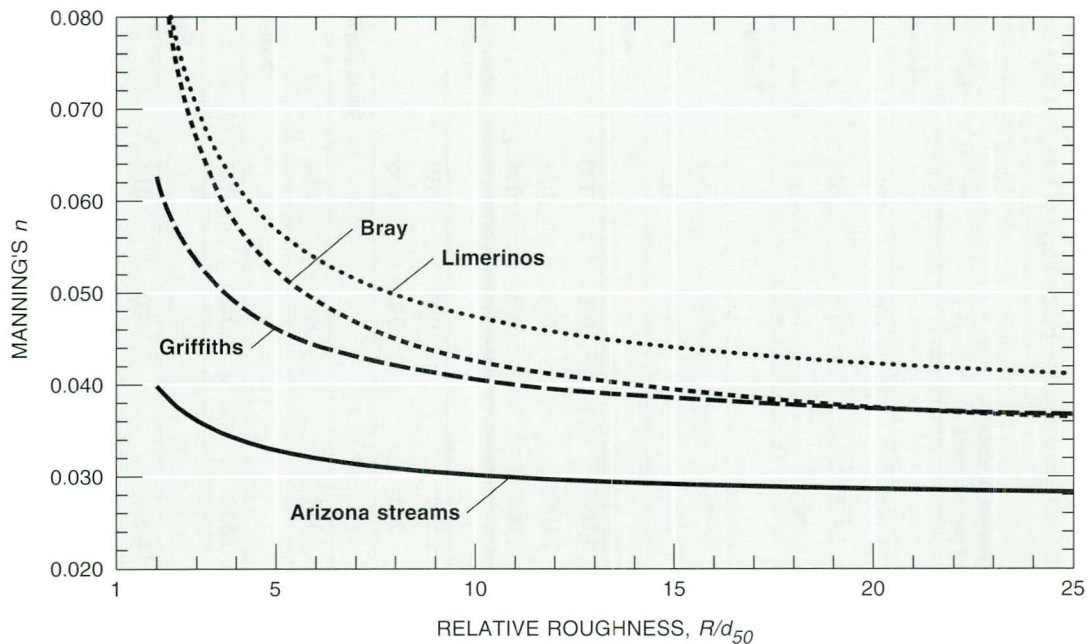


Figure 18. Relation of Manning's n and relative roughness for gravel-bed stream channels in Arizona and throughout the world. All trend lines are plotted for values of d_{50} equal to 0.30 foot, and values of R range from 0.6 to 7.5 feet.

A discussion, therefore, follows that presents potential factors that may account for the differences between the relations (fig. 18).

Possible explanations for the apparent shift in relations may be found by examining differences in channel and flow characteristics for the separate regions in which the data for the equations were obtained. For example, most of the streams used in the derivation of equations 10, 11, and 12 (table 30) for California, New Zealand, and Canada, respectively, are perennial and in relatively humid climates; whereas many of the streams that were studied in Arizona are ephemeral and in an arid to semiarid climate. Channels of ephemeral streams in dry climates, such as Skunk Creek above Interstate 17, may contain substantial amounts of fine-grained particles between the larger cobble-sized particles primarily because of the lack of regular base-flow conditions required for sediment transport. The presence of a fine-grained matrix may result in mitigated turbulence around the cobbles. The overall hydraulic effect would be a lower expenditure of energy by the fluid during flow resulting in lower values of n_b .

The substantial shift in trendlines also may reflect extraneous flow-retarding effects associated with irregularities in bank shape and changes in channel alignment. Many of the sites used to develop equations 10, 11, and 12 are located in relatively pristine areas where streams are not substantially affected by human influences. Three of the sites used to derive equation 13, however, are located in river reaches that have been channelized. In addition to stabilizing channel banks, channelization projects generally tend to increase conveyance by straightening rivers, potentially resulting in a decrease of flow-retarding effects associated with channel meanders and other irregularities (Phillips and Ingersoll, 1997).

A third possible reason for the lower values of n_b for gravel-bed streams in Arizona may be the result of the location of the selected sites with respect to the stream's headwaters. Many of the selected sites in Arizona are at great distances from the stream's source, where the stream is considered base level. Particles in base-level streams generally are rounder and reflect better sorting and homogeneity than higher-gradient piedmont channels (Leopold and others, 1964). For piedmont streams where homogeneity of particles may be relatively low, the particles that are substantially larger than the median size can play an important role in flow resistance (Leopold and others, 1964). For

similar values of d_{50} , therefore, greater turbulence may occur near channel beds of piedmont streams than near channel beds of base-level streams resulting in larger values of n_b . Several of the n -verification measurements used for calibration of equations 10, 11, and 12 (table 30) were made in piedmont streams. Additionally, the range in median diameter of particles for streams in central Arizona is much narrower than the range used to develop equations for gravel-bed streams in other regions of the world (table 30). The sites with relatively large median grain sizes that were employed in the development of equations 10, 11, and 12 may have had a disproportionate effect on roughness, a consequence that may weight the relations toward higher values of n (fig. 18; Phillips and Ingersoll, 1997).

A final explanation for the apparent shift in relations may be found by examining potential extraneous flow-retarding elements in the streams that were used in the derivation of each equation. Although the previous investigators attempted to incorporate gravel-bed stream sites in which n_b was the only flow-retarding factor, examination of several sites indicates that the flow-retarding effects associated with bank vegetation may have contributed to the overall value of n . As discussed previously, Manning's n generally decreases with depth until a constant value is asymptotically reached. For channels that contain an appreciable amount of bank vegetation, however, the inverse is likely, and n can increase substantially with flow depth (Barnes, 1967; Jarrett, 1985; and Coon, 1995). One of the sites used by Limerinos (1970), for example, is the Merced River at Happy Isles Bridge, near Yosemite, California. According to site-description information and visual examination of the major flow-retarding elements for this site (Barnes, 1967, p. 194–197), an extensive amount of vegetation in the form of trees was present along the channel banks, which may have had an influence on computed n values (Limerinos, 1970, table 1). Additionally, in the derivation of the equation for gravel-bed streams in New Zealand (table 30, equation 11), Griffiths (1981) used several streams that also contain bank vegetation that may have influenced the overall computed roughness coefficient (Hicks and Mason, 1991). If the flow retarding effect of bank vegetation contributed to total flow retardance at a substantial number of sites used to derive the respective equations, the result could be an apparent upward shift for the relation between n and relative roughness (fig. 18). The contribution of

bank vegetation to total flow retardance for sites used to develop equation 13 appeared to be negligible.

Whatever the reason for the difference between the separate equations, it seems that the relations presented generally are subject to the hydraulic, hydrologic, and geologic conditions of the respective research areas. Because the established equations are limited to the range in hydraulic and channel components used in their derivation, application of equation 13 to similar gravel-bed dryland streams also is limited to this same range. For example, when transferring results to similarly characterized dryland stream channels, caution must be used for sites where values of hydraulic radius are above about 4 ft (fig. 18), and values of d_{50} are outside the range of the data set (table 29). Further research is required to extend the relation developed for gravel-bed streams in Arizona to larger magnitude flows that occur less frequently.

Influence of Vegetation on Manning's n

For 19 of the 37 n -verification measurements made in dryland streams, vegetation was determined to have contributed to total roughness and, therefore, required quantifying (table 29). The vegetation component for several of the gravel-bed streams that contained an appreciable amount of vegetation was determined indirectly. Using equation 13, base n values were computed for five verification measurements made at Skunk Creek above Interstate 17 and two verification measurements made at Cave Creek above Deer Valley Road (table 29). Because n_1 through n_3 were considered to have no effect on total roughness at these two study reaches, the corresponding effect of vegetation on total roughness was quantified for each measurement by subtracting the computed base n value from total verified n (table 29).

For each of the seven n -verification measurements, the average percent area of flow blocked by vegetation was estimated. The vegetation component data obtained indirectly using equation 13 and the corresponding percent area of flow blocked by vegetation were used to develop a simple best-fit relation that can be used to estimate n_4 in similarly vegetated stream channels (equation 14 and figure 19).

$$n_4 = 0.0008B - 0.0007 \quad (14)$$

where

- n_4 = vegetation component of Manning's n , and
- B = percentage of flow blocked by vegetation.

Equation 14 was used to estimate n_4 for the twelve other n -verification measurements that contained an appreciable amount of vegetation (table 29). For 3 of the 12 measurements, an estimate of n_2 was required to adequately account for variations in channel shape and size (table 29). The estimates of n_2 primarily were made using standard guidelines for assigning components of n to dryland streams (Aldridge and Garrett, 1973; Thomsen and Hjalmarson, 1991).

SUMMARY AND CONCLUSIONS

Thirty-seven roughness coefficients were determined for 14 selected natural and constructed stream channels in Arizona. The sites were selected to represent a wide range of channel conditions that include alluvial, boulder, and constructed channels that contain varying amounts of riparian vegetation. Computed roughness-coefficient values ranged from 0.017 for constructed channels to 0.067 for boulder channels.

This report is intended to be used in conjunction with current guidelines that describe techniques and methods for assigning Manning's n . The descriptions of hydraulic and physical characteristics and photographs that reflect the major flow-retarding elements in channel reaches for which n values have been verified can be used as comparison standards to aid in assigning n values to similarly characterized channels.

Relations derived from the data in this study relate Manning's n values to various hydraulic and channel components. For gravel-bed channels that have a median bed-material size from 0.28 to 0.36 ft, the median diameter of bed material, hydraulic radius, and the verified n values are used to develop an equation that can be used to determine n_b for similarly characterized dryland streams. This equation indicates substantially lower n values compared to similarly developed equations for gravel-bed channels in other regions of the world. The larger verified base values of Manning's n for gravel-bed channels in California, New Zealand, and Canada may be the result of the flow-retarding effects associated with channel

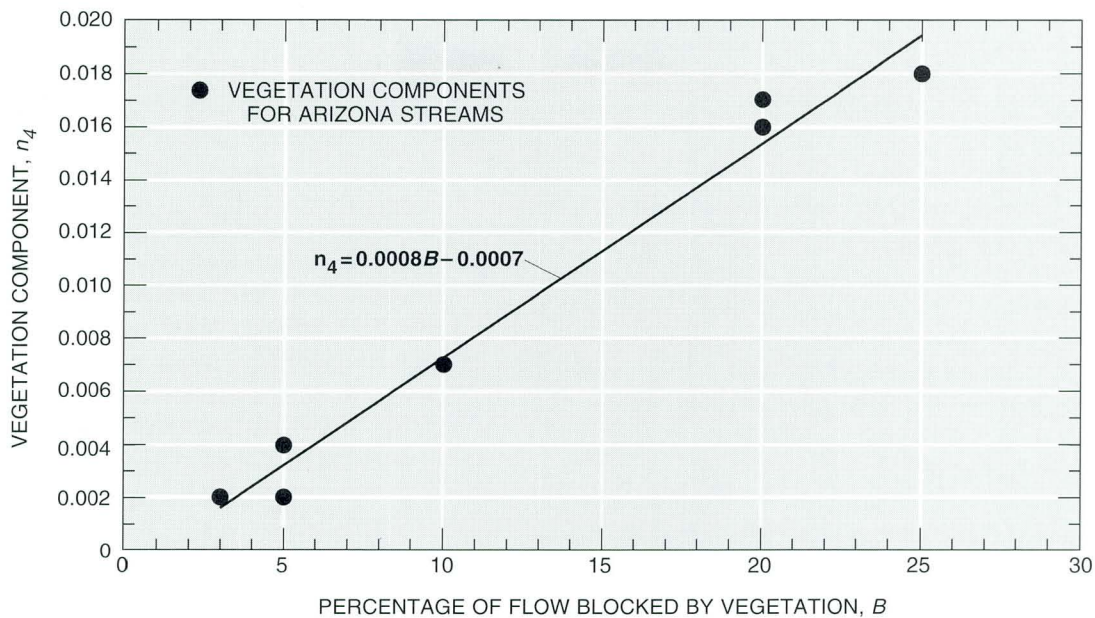


Figure 19. Relation of vegetation components for vegetated channels studied and the estimated percentage of flow blocked by vegetation (average vegetation conditions for all cross sections at each site).

irregularities, poorly sorted bed material, or bank vegetation.

The equation developed for base n values in gravel-bed streams also is used to quantify the magnitude of the vegetation component of Manning's n value for several gravel-bed channels where vegetation was present. A simple relation was developed for the estimated percent area of flow blocked by vegetation and the vegetation component. This relation can be used at similar sites in the arid to semiarid southwestern United States for which the effect of vegetation on total roughness must be determined. Further study is needed to extend the relations developed for this study beyond current limitations of the data sets presented in this report.

SELECTED REFERENCES

- Aldridge, B.N., and Eychaner, J.H., 1984, Floods of October 1977 in southern Arizona and March 1978 in central Arizona: U.S. Geological Survey Water-Supply Paper 2223, 143 p.
- Aldridge, B.N., and Garrett, J.M., 1973, Roughness coefficients for stream channels in Arizona: U.S. Geological Survey unnumbered open-file report, 87 p.

- Arcement, G.J., and Schneider, V.R., 1989, Guide for selecting Manning's roughness coefficient for natural channels and flood plains: U.S. Geological Survey Water-Supply Paper 2339, 38 p.
- Barnes, H.H., Jr., 1967, Roughness characteristics of natural channels: U.S. Geological Survey Water-Supply Paper 1849, 213 p.
- Benson, M.A., and Dalrymple, Tate, 1967, General field and office procedures for indirect discharge measurements: U.S. Geological Survey Techniques of Water-Resources Investigations, book 3, chap. A1, 30 p.
- Birkeland, P.W., 1984, Soils and geomorphology: New York, Oxford University Press, 365 p.
- Blodgett, J.C., 1986, Rock riprap design for protection of stream channels near highway structures: U.S. Geological Survey Water-Resources Investigations Report 86-4127, 60 p.
- Bray, D.I., 1979, Estimating average velocity in gravel-bed rivers: American Society of Civil Engineers, Journal of the Hydraulics Division, v. 105, no. HY9, p. 1103-1122.
- Burkham, D.E., 1970, Precipitation, streamflow, and major floods at selected sites in the Gila River drainage basin above Coolidge Dam, Arizona: U.S. Geological Survey Professional Paper 655-C, p. C1-C13.
- , 1976, Hydraulic effects of changes in bottom-land vegetation on three major floods, Gila River in southeastern Arizona: U.S. Geological Survey Professional Paper 655-J, p. 14.

- Chow, V.T., 1959, *Open-channel hydraulics*: New York, McGraw-Hill, 680 p.
- Coon, W.F., 1995, Estimates of roughness coefficients for selected natural stream channels with vegetated banks in New York: U.S. Geological Survey Open-File Report 93-161, 127 p.
- Costa, J.E., 1987, Hydraulics and basin morphology of the largest flash floods in the conterminous United States: *Journal of Hydrology*, v. 93, p. 313-338.
- Cowan, W.L., 1956, Estimating hydraulic roughness coefficients: *Agricultural Engineering*, v. 37, no. 7, p. 473-475.
- Culbertson, J.K., and Dawdy, D.R., 1964, A study of fluvial characteristics and hydraulic variables middle Rio Grande, New Mexico: U.S. Geological Survey Water-Supply Paper 1498-F, 74 p.
- Dalrymple, Tate, and Benson, M.A., 1967, Measurement of peak discharge by slope-area method: U.S. Geological Survey Techniques of Water-Resources Investigations, book 3, chap. A2, 12 p.
- Fossum, K.D., and Davis, K.G., 1996, Physical, chemical, biological, and toxicity data from the study of urban stormwater and ephemeral streams, Maricopa County, Arizona, water years 1992-95: U.S. Geological Survey Open-File Report 96-394, 71 p.
- Glancy, P.A., and Williams, R.P., 1994, Problems with indirect determinations of peak streamflows in steep, desert stream channels: New York, American Society of Civil Engineers Proceedings of the 1994 National Conference on Hydraulic Engineering, v. 1, p. 635-639.
- Graf, W.L., 1988, *Fluvial processes in dryland rivers*: Berlin, Springer-Verlag, 346 p.
- Griffiths, G.A., 1981, Flow resistance in coarse gravel bed rivers: American Society of Civil Engineers, *Journal of Hydraulics Division*, v. 107, no. HY7, p. 899-918.
- Hicks, D.M., and Mason, P.D., 1991, Roughness characteristics of New Zealand Rivers: New Zealand Water Resources Survey, DSIR Marine and Freshwater, 329 p.
- Hirschboeck, K.K., 1985, Hydroclimatology of flow events in the Gila River basin, central and southern Arizona: Tucson, University of Arizona, doctoral dissertation, 335 p.
- Hjalmarson, H.W., 1994, Potential flood hazards and hydraulic characteristics of tributary-flow areas in Maricopa County, Arizona: U.S. Geological Survey Water-Resources Investigations Report 93-4169, 55 p.
- Hoyt, W.G., and Langbein, W.B., 1955, *Floods*: Princeton, N.J., Princeton University Press, 469 p.
- Jarrett, R.D., 1985, Determination of roughness coefficients for streams in Colorado: U.S. Geological Survey Water-Resources Investigations Report 85-4004, 54 p.
- , 1987, Errors in slope-area computation of peak discharges in mountain streams: *Journal of Hydrology*, v. 96, p. 53-67.
- Jarrett, R.D., and Petsch, H.E., Jr., 1985, Computer program NCALC user's manual—Verification of Manning's roughness coefficient in channels: U.S. Geological Survey Water-Resources Investigations Report 85-4317, 27 p.
- Karim, F., 1995, Bed configuration and hydraulic resistance in alluvial-channel flows: *Journal of Hydraulic Engineering*, v. 121, no. 1, p. 15-25.
- Koloseus, H.J., and Davidian, Jacob, 1966, Free-surface instability correlations: U.S. Geological Survey Water-Supply Paper 1592-C, 72 p.
- Leopold, L.B., Wolman, M.G., and Miller, J.P., 1964, *Fluvial processes in geomorphology*: New York, Dover Books on Earth Sciences, 503 p.
- Limerinos, J.T., 1970, Determination of the Manning's coefficient from measured bed roughness in natural channels: U.S. Geological Survey Water-Supply Paper 1898-B, 47 p.
- NBS Lowry Engineers and Planners, and McLaughlin Water Engineers, Ltd., 1992, *Drainage design manual for Maricopa County, Arizona, Volume II, Hydraulics*: Phoenix, Arizona Flood Control District of Maricopa County.
- Parker, J.T.C., 1995, Channel change and sediment transport in two desert streams in central Arizona, 1991-92: U.S. Geological Survey Water-Resources Investigations Report 95-4059, p. 1-42.
- Phillips, J.V., and Hjalmarson, H.W., 1994, Floodflow effects on riparian vegetation in Arizona: New York, American Society of Civil Engineers Proceedings of the 1994 National Conference on Hydraulic Engineering, v. 1, p. 707-711.
- Phillips, J.V., and Ingersoll, T.L., 1997, Comparison of verified roughness coefficients for gravel-bed streams in central Arizona with other areas of the western United States, in *Floodplain Management in a Multi-faceted World*, 21st Annual Conference of the Association of State Floodplain Managers, Proceedings, Little Rock, Arkansas, April 27-May 2, 1997: Boulder, Colorado, Natural Hazards Research Center, University of Colorado, p. 153-158.
- Rantz, S.E., and others, 1982, Measurement and computation of streamflow—Volume I. Measurement of stage and discharge: U.S. Geological Survey Water-Supply Paper 2175, 284 p.
- Roeske, R.H., Garrett, J.M., and Eychaner, J.H., 1989, Floods of October 1983 in southeastern Arizona: U.S. Geological Survey Water-Resources Investigations Report 85-4225C, 77 p.
- Sabol, G.V., Rumann, J.M., Khalili, D., and Waters, S.D., 1990, *Hydrologic design manual for Maricopa County, Arizona*: Phoenix, Arizona, Flood Control District of Maricopa County.
- Sargent, R.J., 1979, Variation of Manning's n roughness coefficient with flow in open river channels: *Journal of*

- the Institution of Water Engineers and Scientists, v. 33, no. 3, p. 290–294.
- Sellers, W.D., Hill, R.H., and Sanderson-Rae, Margaret, eds., 1985, *Arizona climate—The first hundred years*: Tucson, University of Arizona Press, 80 p.
- Simons, D.B., and Richardson, E.V., 1966, Resistance to flow in alluvial channels: U.S. Geological Survey Professional Paper 422–J, 61 p.
- Thomsen, B.W., and Hjalmanson, H.W., 1991, Estimated Manning's roughness coefficients for stream channels and flood plains in Maricopa County, Arizona: Phoenix, Arizona, Flood Control District of Maricopa County, 126 p.
- Wahl, K.L., 1994, Bias in regression estimates of Manning's n : New York, American Society of Civil Engineers Proceedings of the 1994 National Conference on Hydraulic Engineering, v. 1, p. 727–731.
- Webb, R.H., and Betancourt, J.L., 1992, Climatic variability and flood frequency of the Santa Cruz River, Pima County, Arizona: U.S. Geological Survey Water-Supply Paper 2379, 40 p.
- Wolman, M.G., 1954, A method of sampling coarse riverbed material: American Geophysical Union, Transactions, v. 35, no. 6, p. 951–956.